Indicators of Global Climate Change 2024: annual update of key indicators of the state of the climate system and human influence

Piers M. Forster [1], Chris Smith [2,3], Tristram Walsh [4], William F. Lamb [1, 5], Robin Lamboll [6], Christophe Cassou [7, 8], Mathias Hauser [9], Zeke Hausfather [10, 11], June-Yi Lee [12, 13], Matthew D. Palmer[14, 15], Karina von Schuckmann [16], Aimée B.A. Slangen [17], Sophie Szopa [18], Blair Trewin [19], Jeongeun Yun [12], Nathan P. Gillett [20], Stuart Jenkins [4], H. Damon Matthews [21], Krishnan Raghavan [22], Aurélien Ribes [23], Joeri Rogelj [3, 6, 24], Debbie Rosen [1], Xuebin Zhang [25], Myles Allen [4, 26], Lara Aleluia Reis [27, 28], Robbie M. Andrew [29], Richard A. Betts [14, 30], Alex Borger [31], Jiddu A. Broersma [31], Samantha N. Burgess [32], Lijing Cheng [33], Pierre Friedlingstein [7, 30], Catia M. Domingues [34, 35], Marco Gambarini [27, 28], Thomas Gasser [3], Johannes Gütschow [36], Masayoshi Ishii [37], Christopher Kadow [38], John Kennedy [39], Rachel E. Killick [14], Paul B. Krummel [40], Aurélien Liné [8, 16, 41], Didier P. Monselesan [42], Colin Morice [14], Jens Mühle [43], Vaishali Naik [44], Glen P. Peters [29], Anna Pirani [45], Julia Pongratz [46, 47], Jan. C. Minx [1, 5], Matthew Rigby [48], Robert Rohde [10], Abhishek Savita [49, 50], Sonia I. Seneviratne [9], Peter Thorne [51], Christopher Wells [1], Luke M. Western [48], Guido R. van der Werf [52], Susan E. Wijffels [42, 53], Valérie Masson-Delmotte [18], Panmao Zhai [54]

1. Priestley Centre for Climate Futures, University of Leeds, Leeds, LS2 9JT, UK
2. Department of Water and Climate, Vrije Universiteit Brussel, Brussels, Belgium
3. International Institute for Applied Systems Analysis (IIASA), Vienna, Austria
4. Environmental Change Institute, University of Oxford, Oxford, UK
5. Potsdam Institute for Climate Impact Research (PIK), Member of the Leibniz Association, Potsdam, Germany
6. Centre for Environmental Policy, Imperial College London, London, UK
7. Laboratoire de Météorologie Dynamique/Institut Pierre-Simon Laplace, CNRS, Ecole Normale Supérieure/Université PSL, Paris, France
8. CECI, Université de Toulouse, CERFACS, CNRS, Toulouse, France
9. Institute for Atmospheric and Climate Science, Department of Environmental Systems Science, ETH Zurich, Zurich, Switzerland
10. Berkeley Earth, Berkeley, CA, USA
11. Stripe Inc., South San Francisco, CA, USA
12. Research Center for Climate Sciences, Pusan National University, Busan, Republic of Korea
13. Center for Climate Physics, Institute for Basic Science, Busan, Republic of Korea
14. Met Office Hadley Centre, Exeter, UK
15. School of Earth Sciences, University of Bristol, Bristol, UK
16. Mercator Ocean international, Toulouse, France

17. NIOZ Royal Netherlands Institute for Sea Research, Department of Estuarine and Delta Systems, Yerseke, the Netherlands
18. Institut Pierre Simon Laplace, Laboratoire des Sciences du Climat et de l'Environnement (UMR 8212 CEA-CNRS-UVSQ), Université Paris-Saclay, Gif-sur-Yvette, France
19. Bureau of Meteorology, Melbourne, Australia
20. Canadian Centre for Climate Modelling and Analysis, Environment and Climate Change Canada, Victoria, BC, Canada
21. Concordia University, Montreal, Canada
22. Indian Institute of Tropical Meteorology, Pune, India
23. CNRM, Université de Toulouse, Météo France, CNRS, Toulouse, France
24. Grantham Institute for Climate Change and Environment, Imperial College London, United Kingdom
25. Pacific Climate Impacts Consortium, University of Victoria, Victoria, Canada
26. Atmospheric, Oceanic and Planetary Physics, Department of Physics, University of Oxford, UK
27. CMCC Foundation, Euro-Mediterranean Center on Climate Change, Lecce, Italy
28. RFF-CMCC, European Institute on Economics and the Environment, Milan, Italy
29. CICERO Center for International Climate Research, Oslo, Norway
30. Global Systems Institute, Science and Economy, University of Exeter, Exeter, UK
31. Climate Change Tracker, Data for Action Foundation, Amsterdam, the Netherlands
32. European Centre for Medium-Range Weather Forecasts, ECWMF, Reading, United Kingdom
33. State Key Laboratory of Earth System Numerical Modeling and Application, Institute of Atmospheric Physics, Chinese Academy of Sciences, Beijing, China
34. Marine Physics and Ocean Climate, National Oceanography Centre, Southampton, UK
35. Environmental Business Unit, CSIRO, Hobart, Australia
36. Climate Resource, Melbourne, Australia
37. Meteorological Research Institute, Tsukuba, Japan
38. German Climate Computing Center, Hamburg, Germany (DKRZ)
39. No affiliation, Verdun, France
40. CSIRO Environment, Aspendale, Australia
41. Institut de Mécanique des Fluides de Toulouse, Université de Toulouse, INP, CNRS, Toulouse, France
42. CSIRO, Environment Research Unit, Climate Intelligence, Climate variability and hazards, Hobart, Tasmania, Australia
43. Scripps Institution of Oceanography, University of California San Diego, La Jolla, CA, USA
44. NOAA Geophysical Fluid Dynamics Laboratory, Princeton, NJ, USA
45. Euro-Mediterranean Center on Climate Change (CMCC), Venice, Italy; Università Cà Foscari,Venice, Italy
46. Ludwig-Maximilians-Universität München, München, Germany
47. Max Planck Institute for Meteorology, Hamburg, Germany

48. School of Chemistry, University of Bristol, Bristol, United Kingdom
49. Centre for Atmospheric Sciences, Indian Institute of Technology Delhi, Delhi, India
50. Department of Atmospheric Sciences, Rosenstiel School of Marine, Atmospheric and Earth Science, Miami, USA
51. ICARUS Climate Research Centre, Maynooth University, Maynooth, Ireland
52. Wageningen University and Research, Wageningen, The Netherlands
53. Physical Oceanography, Woods Hole Oceanographic Institution, Woods Hole, Massachusetts, USA
54. Chinese Academy of Meteorological Sciences, Beijing, China

Correspondence to: Piers. M. Forster (p.m.forster@leeds.ac.uk)

Abstract.

In a rapidly changing climate, evidence-based decision-making benefits from up-to-date and timely information. Here we compile monitoring datasets (published here, https://doi.org/10.5281/zenodo.15639576 Smith et al., 2025a) to produce updated estimates for key indicators of the state of the climate system: net emissions of greenhouse gases and short-lived climate forcers, greenhouse gas concentrations, radiative forcing, the Earth's energy imbalance, surface temperature changes, warming attributed to human activities, the remaining carbon budget, and estimates of global temperature extremes. This year, we additionally include indicators for sea-level rise and land precipitation change. We follow methods as closely as possible to those used in the IPCC Sixth Assessment Report (AR6) Working Group One report.

The indicators show that human activities are increasing the Earth's energy imbalance and driving faster sea-level rise compared to the AR6 assessment. For the 2015–2024 decade average, observed warming relative to 1850-1900 was 1.24 [1.11 to 1.35] °C, of which 1.22 [1.0 to 1.5] °C was human-induced. The 2024 observed best estimate of global surface temperature (1.52 °C) is well above the best estimate of human-caused warming (1.36°C). However, the 2024 observed warming can still be regarded as a typical year, considering the human induced warming level and the state of internal variability associated with the phase of El Niño and Atlantic variability. Human-induced warming has been increasing at a rate that is unprecedented in the instrumental record, reaching 0.27 [0.2 - 0.4] °C per decade over 2015-2024. This high rate of warming is caused by a combination of greenhouse gas emissions being at an all-time high of 53.6 ± 5.2 $GtCO_2e$ per year over the last decade (2014-2023), as well as reductions in the strength of aerosol cooling. Despite this, there is evidence that the rate of increase in CO_2 emissions over the last decade has slowed compared to the 2000s, and depending on societal choices, a continued series of these annual updates over the critical 2020s decade could track decreases or increases in the rate of the climatic changes presented here.

1 Introduction

IPCC AR6 provided an assessment of human influence on key indicators of the state of climate grounded in available data at the time of publication. The preparation for the next IPCC report, the Seventh Assessment Report (AR7), has started and the assessment is due in around 5 years. Given the speed of recent change, and the need for updated climate knowledge to inform evidence-based decision-making, the Indicators of Global Climate Change (IGCC) was initiated to provide policymakers with annual updates of the latest scientific understanding on the state of selected critical indicators of the climate system and where possible of the quantified human influence upon these.

IGCC compliments other annual updates, most notably, the BAMS State of the Climate Report (Dunn et al., 2024) and the WMO State of the Global Climate (WMO, 2024). The main difference is that this work goes beyond the observations to make process level estimates of effective radiative forcing and attributed human-induced response using methods rigorously assessed in AR6.

This third annual update follows broadly the format of last year (Forster et al., 2024), which extended indicators through 2023. The work focuses on indicators related to heating of the climate system, building from greenhouse gas emissions towards estimates of human-induced warming and the remaining carbon budget for 1.5 °C and other policy-relevant temperature thresholds.. Fig. 1 presents an overview of the aspects assessed and their interlinkages from cause (emissions) through effect (changes in physical indicators) to Climatic Impact-Drivers. It also provides a visual roadmap as to the structure of remaining sections in this paper to guide the reader.

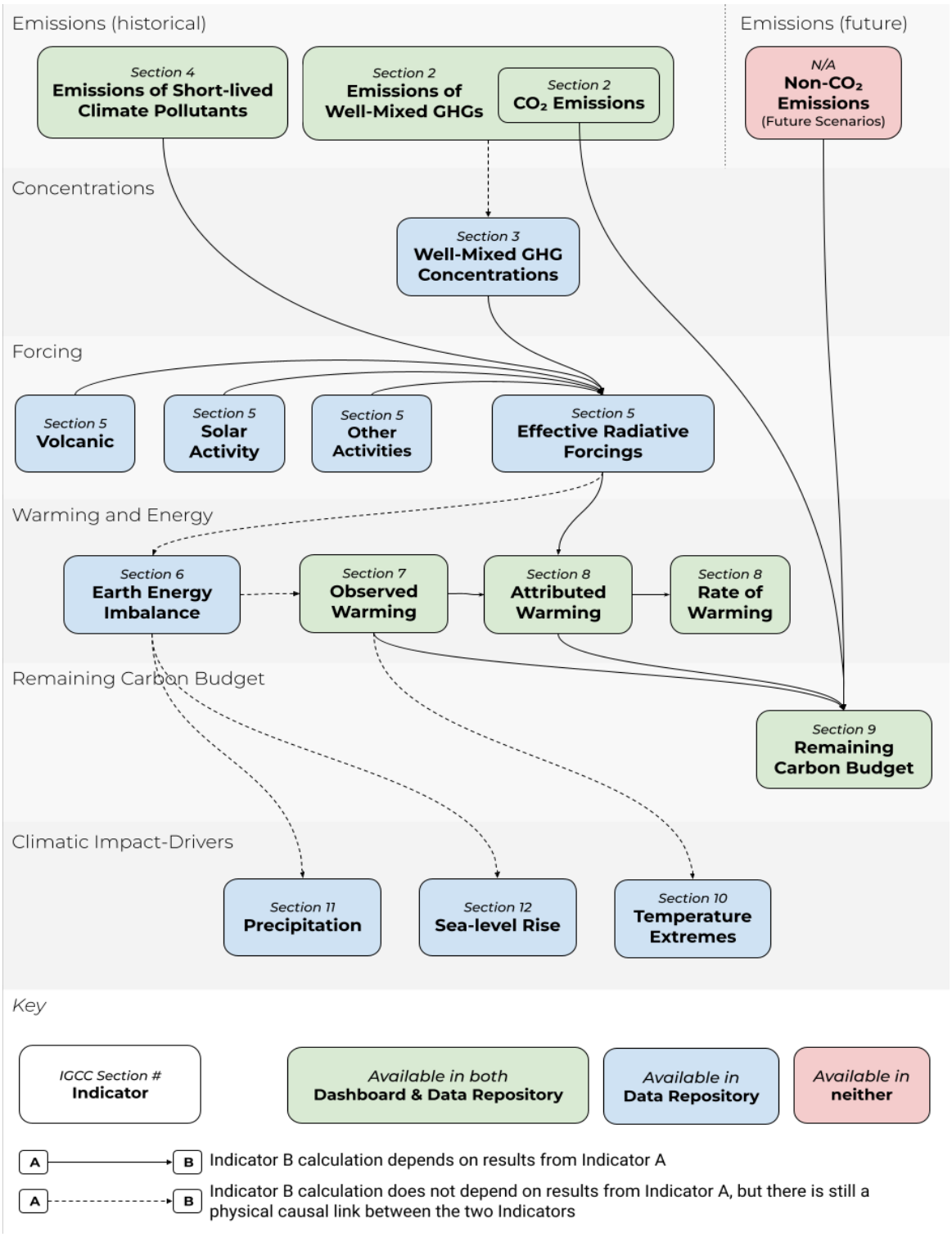
Emissions (historical)
Emissions (future)
Section 4
Emissions of Short-lived Climate Pollutants
Section 2
Emissions of Well-Mixed GHGs
Section 2
CO₂ Emissions
N/A
Non-CO₂ Emissions
(Future Scenarios)
Concentrations
Section 3
Well-Mixed GHG Concentrations
Forcing
Section 5
Volcanic
Section 5
Solar Activity
Section 5
Other Activities
Section 5
Effective Radiative Forcings
Warming and Energy
Section 6
Earth Energy Imbalance
Section 7
Observed Warming
Section 8
Attributed Warming
Section 8
Rate of Warming
Remaining Carbon Budget
Section 9
Remaining Carbon Budget
Climatic Impact-Drivers
Section 11
Precipitation
Section 12
Sea-level Rise
Section 10
Temperature Extremes
Key
IGCC Section #
Indicator
Available in both
Dashboard & Data Repository
Available in
Data Repository
Available in
neither
A
B
Indicator B calculation depends on results from Indicator A
A
B
Indicator B calculation does not depend on results from Indicator A, but there is still a physical causal link between the two Indicators

121

Figure 1 The flow chart of data production from emissions to human induced warming, the remaining carbon budget, and changes to Climatic Impact-Drivers, illustrating both the rationale and workflow within the paper production.

The update is based on methodologies assessed by the IPCC Sixth Assessment Report (AR6) of the physical science basis of climate change (Working Group One (WGI) report; IPCC, 2021a) as well as Chap. 2 of the WGIII report (Dhakal et al., 2022) and is aligned with the efforts initiated in AR6 to implement FAIR (Findable, Accessible, Interoperable, Reusable) principles for reproducibility and reusability (Pirani et al., 2022; Iturbide et al., 2022). IPCC reports make a much wider assessment of the science and methodologies – we do not attempt to reproduce the comprehensive nature of these IPCC assessments here. We also do not consider adopting fundamentally different approaches to AR6. Rather, our aim is to rigorously track both climate system change and evolving methodological improvements between IPCC report cycles, thereby increasing transparency and consistency in between successive reports.

This annual update is organised as follows: greenhouse gas (GHG) emissions (Sect. 2), greenhouse gas concentrations (Sect. 3) and emissions of short-lived climate forcers (Sect. 4) are used to develop updated estimates of effective radiative forcing (Sect. 5). The Earth energy imbalance (Sect. 6) and observations of global surface temperature change (Sect. 7) are key global indicators of a warming world. The contributions to global surface temperature change from human and natural influences are formally attributed in Sect. 8, which tracks the level and rate of human-induced warming. Sect. 9 updates the remaining carbon budget for policy-relevant temperature thresholds. Sect. 10 gives an example of global-scale indicators associated with climate extremes of maximum land surface temperatures and Sect. 11 shows land-surface precipitation trends traceable to AR6, a new addition to this year's update. Sect. 12 presents updated estimates of global mean sea-level rise, also a new addition. Code and data availability are given in Sect. 13, and conclusions are presented in Sect. 14. Data are available at https://doi.org/10.5281/zenodo.15639576 (Smith et al., 2025a).

2 Greenhouse gas emissions

Historic GHG emissions from human activity were assessed in both AR6 WGI and WGIII. Chapter 5 of WGI assessed CO_2 and CH_4 emissions in the context of the carbon cycle (Canadell et al., 2021). Chapter 2 of WGIII, published one year later (Dhakal et al., 2022), assessed the sectoral sources of emissions and gave the most up-to-date understanding of the current level of emissions. This section bases its methods and data on those employed in this WGIII chapter.

2.1 Methods of estimating greenhouse gas emissions changes

Like in AR6 WGIII, net GHG emissions in this paper refer to releases of GHGs from anthropogenic sources minus removals by anthropogenic sinks, for the set of GHGs outlined in the United Nations Framework Convention on Climate Change (UNFCCC). These include: CO_2 emissions from fossil fuels and industry (CO_2-FFI); net CO_2

emissions from land use, land-use change and forestry (CO_2-LULUCF); CH_4 emissions; N_2O emissions; and fluorinated gas (F-gas) emissions comprising hydrofluorocarbons (HFCs), perfluorocarbons (PFCs), sulphur hexafluoride (SF_6) and nitrogen trifluoride (NF_3) - hereafter the "UNFCCC F-gases".

Despite an extensive literature on GHG emissions, there remains important differences in reporting conventions and system boundaries between assessments. These differences relate to three underlying issues: (1) emissions data sets vary in their coverage of sources and sectors; (2) there are different approaches to determining the 'anthropogenic' component of LULUCF emissions and removals; and (3) the Paris Agreement does not cover all relevant sources of emissions (Lamb et al., 2025).

Concerning the first issue, there are several possible emissions datasets to draw from, each with varying coverage and update schedules. Emissions data are gathered by countries and submitted to the UNFCCC in the form of national inventory reports and common reporting tables. However, these "national inventories" are generally incomplete and are not kept up to date for all countries. Emissions reporting therefore often relies on "third-party" datasets compiled by research organisations, including: the Global Carbon Budget (GCB; Friedlingstein et al., 2024); the Emissions Database for Global Atmospheric Research (EDGAR; Crippa et al., 2023); the Potsdam Real-time Integrated Model for probabilistic Assessment of emissions Paths (PRIMAP-hist; Gütschow et al., 2016; Gütschow et al., 2025)[1]; the Community Emissions Data System (CEDS; Hoesly et al., 2018; Hoesly and Smith, 2024); and the Global Fire Emissions Database (GFED; van der Werf et al., 2017). As detailed below, for various reasons not all these datasets were employed in this update.

Concerning the second issue, there are varying conventions used to quantify CO_2-LULUCF fluxes. These include the use of bookkeeping models and aggregated national inventory reporting (Pongratz et al., 2021), which differ in terms of their applied system boundaries and definitions, and in particular how they treat "indirect anthropogenic effects" such as the influence of increased atmospheric CO_2 on vegetation growth. As such, the CO_2-LULUCF emissions estimates generated using bookkeeping models versus national inventories are not directly comparable and differ by about 7.5GtCO2yr-1 (2013-2022 average), but there are now methods to "translate" between these two approaches (Friedlingstein et al., 2022; Grassi et al., 2023; Schwingshackl et al., 2022). Assessments also differ with respect to biomass fire emissions and to what extent components of these are treated as anthropogenic (Lamb et al., 2025).

Finally, two categories of emissions are not directly covered by the Paris Agreement but might be considered depending on the objectives of an assessment. These include the Ozone Depleting Substances (hereafter the "ODS F-gases") comprising halons, chlorofluorocarbons (CFCs) and hydrochlorofluorocarbons (HCFCs). The ODS F-gases

[1] PRIMAP is a synthetic dataset that includes two time-series: PRIMAP Hist-TP, which is compiled from other underlying products such as EDGAR; and PRIMAP Hist-CR, which prioritises data from national inventories but gap-fills these where necessary.

were initially controlled under the Montreal Protocol and its amendments and are therefore not included in national inventories submitted to the UNFCCC, nor in many third-party emissions datasets - in contrast to the UNFCCC F-gases. Another important omission is the cement carbonation sink. To date this has also been excluded from national reporting under the UNFCCC, but plans for a new chapter covering these removals in the IPCC Task Force on National Greenhouse Gas Inventory Guidelines indicates a pathway for its eventual inclusion (IPCC, 2025).

The IPCC AR6 WGIII addressed these issues as follows. Total net GHG emissions were calculated as the sum of CO_2-FFI, CH_4, N_2O and UNFCCC F-gases from EDGAR (version 6, with a fast-track methodology applied for the final year of data - 2019), and net CO_2-LULUCF emissions from the GCB (the 2020 version; Friedlingstein et al., 2020). Net CO_2-LULUCF emissions followed the GCB convention and were derived from the average of three bookkeeping models (Hansis et al., 2015; Houghton and Nassikas, 2017; Gasser et al., 2020). "Indirect anthropogenic effects" on the terrestrial carbon fluxes were therefore excluded from totals (i.e., they were treated as part of the natural land sink). Further, the GCB methodology (and thus reporting in IPCC AR6 WGIII) includes CO_2 emissions from deforestation and forest degradation fires, but excludes those from wildfires, which are classified as natural even if climate change affects their intensity and frequency. Similarly, the EDGAR dataset used in AR6 includes some non-CO_2 biomass fire emissions in the agricultural sector, but otherwise excludes those from wildfires. Sources not covered by inventories or the Paris Agreement (ODS F-gases and cement carbonation) were also excluded. Together these choices ensured consistency with the Integrated Assessment Model (IAM) benchmarks reported in WGIII and were closely focused on direct anthropogenic emissions under the UNFCCC, reflecting the importance of human-driven technology and policy options in shaping the future climate response.

The analysis presented here continues to provide an "WGIII update" estimate that tracks the same system boundary and compilation of GHGs as in AR6 WGIII, albeit with some differences in the selected data sources. As in previous years, we use GCB data for CO_2-FFI. We also continue to use GCB for CO_2-LULUCF, which has now been updated to use the average of four (rather than three) bookkeeping models (BLUE by Hansis et al., 2015; H&C by Houghton and Castanho, 2023; OSCAR by Gasser et al., 2020; LUCE by Qin et al., 2024). We use PRIMAP Hist-TP data for CH_4 and N_2O, and inversions of atmospheric concentrations tracked by NOAA and AGAGE with best-estimate lifetimes for UNFCCC F-gas emissions based on analysis in the subsequent Section 3 (Lan et al., 2025; Dutton et al., 2024; Prinn et al., 2018). We follow the same approach for estimating uncertainties and CO_2-equivalent emissions as in AR6, as described in the Supplement.

In addition to the WGIII update, we provide two further estimates that provide clarity and comparison to other assessment approaches. This reflects the fact that other decision criteria for tracking emissions are possible. First, in cases where assessments prioritise calculating the best estimate of fluxes to the atmosphere, it would be important to include ODS F-gases, cement carbonation and all non-CO_2 biomass fire emissions, including those from wildfires. Indeed, these are included in this article in subsequent assessments of concentration change (including compounds

formed in the atmosphere as ozone), effective radiative forcing, human-induced warming, carbon budgets and climate impacts, in line with the WGI assessment. We therefore provide an "IPCC update + additional sources and sinks" estimate that shows the change implied by including these three components in the global total. Second, the IPCC AR7 report outline foresees the tracking of "inventory-aligned" emissions that are consistent with national reporting. Full alignment between emissions inventories and WGIII emissions consistent with IAM benchmarks is essential for an accurate assessment and stocktake of the Nationally Determined Contributions (NDCs) and pathways to net-zero emissions (Grassi et al., 2021; Gidden et al., 2023; Allen et al., 2025). We therefore provide an "Inventory-aligned" estimate that follows the inventory approach to accounting for LULUCF emissions, while also integrating the latest national inventory data from the Common Reporting Tables. The data sources associated with these additional estimates are detailed in Table S1 in the Supplement.

We expect to see differences between the three estimates, most notably between the "WGIII update" and "Inventory-aligned" estimates. As discussed above, these differ conceptually in their treatment of the LULUCF sector. However, national inventory reporting can also differ from third-party datasets in terms of underlying methods: in some countries, investments into statistical infrastructures have enabled the use of more precise emissions factors in inventories to estimate fluxes according to local or national conditions, while in others this may not be the case. In contrast, third-party datasets often use globally consistent emissions factors. Notably, the PRIMAP Hist-CR dataset, which is here used to represent national inventories, has significantly lower total CH_4 emissions relative to other datasets reported here, as well as the global atmospheric inversion estimates evaluated in this paper. A substantive body of literature has found that, on average, national inventories tend to underestimate CH_4 compared to inversions (Deng et al., 2022; Tibrewal et al., 2024; Janardanan et al., 2024; Scarpelli et al., 2022).

2.2 Updated greenhouse gas emissions

Updated GHG emission estimates following the WGIII assessment are presented in Fig. 2 and Table 1. Total global GHG emissions were 55.4± 5.1 $GtCO_2e$ in 2023. Of this total, CO_2-FFI contributed 37.8 ± 3.0 $GtCO_2$, CO_2-LULUCF contributed 3.6 ± 2.5 $GtCO_2$, CH_4 contributed 9.2 ± 2.7 $GtCO_2e$, N_2O contributed 2.9 ± 1.7 $GtCO_2e$ and F-gas emissions contributed 1.9 ± 0.6 $GtCO_2e$.

Note the recent history of emissions in these datasets are continually revised, so there are small differences between each annual update in emission estimates over the recent past. Initial projections for 2024 indicate that CO_2 emissions from fossil fuels and industry increased to 38.2 ± 3.0, and CO_2 emissions from land-use change increased to 4.2 ± 2.8 $GtCO_2$ (Friedlingstein et al., 2024; Deng et al., 2024). The significant increase in land-use change emissions is connected to high emissions from tropical deforestation and degradation fires in the aftermath of the El Niño with droughts in South America continuing since 2023. Synchronous large fires occurred in North America, where the record-breaking Canadian fires of 2023 were followed by another well above average year in 2024, but are attributable to climate variability and climate change, and not anthropogenic land-use change (Friedlingstein et al., 2024).

Average annual GHG emissions for the decade 2014–2023 were 53.6 ± 5.2 $GtCO_2e$. Average decadal GHG emissions have increased steadily since the 1970s across all major groups of GHGs, driven primarily by increasing CO_2 emissions from fossil fuel and industry but also rising emissions of CH_4 and N_2O. Emissions of UNFCCC F-gases have grown more rapidly than other GHG, but from low levels. Both the magnitude and trend of CO_2 emissions from land-use change remain highly uncertain, with the latest data indicating an average net flux between 4–5 $GtCO_2\ yr^{-1}$ for the past few decades.

The fossil fuel share of global GHG emissions was approximately 70% in 2023 (GWP100 weighted), based on the EDGAR v9 dataset (Crippa et al., 2023) and net land-use CO_2 emissions from the Global Carbon Budget (Friedlingstein et al. 2024). The remaining share of non-fossil fuel emissions are mostly from land-use change, agriculture, cement production, waste and F-gas emissions.

Different emissions assessment approaches are shown in Fig. 3. Increasing the scope of the WGIII update to include ODS F-gases, cement carbonation, and CH_4 and N_2O from biomass burning results in emissions of 56.9 ± 5.2 GtCO2e yr^{-1} in 2023, or a total change of +1.6 GtCO2e yr^{-1}. ODS F-gas emissions have declined substantially since the 1990s under the Montreal Protocol and its amendments, reaching 1.3 GtCO2e yr^{-1} in 2023, with a stalling rate of reduction in the past decade. The cement carbonation sink has steadily increased alongside cement production to reach -0.8 GtCO2e yr^{-1} in 2023. Biomass fire emissions have a more variable trend and 2023 was a relatively extreme year at 1 GtCO2e yr^{-1}, compared to an average of 0.7 GtCO2e yr^{-1} in the preceding decade.

Emissions according to national inventories were 47.1 ± 4.7 GtCO2e yr^{-1} in 2023, or 8.3 GtCO2e yr^{-1} lower than the WGIII update (Fig. 3). The main reason is due to diverging estimates of net LULUCF emissions, which according to inventory accounts were on average 7.5 $GtCO_2$ lower over the past decade (2014-2023). Additional differences result from a lower estimate of Energy, Industrial Process, Agriculture and Waste emissions in inventories (-1.8 GtCO2e yr^{-1}), particularly for CH_4 (-0.7 GtCO2e yr^{-1}).

Emerging literature, published after AR6, suggests that increases in atmospheric CH_4 concentrations may also be driven by methane emissions from wetland changes resulting from climate change and variability (e.g. Basu et al., 2022; Hardy et al., 2023; Peng et al., 2022; Nisbet et al., 2023; Zhang et al., 2023). There is also a possible effect from CO_2 fertilisation (Feron et al., 2024; Hu et al., 2023). The latest global methane budget estimates indirect anthropogenic CH_4 fluxes from wetlands and freshwater bodies of approximately 2.4 $GtCO_2e\ yr^{-1}$ (Saunois et al., 2024). Such emissions are not captured in the WGIII estimate here as they are not a direct emission from human activity, but rather a feedback induced by a changing climate, yet they will contribute to GHG concentration rise, forcing and energy budget changes discussed in the next sections. They will become more important to properly

account for in future years. Note that these indirect CH_4 emissions are not used to determine the effective radiative forcing in Sect. 5.

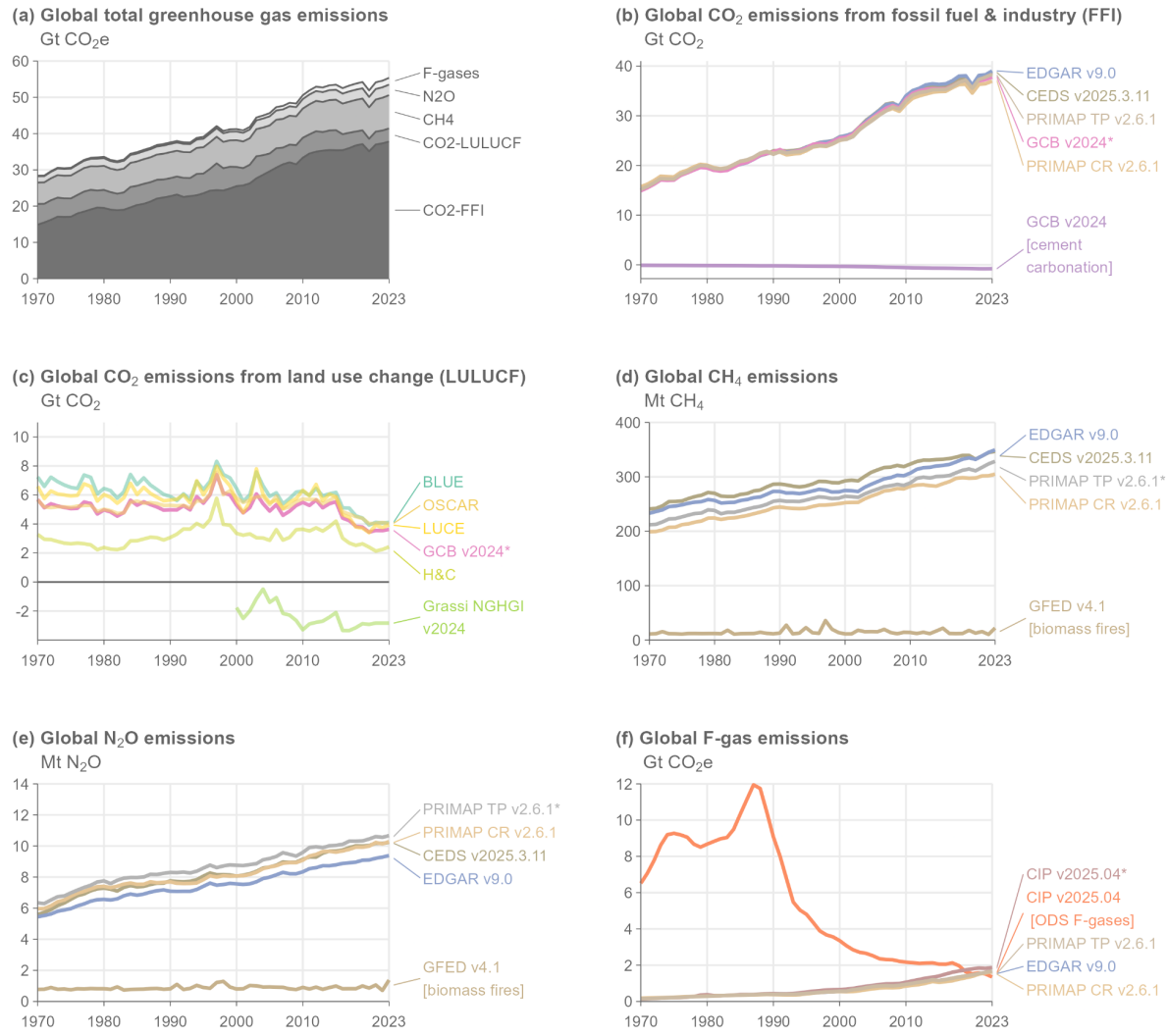

Figure 2 Annual global anthropogenic GHG emissions by source, 1970–2023. Refer to Sect. 2.1 and Table S1 for a list of datasets. Datasets with an asterisk (*) indicate the sources used to compile global total greenhouse gas emissions following the WGIII assessment in (a). CO_2-equivalent emissions in (a) and (f) are calculated using GWP100 from the AR6 WGI Chap. 7 (Forster et al., 2021). F-gas emissions in (a) comprise only UNFCCC F-gas emissions (see Sect. 2.1 for a list of species). F-gas emissions in (f) refer to UNFCCC F-gases, except for "CIP v2024.04 [ODS F-gases]". Some of the major depicted differences between datasets (e.g. between GCB v2024 and Grassi NGHGI v2024 in panel c) are due to varying system boundaries, rather than underlying uncertainties in activity levels or emissions factors.

Table 1 Global anthropogenic greenhouse gas emissions by source and decade following the WGIII assessment. All numbers refer to decadal averages, except for annual estimates in 2023 and 2024. CO_2-equivalent emissions are calculated using GWP100 from AR6 WGI Chap. 7 (Forster et al., 2021). Projections of non-CO_2 GHG emissions in 2024 remain unavailable at the time of publication. Uncertainties are ±8 % for CO_2-FFI, ±70 % for CO_2-LULUCF, ±30 % for CH_4 and F-gases, and ±60 % for N_2O, corresponding to a 90 % confidence interval. "GHG" in row one is the sum of the other rows.

Units: $GtCO_2e$	1970-1979	1980-1989	1990-1999	2000-2009	2010-2019	2014-2023	2023	2024 (projection)
GHG	30.9±4.5	34.6±4.6	39.3±5.1	45.1±5.1	52.9±5.4	53.6±5.2	55.4±5.1	
CO_2-FFI	17.3±1.4	20.3±1.6	23.6±1.9	28.9±2.3	35.4±2.8	36.3±2.9	37.8±3.0	38.2±3.0
CO_2-LULUCF	5.2±3.7	5.1±3.6	5.7±4.0	5.2±3.6	4.9±3.4	4.1±2.9	3.6±2.5	4.2±2.8
CH_4	6.3±1.9	6.7±2	7.2±2.2	7.7±2.3	8.4±2.5	8.7±2.6	9.2±2.7	
N_2O	1.9±1.1	2.2±1.3	2.3±1.4	2.5±1.5	2.7±1.6	2.8±1.7	2.9±1.7	
UNFCCC F-gases	0.2±0.01	0.4±0.1	0.5±0.2	0.8±0.3	1.4±0.4	1.6±0.5	1.9±0.6	

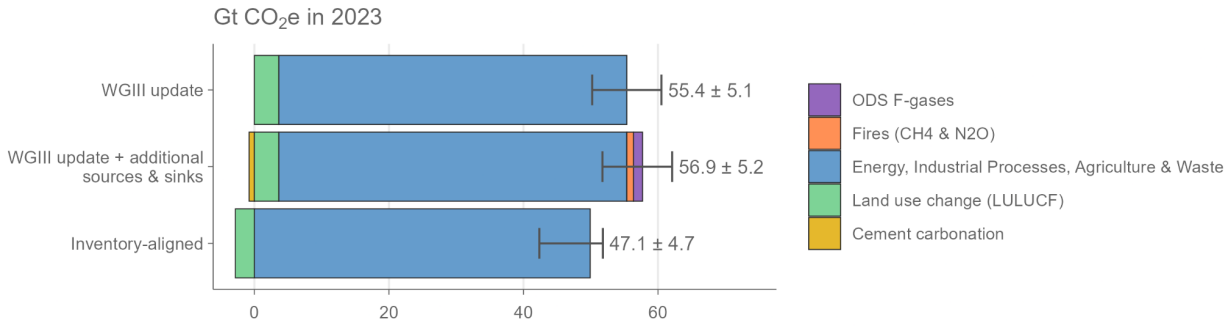

Figure 3 Annual global anthropogenic greenhouse gas emissions by assessment convention in 2023. Refer to Table 1 for a list of underlying datasets. Differences between conventions are primarily due to differences in system boundaries (Lamb et al., 2025). Uncertainties are ±8 % for CO_2-FFI, ±70 % for CO_2-LULUCF, ±30 % for CH_4 and F-gases, and ±60 % for N_2O, corresponding to a 90 % confidence interval.

3 Well-mixed greenhouse gas concentrations

As in Forster et al. (2024), we report best-estimate global mean concentrations for 52 well-mixed GHGs. These concentrations are updated to 2024. CO_2 mixing ratios were taken from the NOAA Global Monitoring Laboratory (GML) and are updated here through 2024 (Lan et al., 2025a). As in Forster et al. (2023, 2024), CO_2 is reported on the WMO-CO_2-X2019 scale, which differs from the WMO-CO_2-X2007 scale used in AR6 with WMO-CO_2-X2019 being around 0.18 ppm higher than WMO-CO_2-X2007 in recent years. For consistency with WMO-CO_2-X2019, the AR6 CO_2 concentrations that make up the 1750 to 1978 period in the IGCC dataset (before recent NOAA updates) have been converted to the WMO-CO_2-X2019 scale. Other GHG records were compiled from NOAA and AGAGE global networks or extrapolated from literature. An average of NOAA and AGAGE data, updated through 2024, were used for N_2O, CH_4, CFC-11, CFC-12, CCl_4, HCFC-22, HFC-134a, and HFC-125 (Lan et al., 2025; Dutton et al., 2024; Prinn et al., 2018), which, along with CO_2, account for over 97% of the ERF from well-mixed GHGs. Several other species also use means from the NOAA and AGAGE networks, where the NOAA data is updated to 2024 from the values given in the BAMS State of the Climate Report (Dunn et al., 2024) and AGAGE data up until 2022 is available; for 2023 and 2024, an offset to the NOAA data was applied which was equal to the mean difference between the NOAA and AGAGE datasets over the recent past. In cases where no updated information is available, global estimates were extrapolated from Vimont et al. (2022), Western et al. (2023, 2024), or other literature and scaled to be consistent with those reported in AR6. Some extrapolations are based on data from the mid-2010s (Droste et al., 2020; Laube et al., 2014; Simmonds et al., 2017; Vollmer et al., 2018), but have an imperceptible effect on the total ERF assessed in Sect. 5, and are included to maintain consistency with AR6. Mixing ratio uncertainties for 2024 are assumed to be like 2019, and we adopt the same uncertainties as assessed in AR6 WGI.

Fig. 4 shows recent GHG concentrations and their changes. Table S2 in the Supplement shows specific updated concentrations for all the GHGs considered. The global surface mean concentrations of CO_2, CH_4 and N_2O in 2024 were 422.8 [±0.4] parts per million (ppm), 1929.7 [±3.3] parts per billion (ppb) and 337.9 [±0.4] ppb, respectively. Concentrations of all three major GHGs have increased since 2019, with CO_2 increasing by 12.7 ppm, CH_4 by 63.3 ppb, and N_2O by 5.8 ppb. Increases since 2019 are consistent with those from the CSIRO network (Francey et al., 1999), which are 13.0 ppm, 61.9 ppb, and 6.0 ppb for CO_2, CH_4, and N_2O, respectively. With few exceptions, concentrations of ozone-depleting substances, such as CFC-11 and CFC-12, continue to decline, while those of replacement compounds (HFCs) have increased. HFC-134a, for example, has increased 25% since 2019 from 107.6 to 134.7 parts per trillion (ppt). Aggregated across all gases, PFCs have increased from 109.7 to an estimated 117.4 ppt CF_4-eq from 2019 to 2024, HFCs from 237 to 3212 ppt HFC-134a-eq, while ozone depleting gases have declined from 1032 to 995 ppt CFC-12-eq. Mixing ratio equivalents are determined by the radiative efficiencies of each GHG from Hodnebrog et al. (2020).

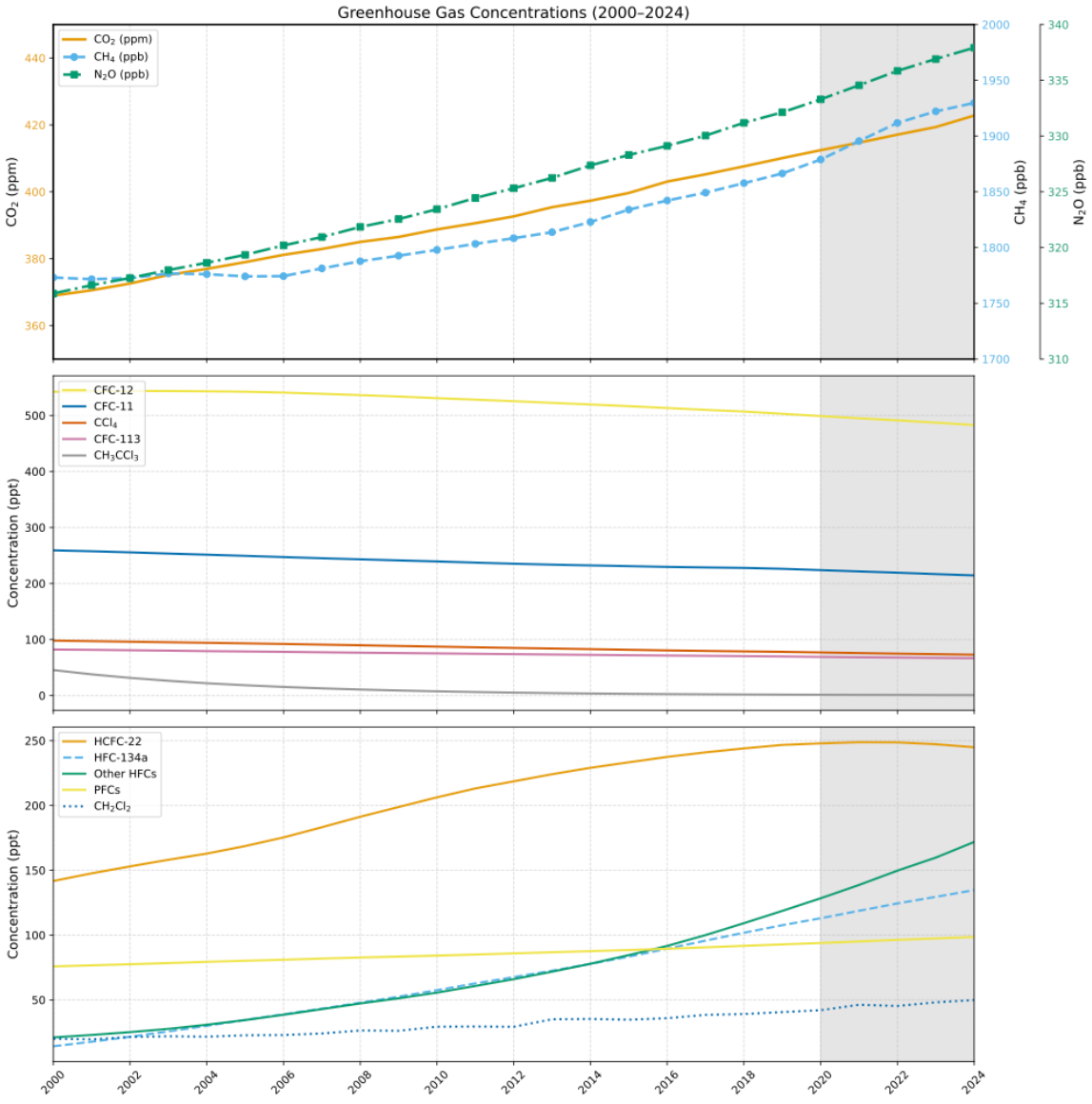

Figure 4 Atmospheric concentrations of a set of well mixed greenhouse gases over 2000-2024. The grey shaded region represents continuing changes since AR6. Note the different vertical scales.

Ozone and other non-methane SLCFs are not well-mixed in the atmosphere and are thus discussed separately (in Section 4). For this reason, the warming impact of ozone, the third most important GHG (in terms of current

contribution to warming) is not included in the contribution of well-mixed GHGs to observed warming, consistently with AR6. Note that change in methane concentration affects ozone, but this indirect effect is not accounted for in the estimate of the warming due to the evolution of well mixed GHG concentrations.

4 Non-methane short-lived climate forcers

Chapter 6 of WGI assessed emissions in the context of understanding the climate and air quality impacts of SLCFs (Szopa et al., 2021). Methane is a SLCF but also a well mixed GHG and is discussed in Sections 2 and 3. Trends in SLCFs emissions are spatially heterogeneous (Szopa et al., 2021), with strong shifts in the locations of reductions and increases over the decade 2010–2019 (Hodnebrog et al., 2024). Concentrations of non-methane SLCFs are heterogeneously distributed in the atmosphere and the observation networks are too sparse to report globally averaged concentrations. Typically, a combination of satellite data, where available, and global models and reanalysis are relied upon for producing global-scale distributions. In the case of models, production of near-real time information relies upon the availability of near-real time updates to SLCF emissions which are still challenging. Little information, whether from observations from local monitoring networks, satellite data or from global model reanalysis, is released in near real time.

In addition to GHG emissions, we provide an update of anthropogenic emissions of non-methane SLCFs (SO_2, black carbon (BC), organic carbon (OC), NOx, volatile organic compounds (VOCs), CO and NH_3). Data are presented in Table 2 and the evolution of SLCF emission estimates from the AR6 to this study is presented in Sect. S4 of the Supplement. Consistency between emission trends and concentrations is considered whenever feasible. HFCs, whatever their lifetimes, were considered in Sect. 2.2.

Sectoral emissions of SLCFs are derived from two sources: CEDS, which was used in the AR6 and in CMIP6 to assess historical evolution of atmospheric composition and that has been updated since then, and the Copernicus Atmosphere Monitoring Service (CAMS). The most recent release of the CEDS anthropogenic emissions dataset (Hoesly et al., 2025) covers the 1750-2023 period (Hoesly et al., 2018; Hoesly and Smith, 2024). Since 2023, CAMS has released regular updates of their global emission dataset (Soulie et al., 2023). For the year 2024, we apply, for each compound, the trend in emission from the CAMS dataset to the 2023 CEDS emission. The CAMS dataset is essentially based on the EDGARv6/v7 emissions as well as on CEDS, so CEDS and CAMS are not entirely independent. The temporal extension is based on evolution of drivers of emissions (energy consumption, production rates) and trends in technologies that affect the emissions factors (e.g. fleet renewal and abatement systems) (Denier van der Gon et al., 2023).

The CAMS v6.2 emission dataset (ECCAD, 2025) indicates a decrease in global anthropogenic emissions of the primary SLCFs (NOx, CO, NMVOCs, SO_2, BC and OC) since the COVID hiatus in emissions, except for NH_3,

whose emissions are steadily increasing. SLCF emissions from biomass burning are taken from GFED (van der Werf et al., 2017) with small fires (GFED4.1s) updated to 2024 (following AR6 WGIII (Dhakal et al., 2022)). Estimates from GFED for 2017 to 2024 are provisional and will be updated with GFED5 in future datasets which will provide substantially higher emissions for most species. The estimate of global carbon emissions due to wildfires in 2024 is slightly lower than in 2023 (both were higher than average fire years). These lower overall carbon emissions in 2024 hide an increase in CO_2 emissions (accompanied by an increase in NOx emissions) but a decrease in CH_4 and CO emissions accompanied by a decrease in carbonaceous aerosols and NMVOC emissions.

The decrease of global NOx emissions, despite very heterogeneous regional trends (Szopa et al., 2021), is confirmed by global NO_2 satellite observations from OMI (tropospheric NO_2 column from OMI visualised through the Giovanni system, Acker and Leptoukh, 2007). The trends in global CO concentration are less clear. Surface data from MOPITT and AIRS show a slight increase over the last three years. CO does not result solely from CO emissions but also from VOC including methane oxidation which can explain differences in trends between emissions and concentrations.

Overall, the trends in emissions were similar (see Supplement Sect. S4) over the 2020-23 period in the most recent CEDS dataset to our previous estimate (Forster et al., 2024) but with a lower post COVID rebound for NOx and SO_2. Regarding SO_2, the CEDS datasets (v2024_04_01 used in Forster et al., 2024 and v2025_03_18 used here) account for the introduction of strict fuel sulphur controls brought in by the International Maritime Organization in January 2020. Total SO_2 emissions in 2019 were 80.9 $TgSO_2$ (Table 2). The SO_2 emissions from international shipping declined by 8.4 $TgSO_2$ from 10.4 $TgSO_2$ in 2019 to 2.0 $TgSO_2$ in 2020, which is close to the expected 8.5 $TgSO_2$ reduction estimated by the International Maritime Organization. This decrease was estimated at 7.4 $TgSO_2$ in the previous CEDS version used in Forster et al. (2024). More generally, the reduction pace of the global SO_2 emission over the last ten years corresponds to that of the first ten years of the SSP scenarios assuming strong air pollution control (SSP1 and SSP5).

Using our combined estimate of GFED, and CEDS (with a 2024 extrapolation based on CAMS), emissions of all SLCFs were reduced in 2022 relative to 2019, but rebounded in 2023 and then slightly decreased in 2024 (relative to 2023) for all compounds except NOx whose increase is partly driven by increased emissions from biomass burning (Table 2 and Supplement Sect. S4). 2023 was a record year for emissions of organic carbon (driven again by a very active biomass burning season) and ammonia (driven by a steady background increase in agricultural sources, plus a contribution from biomass burning). Fires can be worsened by climate change, because of increased fire prone weather conditions (Burton et al., 2024). Strictly speaking, such fires could sometimes be considered as feedbacks and not be included in anthropogenic forcings. However, we choose to include fires in our tracking, as historical biomass burning emissions inventories have previously been consistently treated as an anthropogenic forcing (for example in CMIP6), though this assumption may need to be revisited in the future (see also discussion in Sect. 5). This differs from the treatment of accounting for CO_2 and CH_4 emissions at present (Sect. 2.2), where we do not include natural emissions

in the inventories. As described in Sect. 5, this treatment of all biomass burning emissions as a forcing has implications for several categories of anthropogenic radiative forcing.

Table 2 Emissions of the major SLCFs in 1750, 2019, and 2024 from a combination of CEDS and GFED. Emissions of SO_2+SO_4 use SO_2 molecular weights. Emissions of NO_x use NO_2 molecular weights. VOCs are for the total mass. Note that estimates for previous years have been revised and updated. WGI 2019 estimates from Smith et al. (2021).

Compound	SLCF emissions (Tg yr^{-1})				
	1750	2019 (WGI for ERF estimates)	2019 (updated)	2023 (updated)	2024 (updated)
Sulphur dioxide (SO_2) + sulfate (SO_4^{2-})	2.8	83.7	80.9	72.7	71.2
Black carbon (BC)	2.1	7.8	7.3	7.6	7.5
Organic carbon (OC)	15.5	29.8	33.0	41.0	36.1
Ammonia (NH_3)	6.6	64.9	66.3	72.7	70.6
Oxides of nitrogen (NO_x)	19.4	135.3	133.6	128.4	130.4
Volatile organic compounds (VOCs)	60.9	209.1	204.8	224.1	212.7
Carbon monoxide (CO)	348.4	855.0	816.1	896.0	845.3

Uncertainties associated with these emission estimates are difficult to quantify. From the non-biomass-burning sectors they are estimated to be smallest for SO_2 (±14 %), largest for black carbon (BC) (a factor of 2) and intermediate for other species (Smith et al., 2011; Bond et al., 2013; Hoesly et al., 2018). Relative uncertainties are also likely to increase both backwards in time (Hoesly et al., 2018) and again in the most recent years. Future updates of CEDS are expected to include uncertainties (Hoesly et al., 2018).

5 Effective radiative forcing (ERF)

ERFs were principally assessed in Chap. 7 of AR6 WGI (Forster et al., 2021), which focussed on assessing ERF from changes in atmospheric concentrations; it also supported estimates of ERF in Chap. 6 that attributed forcing to specific precursor emissions (Szopa et al., 2021) and generated the time history of ERF shown in AR6 WGI Fig. 2.10 and discussed in Chap. 2 (Gulev et al., 2021).

The ERF calculation follows the methodology used in AR6 WGI (Smith et al., 2021) as updated by Forster et al. (2024) and described in the Supplement Sect. S5). One methodological update is incorporated in IGCC 2024 for the ERF from land use surface reflection and irrigation (Supplement Sect. S5.4). For each category of forcing, a 100,000-member probabilistic Monte Carlo ensemble is sampled to span the assessed uncertainty range in each forcing. Uncertainties account for systematic, structured random and random components. All uncertainties are reported as 5 %–95 % ranges and provided in square brackets. The methods are all detailed in the Supplement, Sect. S5.

The summary results for the anthropogenic constituents of ERF and solar irradiance in 2024 relative to 1750 are shown in Fig. 5a. In Table 3 these are summarised alongside the equivalent ERFs from AR6 (1750–2019) and last year's Climate Indicators update (1750-2023). Fig. 5b shows the time evolution of ERF from 1750 to 2024.

Table 3 Contributions to anthropogenic effective radiative forcing (ERF) for 1750–2024 assessed in this section. Data is for single year estimates unless specified. All values are in watts per square metre (W m^{-2}), and 5 %–95 % ranges are in square brackets. As a comparison, the equivalent assessments from AR6 (1750–2019) and last year's Climate Indicators (1750-2023) are shown. Solar ERF is included and unchanged from AR6, based on the most recent solar cycle (2009–2019), thus differing from the single-year estimate in Fig. 5a. Volcanic ERF is excluded due to the sporadic nature of eruptions.

Forcer	1750-2019 [W m^{-2}] (AR6)	1750-2023 [W m^{-2}] (Forster et al., 2024)	1750-2024 [W m^{-2}]	Reason for change since last year
CO_2	2.16 [1.90 to 2.41]	2.28 [2.01 to 2.56]	2.33 [2.05 to 2.61]	Increases in GHG concentrations resulting from increases in emissions
CH_4	0.54 [0.43 to 0.65]	0.56 [0.45 to 0.68]	0.57 [0.45 to 0.68]	
N_2O	0.21 [0.18 to 0.24]	0.22 [0.19 to 0.26]	0.23 [0.20 to 0.26]	
Halogenated GHGs	0.41 [0.33 to 0.49]	0.41 [0.33 to 0.49]	0.41 [0.33 to 0.49]	
Ozone	0.47 [0.24 to 0.71]	0.51 [0.25 to 0.76]	0.50 [0.25 to 0.75]	
Stratospheric water vapour	0.05 [0.00 to 0.10]	0.05 [0.00 to 0.10]	0.05 [0.00 to 0.11]	

Aerosol-radiation interactions	-0.22 [-0.47 to +0.04]	-0.26 [-0.50 to -0.03]	-0.22 [-0.44 to +0.01]	Decrease in most aerosol and aerosol precursor emissions (Table 2)
Aerosol-cloud interactions	-0.84 [-1.45 to -0.25]	-0.91 [-1.80 to -0.27]	-0.85 [-1.65 to -0.25]	
Land use (surface albedo changes and effects of irrigation)	-0.20 [-0.30 to -0.10]	-0.20 [-0.31 to -0.10]	-0.19 [-0.30 to -0.05]	Separation of albedo and irrigation components; updated data source and methodology
Light-absorbing particles on snow and ice	0.08 [0.00 to 0.18]	0.08 [0.00 to 0.17]	0.08 [0.00 to 0.19]	
Contrails and contrail-induced cirrus	0.06 [0.02 to 0.10]	0.05 [0.02 to 0.09]	0.06 [0.02 to 0.10]	
Total anthropogenic	2.72 [1.96 to 3.48]	2.79 [1.78 to 3.61]	2.97 [2.05 to 3.77]	Increasing positive GHG forcing and decreasing negative aerosol forcing
Solar irradiance	0.01 [-0.06 to 0.08]	0.01 [-0.06 to 0.08]	0.01 [-0.06 to 0.08]	

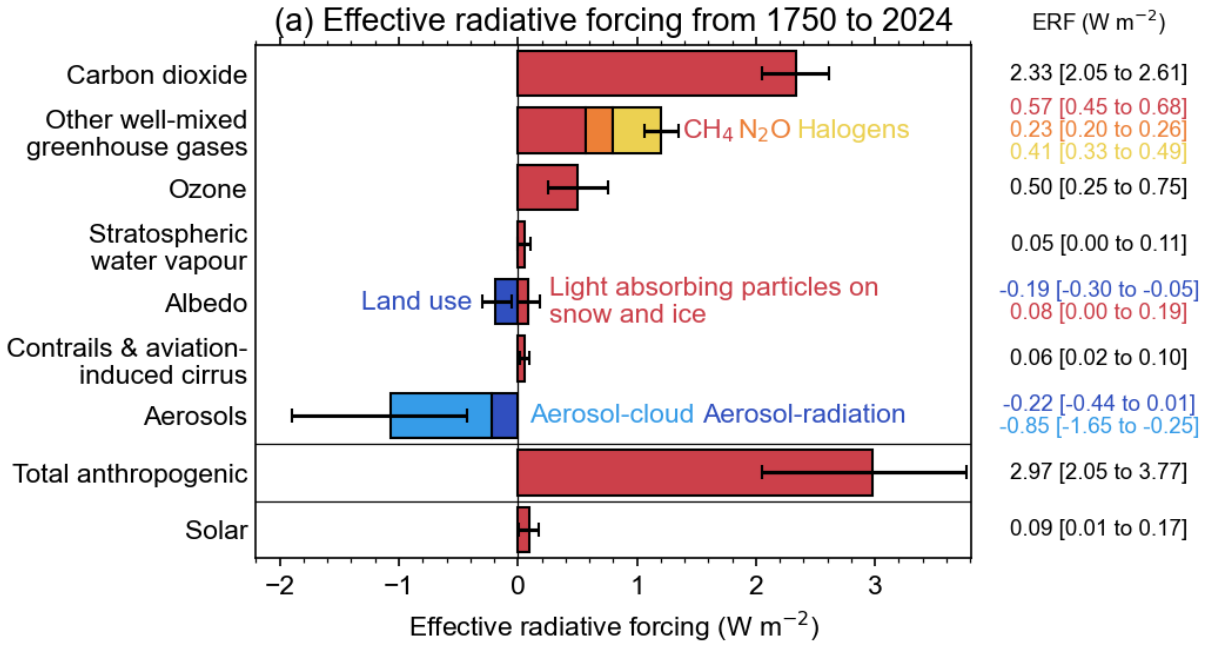

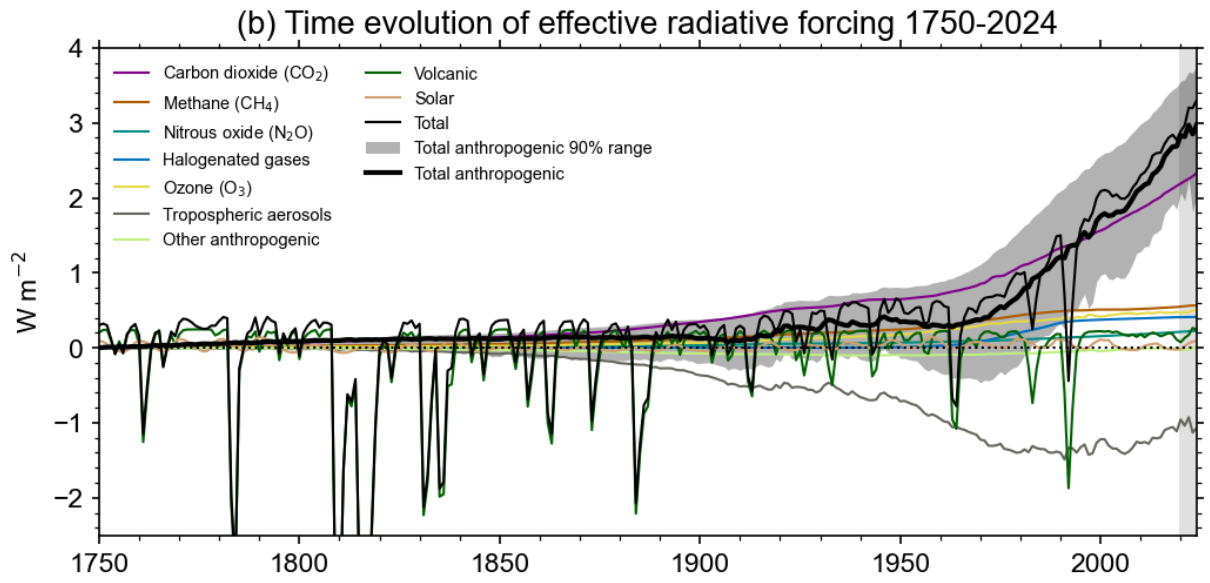

Figure 5 Effective radiative forcing (ERF) from 1750–2024. (a) 1750–2024 change in ERF, showing best estimates (bars) and 5 %–95 % uncertainty ranges (lines) from major anthropogenic components to ERF, total anthropogenic ERF and solar forcing. Note that solar forcing in 2024 is a single-year estimate and hence differs from Table 3. (b) Time evolution of ERF from 1750 to 2024. Best estimates from major anthropogenic categories are shown along with solar and volcanic forcing (thin coloured lines), total (thin black line), and anthropogenic total (thick black line). The 5 %–95 % uncertainty in the anthropogenic forcing is shown by grey shading.

Total anthropogenic ERF has increased to 2.97 [2.05 to 3.77] W m^{-2} in 2024 relative to 1750, compared to 2.72 [1.96 to 3.48] W m^{-2} for 2019 relative to 1750 in AR6. The ERF has increased considerably from the 2023 estimate of 2.79 [1.79 to 3.61] W m^{-2}. 2023 was a year associated with high biomass burning aerosol which resulted in a stronger negative aerosol forcing than recent trends. Biomass burning was also high in 2024, but lower than 2023 levels. Sulphur emissions from shipping have declined since 2020, weakening the aerosol ERF and adding around +0.1 W m^{-2} over 2020 to 2024 (see Sect. 7.2 and Supplement Sects. S5 and S7). The approach of including all biomass burning aerosols is consistent with reporting ERF based on concentration increase of GHGs independent of whether CO_2 and CH_4 are caused by anthropogenic emissions or a smaller part is caused by any feedbacks such as from biomass burning fires or wetlands. Changes in mineral dust and sea salt are not easily relatable to human activity and are not included in the ERF of aerosols.

The ERF from well-mixed GHGs is 3.54 [3.22 to 3.85] W m^{-2} for 1750–2024, of which 2.33 W m^{-2} is from CO_2, 0.57 W m^{-2} from CH_4, 0.23 W m^{-2} from N_2O and 0.41 W m^{-2} from halogenated gases. This is an increase of around 7% from 3.32 [3.03 to 3.61] W m^{-2} for 1750–2019 in AR6. ERFs from CO_2, CH_4 and N_2O have all increased since the AR6 WG1 assessment for 1750–2019, owing to increases in atmospheric concentrations.

The total aerosol ERF (sum of the ERF from aerosol–radiation interactions (ERFari) and aerosol–cloud interactions (ERFaci)) for 1750–2024 is −1.07 [−1.90 to −0.43] W m^{-2} compared to −1.18 [−2.10 to −0.49] W m^{-2} for 1750–2023 (Forster et al., 2024) and −1.06 [−1.71 to −0.41] W m^{-2} assessed for 1750–2019 in AR6 WGI. Attributing year-to-year trends to aerosol forcing is problematic due to the variability in biomass burning emissions. Increasing biomass burning emissions since AR6 have been mostly offset by a decrease in emissions from energy and industrial sectors, leading to best estimates of ERFari and ERFaci that are virtually unchanged from the 1750–2019 AR6 assessment to the 1750–2024 determination here (Table 3).

Ozone ERF is determined to be 0.50 [0.25 to 0.75] W m^{-2} for 1750–2024, slightly higher than the AR6 assessment of 0.47 [0.24 to 0.71] W m^{-2} for 1750–2019. This is due to the increase in emissions of some of its precursors (CO, VOC, CH_4), but this result is highly uncertain since consolidated ozone trends are not yet released. Stratospheric water vapour from methane oxidation is unchanged (to two decimal places) since AR6. ERF from light-absorbing particles on snow and ice being 0.08 [0.00 to 0.19] W m^{-2} for 1750–2024, like AR6. We determine from provisional data that aviation activity in 2024 has returned to pre-COVID levels (IATA, 2024). Therefore, ERF from contrails and contrail-induced cirrus is the same as in AR6, at 0.06 [0.02 to 0.10] W m^{-2} in 2024. The methodology to determine land-use ERF has been updated (Sect. S5.4) but this forcing has a similar best estimate to 2023 and AR6, with a wider uncertainty range that accounts for the separate assessment of irrigation forcing.

The headline assessment of solar ERF has not been re-assessed, at 0.01 [−0.06 to +0.08] W m^{-2} from pre-industrial to the 2009–2019 solar cycle mean (Table 3). Separate to the assessment of solar forcing over complete solar cycles, we provide a single-year solar ERF for 2024 of +0.09 [+0.01 to +0.17] W m^{-2} (Fig. 5a). This is higher than the single-year estimate of solar ERF for 2019 (a solar minimum) of −0.02 [−0.08 to 0.06] W m^{-2}.

Volcanic ERF is included in the overall time series (Fig. 5b) but following IPCC convention we do not provide a single-year estimate for 2024 given the sporadic nature of volcanoes. Alongside the time series of stratospheric aerosol optical depth derived from proxies and satellite products, for 2022–2024 we include the stratospheric water vapour contribution from the Hunga Tonga-Hunga Ha'apai (HTHH) eruption derived from Microwave Limb Sounder (MLS) data. We estimate a net positive (positive forcing from stratospheric water vapour more than outweighing negative forcing from stratospheric aerosols) forcing from HTHH through 2024 (Supplementary Material Sect. S5), though note that other studies find the net HTHH forcing to be negative (Gupta et al., 2025) or close to zero (Schoeberl et al., 2024).

6 Earth energy imbalance (EEI)

EEI, assessed in Chap. 7 of AR6 WGI (Forster et al., 2021), provides a measure of accumulated surplus energy (heating) in the climate system, and is hence an essential indicator to monitor the current and future status of global warming. It represents the difference between the radiative forcing acting to warm the climate, and Earth's radiative response, which acts to oppose this warming. Under stable climate conditions, i.e., in the absence of anthropogenic climate forcing, this difference would be balanced over interdecadal time scales. Since at least 1970 there has been a persistent imbalance in the energy flows that has led to excess energy being absorbed by the climate system (Forster et al., 2021). On annual and longer timescales, the global Earth heat inventory changes associated with EEI are dominated by the changes in global ocean heat content (OHC), which accounts for about 90 % of global heating since the 1970s (Forster et al., 2021). This planetary heating results in changes in all components of the Earth system such as sea-level rise, ocean warming, ice loss, rises in temperature and water vapor in the atmosphere, changes in ocean and atmospheric circulation, continental warming and permafrost thawing (e.g. Cheng et al., 2022; von Schuckmann et al., 2023a), with adverse impacts for ecosystems and human systems (Douville et al., 2021; IPCC, 2022).

On decadal timescales, changes in global surface temperatures (Sect. 5) can become decoupled from EEI by ocean heat rearrangement processes (e.g. Palmer and McNeall, 2014; Allison et al., 2020). Therefore, the increase in the Earth heat inventory arguably provides a more robust indicator of the rate of global change on interannual-to-decadal timescales (Cheng et al., 2019; Forster et al., 2021; von Schuckmann et al., 2023a). AR6 WGI found increased confidence in the assessment of change in the Earth heat inventory compared to previous IPCC reports due to observational advances and joint closure of the energy and global sea level budgets (Forster et al., 2021; Fox-Kemper et al., 2021).

AR6 estimated that EEI increased from 0.50 [0.32–0.69] $\mathrm{W\,m^{-2}}$ during the period 1971–2006 to 0.79 [0.52–1.06] $\mathrm{W\,m^{-2}}$ during the period 2006–2018 (Forster et al., 2021). The contributions to increases in the Earth heat inventory throughout 1971–2018 remained stable: 91 % for the full-depth ocean, 5 % for the land, 3 % for the cryosphere and about 1 % for the atmosphere (Forster et al., 2021). Two recent studies demonstrated independently and consistently that since 1960, the rate of warming of the world ocean is increasing at a relatively consistent pace of 0.15 ± 0.05 $\mathrm{W\,m^{-2}}$ per decade (Minière et al., 2023; Storto and Yang, 2024; Merchant et al., 2025), while the rate of warming for the land, cryosphere, and atmosphere has been increasing at rate of 0.013 ± 0.003 $\mathrm{W\,m^{-2}}$ per decade (Minière et al., 2023). The increase in EEI over the last several decades (Fig. 6) has also been reported by Cheng et al. (2019), von Schuckmann et al. (2020, 2023a), Loeb et al. (2021), Hakuba et al. (2021), Kramer et al. (2021), Raghuraman et al. (2021) and Minère et al. (2023). The observed increase in EEI over the most recent period (i.e. past 2 decades) are helping to drive exceptionally warm conditions (Sect. 7; Minobe et al., 2025). The increase in has been linked to rising concentrations of well-mixed GHGs and recent reductions in aerosol emissions (Sect. 5; Raghuraman et al., 2021; Kramer et al., 2021; Hansen et al., 2023), and to an increase in absorbed solar radiation associated with

decreased reflection by clouds and sea-ice and a decrease in outgoing longwave radiation (OLR) due to increases in trace gases and water vapor (Loeb et al., 2021; Goesling et al., 2025; Allan and Merchant, 2025).

We carry out an update to the AR6 estimate of changes in the Earth heat inventory based on updated observational time series for the period 1971–2020 (Table 4 and Fig. 6). Time series of heating associated with loss of ice and warming of the atmosphere and continental land surface are obtained from the recent Global Climate Observing System (GCOS) initiative (von Schuckmann et al., 2023b; Adusumilli et al., 2022; Cuesta-Valero et al., 2023; Vanderkelen and Thiery, 2022; Nitzbon et al., 2022; Kirchengast et al., 2022). We use the original AR6 time series ensemble OHC time series for the period 1971–2018 and then an updated five-member ensemble for the period 2019–2024. We "splice" the two sets of time series by adding an offset as needed to ensure that the 2018 values are identical. The AR6 heating rates and uncertainties for the ocean below 2000 m are assumed to be constant throughout the period. The time evolution of the Earth heat inventory is determined as a simple summation of time series of atmospheric heating; continental land heating; heating of the cryosphere; and heating of the ocean over three depth layers: 0–700, 700–2000 and below 2000 m (Fig. 6a). While von Schuckmann et al. (2023a) have also quantified heating of permafrost and inland lakes and reservoirs, these additional terms are small and not included here for consistency with AR6 (Forster et al., 2021).

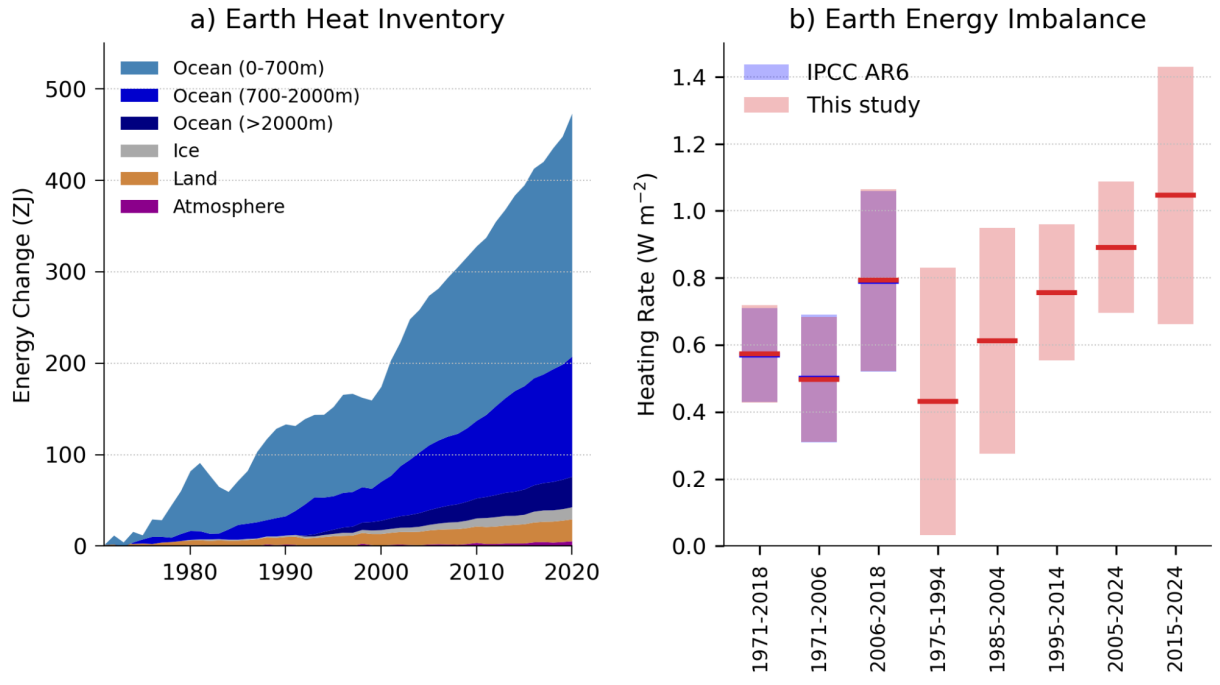

Figure 6 (a) Observed changes in the Earth heat inventory for the period 1971–2020, with component contributions as indicated in the figure legend. (b) Estimates of the Earth energy imbalance for the IPCC AR6 assessment periods, for consecutive 20-year periods and the most recent decade. Shaded regions indicate the *very likely* range (90 % to 100 % probability). Data use and approach are based on the AR6 methods and further described in Supplement Sect. S6. For the IPCC AR6 periods our assessment closely matches that in AR6. Note the periods in our assessment overlap with different IPCC AR6 periods.

In our updated analysis, we find successive increases in EEI for each 20-year period since 1975, with an estimated value of 0.43 [0.03 to 0.83] W m^{-2} during 1975–1994 that more than doubled to 0.89 [0.7 to 1.09] W m^{-2} during 2005–2024 (Fig. 6b). In addition, there is some evidence that the warming signal is propagating into the deeper ocean over time, as seen by a robust increase of ocean warming in the 700-2000m depth layer since the 1990s (von Schuckmann et al., 2020; 2023; Cheng et al., 2019, 2022). The model simulations qualitatively agree with the observational evidence (e.g. Gleckler et al., 2016; Cheng et al., 2019), further suggesting that more than half of the OHC increase since the late 1800s occurs after the 1990s.

The update of the AR6 assessment periods to end in 2024 results in systematic increases of EEI: 0.68 W m^{-2} during 1977–2024 compared to 0.57 W m^{-2} during 1971–2018; and 0.99 W m^{-2} during 2012–2024 compared to 0.79 W m^{-2} 2006–2018 (Table 4). The trend and interannual variability of EEI can largely be explained by a combination of surface temperature changes and radiative forcing (Hodnebrog et al., 2024). However, there was a jump in 2023 and 2024 which is still being investigated (see Sect. 7.2), but which is also discussed in the light of recent exceptional extreme climate conditions (Minobe et al., 2025).

Table 4 Estimates of the Earth energy imbalance (EEI) for AR6 and the present study.

Time Period	Earth energy imbalance (W m^{-2}). Square brackets [show 90% confidence intervals].	
	IPCC AR6	**This Study**
1971-2018	0.57 [0.43 to 0.72]	0.57 [0.43 to 0.72]
1971-2006	0.50 [0.32 to 0.69]	0.50 [0.31 to 0.68]
2006-2018	0.79 [0.52 to 1.06]	0.79 [0.52 to 1.07]
1977-2024	-	0.68 [0.52 to 0.85]

2012-2024	-	0.99 [0.70 to 1.28]

601

602 **7 Observed surface temperature change**

603 **7.1 Change since 1850-1900**

604 AR6 WGI Chap. 2 assessed the 2001–2020 globally averaged surface temperature change above an 1850–1900
605 baseline to be 0.99 [0.84 to 1.10] °C and 1.09 [0.95 to 1.20] °C for 2011–2020 (Gulev et al., 2021). Updated estimates
606 to 2013-2022 of 1.15 [1.00–1.25] °C were given in AR6 SYR (Lee et al., 2023), matching the estimate in Forster et
607 al. (2023).
608
609 There are choices around the methods used to aggregate surface temperatures into a global average, how to correct for
610 systematic errors in measurements, methods of infilling missing data, and whether surface measurements or
611 atmospheric temperatures just above the surface are used. These choices, and others, affect temperature change
612 estimates and contribute to their uncertainty (AR6 WGI Chap. 2, Cross Chap. Box 2.3, Gulev et al., 2021). The
613 methods chosen here closely follow AR6 WGI and are presented in the Supplement Sect. S7. Confidence intervals are
614 taken from AR6 as only one of the employed datasets regularly updates ensembles (see Supplement Sect. S7).
615
616 Based on the updates available as of March 2025, the change in global surface temperature from 1850–1900 to 2015–
617 2024 is presented in Fig. 7. These data, using the same underlying datasets (with some version changes: see
618 Supplement Sect. S7) and methodology as AR6, estimate 1.24 [1.11–1.35] °C of warming, an increase of 0.15 °C
619 within four years from the 2011–2020 value reported in AR6 WGI (Table 5), or 0.14 °C from the 2011–2020 value in
620 the most recent dataset version. The decade 2015-2024 was 0.31 °C warmer than the previous decade (2005–2014).
621 These changes, although amplified somewhat by the exceptionally warm years in 2023 and 2024, are broadly
622 consistent with typical warming rates over the last few decades, which were assessed in AR6 as 0.76 °C over the
623 1980–2020 period (using ordinary-least-square linear trends) or 0.019 °C per year (Gulev et al., 2021). They are also
624 broadly consistent with projected warming rates from 2001–2020 to 2021–2040 reported in AR6, which have a very
625 likely range between 0.016 °C per year and 0.036 °C per year under SSP2-4.5 (Lee et al., 2021, their Table 4.5), and
626 with human-induced warming rates discussed in Sect. 8.4.
627
628 Land temperatures have increased by 1.79 [1.56–2.03] °C from 1850-1900 to 2015-2024, and ocean temperatures by
629 1.02 [0.81-1.13] °C over the same period, implying that most land areas have already experienced more than 1.5 °C
630 of warming from the 1850–1900 period. As was the case for the periods reported in AR6, the ratio of observed land

to ocean warming is in the vicinity of 1.75, somewhat higher than the ratio of 1.5 [1.4–1.7] projected by the end of the century in CMIP6 models (AR6, their Table 4.2 and Section 4.5.1.1.1). The additional observed warming since 2020 in the most recent dataset versions (0.21 °C for land, 0.13 °C for ocean) has a ratio within the CMIP6 projections range.

Table 5 Estimates of global surface temperature change from 1850–1900 [*very likely* (90 %–100 % probability) ranges] for IPCC AR6 and the present study.

Time period	Temperature change from 1850-1900 (°C)	
	IPCC AR6 (as reported)	This study
Global, most recent 10 years	1.09 [0.95 to 1.20] (to 2011-2020)	1.24 [1.11 to 1.35] (to 2015-2024)
Global, most recent 20 years	0.99 [0.84 to 1.10] (to 2001-2020)	1.09 [0.93 to 1.20] (to 2005-2024)
Land, most recent 10 years	1.59 [1.34 to 1.83] (to 2011-2020)	1.79 [1.56 to 2.03] (to 2015-2024)
Ocean, most recent 10 years	0.88 [0.68 to 1.01] (to 2011-2020)	1.02 [0.81 to 1.13] (to 2015-2024)

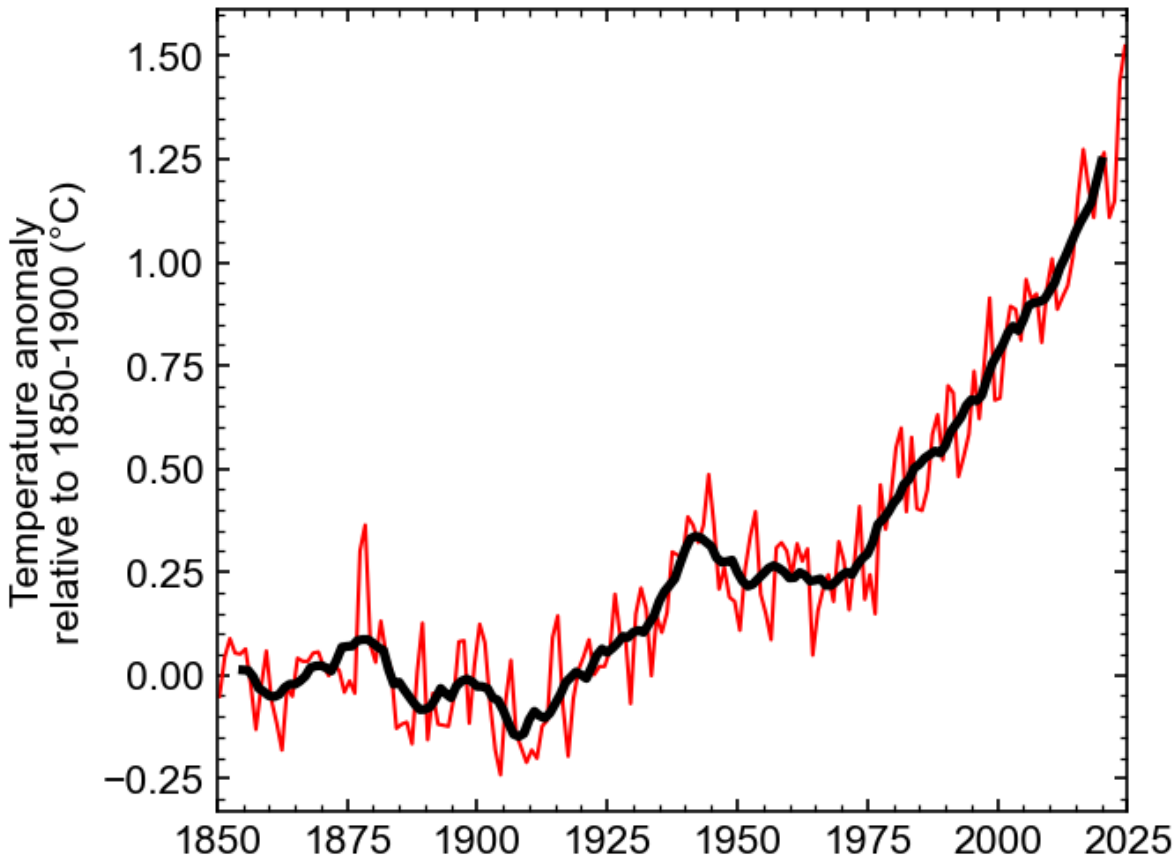

Figure 7 Annual (thin line) and decadal (thick line) means of global surface temperature (expressed as a change from the 1850–1900 reference period). Temperatures are based on an average of four datasets following AR6, see Supplement Sect. S7 for details.

7.2 2023-2024 global mean temperature -anomalies

At the time, 2023 set a new global annual-mean surface temperature change record, with a best estimate of 1.44 ºC, beating 2016 by 0.16 ºC. 2024 surpassed this, reaching 1.52 +/- 0.13 ºC; 2024, becoming the first calendar year since preindustrial more likely than not exceeding 1.5 ºC (Fig. 7). The assessed uncertainty range is based on that in AR6 WGI (Gulev et al., 2021). All four individual datasets are well inside the range (ranging from 1.46 to 1.56 ºC). Natural drivers and internal variability are expected to modulate human-caused warming at interannual-to-decadal timescales. 2024 is assessed to be 0.16 ºC warmer than the updated human-induced value (Table 6) while 2022 was 0.06 ºC colder. These values are not inconsistent with AR6, which estimated the effect of internal variability in any single year be +/- 0.25 ºC based on CMIP6 models, nor with the lower estimated ranges (+/- 0.17 ºC) when calculated from observational products (Trewin, 2022).

The probability of seeing an observed temperature of 1.52 ºC in 2024 considering a human-induced warming equal to 1.36 ºC is about 1 chance out of 6 (Fig. 8a). The methodology to calculate this probability consists in comparing the GSAT observed anomaly to those expected from CMIP6 models following the framework adopted in AR6 in Chapter 3 (Eyring et al., 2021) for decadal trends and adapted here for interannual time scale issues. The same probability but conditional to the fact that 2024 followed an El Niño year and that the Atlantic Multidecadal Variability (AMV) was in a positive phase (Supplement Sect. S7), rises to 1 chance out of 2. 2024 can therefore be treated as a "normal" year, i.e. very much expected at the actual human-caused global warming level when the internal modes of variability are taken into account and when assessed from a very large number of simulations from large ensembles. Based on the same calculation, we estimate that a year as warm as 2023 would occur once in 4 years at human-induced warming equal to 1.31 ºC (Fig. 8b). It drops to 1-in-14 [10-20, CI 5-95%] year event, i.e. a rare-to-exceptional event, when considering that 2023 followed a La Nina year and despite persistent positive AMV. Note that the probability of the large jump in global temperatures was increased by the fact that the El Niño followed an extended La Niña over 2020-2022 (Raghuraman et al., 2024). Within such a framework, 2022, that was colder than human-induced warming, could be interpreted as a normal/expected year considering that 2021 was a La Nina year and AMV positive (Fig. 8c). These results show that human induced warming combined with particular modes of natural variability shifts the odds of global surface temperatures passing 1.5 ºC, making it more likely. Sect. 8 has a fuller discussion of human induced warming.

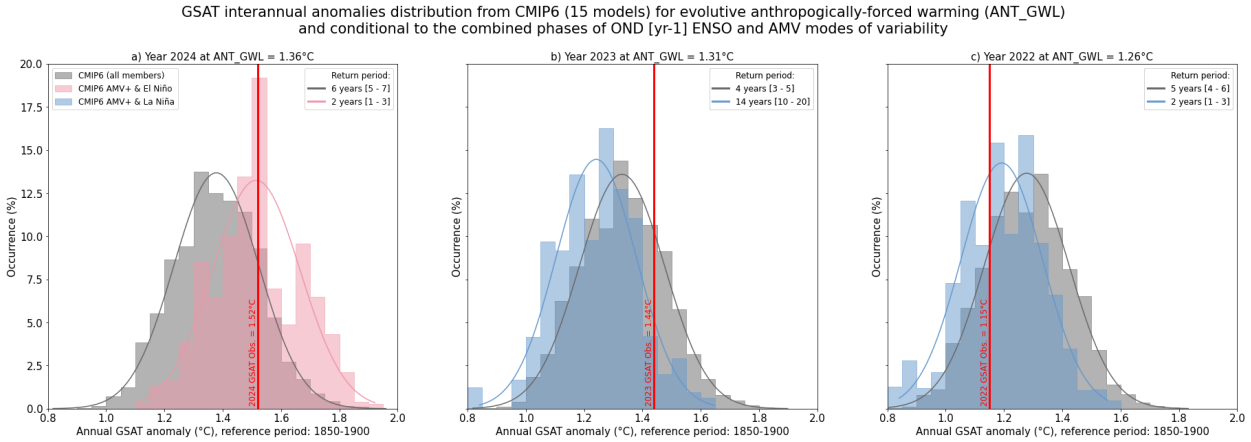

Figure 8 a) Gray histograms of global surface air temperature (GSAT) interannual anomalies estimated from 15 CMIP6 models extracted from all available SSP scenarios (~700 members) at anthropogenic global warming levels (ANT_GWL) corresponding to a) 2024, b) 2023, c) 2022. The red vertical bar stands for the observational consolidated GSAT annual anomalies (Sect. 7.1). The return period of the observed annual GSAT event estimated from the CMIP6 distribution is provided (upper-corner). Associated [5-95%] likely range is assessed through bootstrapping. Interannual anomalies are obtained following Trewin (2022) method over 10-yr sliding windows. Only models providing large-ensembles (n members >5) and having at least one member whose interannual variance of GSAT is compatible with observational estimates, are selected. Colored histograms stand for the same distribution but conditional to the combined phase of El Nino Southern Oscillation (ENSO) and Atlantic Multidecadal Variability (AMV). SST Anomalies for the modes of variability are calculated from the residual of SST obtained after removing the modelled forced response estimated as model ensemble mean. A year is considered as an El Nino/La Nina year if the (October-December) Oceanic Nino Index (ONI) index of the previous year is greater/lower than one standard deviation. A year is considered as an AMV+ year if the annual North Atlantic average SST is greater than one standard deviation. Light pink represents years when ONI and AMV are concomitantly positive and light-blue when ONI is negative.

The increase in global temperature between 2022 and 2023 and in particular in global sea surface temperature is exceptional based on model estimates accounting for projected known human and natural forcings plus internal variability (Rantanen and Laaksonen, 2024; Terhaar et al., 2025, Cattiaux et al., 2024). The La Niña-to-El Niño sequence is of key importance and has been likely reinforced by enhanced energy uptake due to multi-year persistence in the preceding La Niña. The temporal synchronicity between the modes of variability in all basins is hypothesized to have played a role in the jump (Minobe et al., 2025) with the North Atlantic being record warm (Guinaldo et al., 2025) and the austral sea ice extent being record low (Purish and Doddridge, 2023).

Possible specific causes beyond internal variability, many of which are already accounted for in the estimated human-induced warming level, have been postulated e.g.: International Maritime Organization rules on shipping fuel sulphur content that came into force in January 202l; the eruption of Hunga Tonga Hunga Ha'apai in January 2022 and other subsequent smaller volcanic activity; and a faster-than-expected onset of Solar Cycle 25 (see Supplement Section S7 for details and references). A key diagnostic of these changes including both external forcing and internal variability was the exceptional magnitude of the net energy increase into the Earth system from mid-2022 to mid-2023, driven in large part by the reduced reflectance and greater absorption of solar radiation (Hodnebrog et al., 2024; Goessling et al., 2024; Minobe et al. 2025; Allan and Merchant, 2025), which may be influenced by cloud feedbacks (Tselioudis et al., 2024) as well as surface reflectance and atmospheric composition change (see also Sect. 6).

Our analysis, detailed in Supplement Sect. S7, makes use of estimates of variability and radiative forcing contributions and their uncertainty based on Sect 5. and the published literature. It shows that the increase in 2023 and 2024 compared to previous years could be explained by a combination of factors. In summary, our analyses show that, although the relative weight between the physical processes in explaining the high surface temperatures remain to be

712 better quantified, the 2023 and 2024 observed temperatures are not inconsistent with the level of human induced
713 warming assessed next, in Sect. 8.
714

715 **8 Human contribution to surface temperature change**

716 Human-induced warming, also known as anthropogenic warming, refers to the component of observed global surface
717 temperature increase attributable to both the direct and indirect effects of human activities, which are typically grouped
718 as follows: well-mixed GHGs (consisting of CO_2, CH_4, N_2O and F-gases) and other human forcings (consisting of
719 aerosol–radiation interaction, aerosol–cloud interaction, black carbon on snow, contrails, ozone, stratospheric H_2O
720 and land use) (Eyring et al., 2021). The remaining contributors to total warming are natural: consisting of both natural
721 forcings (such as solar and volcanic activity) and internal variability of the climate system (such as variability related
722 to El Niño/La Nina events).
723
724 An assessment of human-induced warming was provided in two reports within the IPCC's Sixth Assessment cycle:
725 first in SR1.5 in 2018 [Chap. 1 Sect. 1.2.1.3 and Fig. 1.2 (Allen et al., 2018), summarised in the Summary for
726 Policymakers (SPM) Sect. A.1 and Fig. SPM.1 (IPCC, 2018)] and second in AR6 in 2021 [WGI Chap. 3 Sect. 3.3.1.1.2
727 and Fig. 3.8 (Eyring et al., 2021), summarised in the WGI Summary for Policymakers (SPM) Sect. A.1.3 and Fig.
728 SPM.2 (IPCC, 2021b)], and quoted again without any updates in SYR [Sect. 2.1.1 and Fig. 2.1 (IPCC,2023a) and
729 SYR Summary for Policymakers (SPM) Sect. A.1.2. (IPCC 2023b)].

730 **8.1 Warming period definitions in the IPCC Sixth Assessment cycle**

731 Temperature increases are defined relative to a baseline; IPCC assessments typically use the 1850–1900 average
732 temperature as a proxy for the climate in pre-industrial times, referred to as the period before 1750, even though a
733 small amount of warming likely occurred over 1750-1850 (see AR6 WGI Cross Chapter Box 1.2). Temperatures in
734 the IPCC were reported as either GMST or GSAT, see Supplement Sect. 8.1 for details.
735
736 Tracking progress towards the long-term global goal to limit warming, in line with the Paris Agreement, requires the
737 assessment of both what the current level of global surface temperatures are and whether a level of global warming,
738 such as 1.5 °C, is being reached. Definitions for these were not specified in the Paris Agreement, and several ways of
739 tracking levels of global warming are in use; here we focus on those adopted within AR6. When determining whether
740 warming thresholds have been passed, both AR6 and SR1.5 adopted definitions that depend on future warming; in
741 practice, levels of current warming were therefore reported in AR6 and SR1.5 using additional definitions that
742 circumvented the need to wait for observations of the future climate, as described next. AR6 defined crossing-time for
743 a level of global warming as the midpoint of the first 20-year period during which the average *observed* warming for
744 that period exceeds that level of warming (see AR6 WGI Chapter 2 Box 2.3) (the level of warming for a given year
745 defined in this way is therefore not known until 10 years after that year). AR6 therefore reported current levels of both

observed and *human-induced* warming as their averages over just the most recent 10 years (which gives warming that lags by only 5 years instead of 10 years) (see AR6 WGI Chapter 3 their Sect. 3.3.1.1.2); we refer to this definition as the "AR6 decade-average" warming. SR1.5 defined the level of warming in a given year as the average *human-induced* warming, in GMST, of a 30-year period centred on that year; when the given year is the *current* year, SR1.5 specified that the future 15 years (required for the mean) are revealed by extrapolating the multidecadal trend (see SR1.5 Chapter 1, their Sect. 1.2.1); we refer to this definition as the "SR1.5 trend-based" warming. If the multidecadal trend is interpreted as being linear (which it has been very close to over recent decades), this definition of current warming is equivalent to the end-point of the trend line through the most recent 15 years of human-induced warming, and therefore provides a definition of warming for the current year that depends only on historical warming. This interpretation produces results that in recent years have been identical (or extremely close) to the current annual mean value of human-induced warming (see results in Sect. 8.2, and Supplement Sect. S8.3), so in practice the attribution assessment in SR1.5 was based not on the trend-based definition, but on the simple annual-year attributed warming; we refer to this definition as the "SR1.5 annual-mean" warming. A diagram of these three definitions is given in Supplement Fig. S11.

8.2 Updated assessment approach of human-induced warming to date

This paper provides an update of the AR6 WGI and SR1.5 human-induced warming assessments including, for completeness, all three definitions (AR6 decade-average, SR1.5 trend-based single year, and SR1.5 annual-mean single year). The 2024 updates in this paper follow the same methods and process as the 2022 and 2023 updates provided in Forster et al. (2023, 2024). Global mean surface temperature (GMST) is adopted as the definition of global surface temperature (see Supplement Sect. S8.1). The three attribution methods used in AR6 are retained: the Global Warming Index (GWI) (building on Haustein et al., 2017), regularised optimal fingerprinting (ROF) (as in Gillett et al., 2021) and kriging for climate change (KCC) (Ribes et al., 2021). Details of each method, their different uses in SR1.5 and AR6, and any methodological changes, are provided in Supplement Sect. S8.2; method-specific results are also provided in Supplement Sect. S8.3. The overall estimate of attributed global warming for each definition (decade-average, trend-based, and annual-mean), is based on a multi-method assessment of the three attribution methods (GWI, KCC, ROF); the best estimate is given as the 0.01 °C-precision mean of the 50th percentiles from each method, and the *likely* range is given as the smallest 0.1 °C-precision range that envelops the 5th to 95th percentile ranges of each method. This assessment approach is identical to last year's update (Forster et al. (2024)); it is directly traceable to and fully consistent with the assessment approach in AR6, though it has been lightly extended in ways that are explained in Supplement Sect. S8.4.

Results are summarised in Table 6 and Fig. 9. Method-specific contributions to the assessment results, along with time series, are given in the Supplement, Sect. S8.3. Where results reported in GSAT differ from those reported in GMST (see Supplement Sect. S8.1), the additional GSAT results are given in Supplement Sect. S8.3.

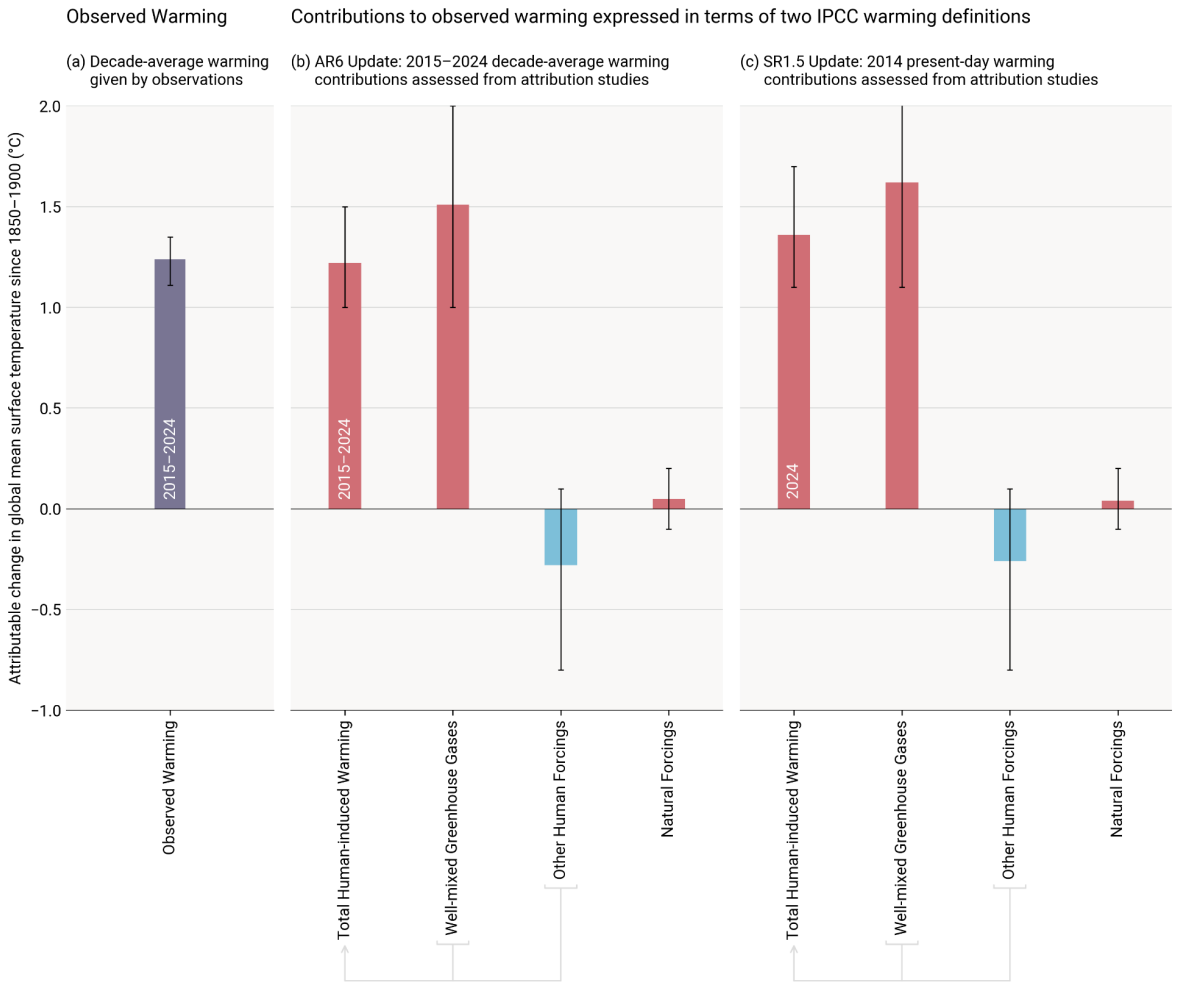

Figure 9 Updated assessed contributions to observed warming relative to 1850–1900; see AR6 WGI SPM.2. Results for all time periods in this figure are calculated using updated datasets and methods. The 2015–2024 average and 2024 results are this year's updated assessments for AR6 and SR1.5, respectively. Panel (a) shows updated observed global warming from Sect. 7, expressed as total global mean surface temperature (GMST), due to both anthropogenic and natural influences. Whiskers give the "*very likely*" range. Panels (b) and (c) show updated assessed contributions to warming, expressed as global mean surface temperature (GMST), from natural forcings and total human-induced forcings, which in turn consist of contributions from well-mixed GHGs and other human forcings. Whiskers give the "*likely*" range. Changes to warming levels since the IPCC sixth assessment cycle are depicted in Supplement Fig. S10.

Table 6 Updates to assessments in the IPCC 6th assessment cycle of warming attributable to multiple influences. Estimates of warming attributable to multiple influences, in °C, relative to the 1850–1900 baseline period. Results are given as best estimates, with the *likely* range in brackets, and reported as global mean surface temperature (GMST). Results from the IPCC 6th assessment cycle, for both AR6 and SR1.5, are quoted in columns labelled (i) and are compared with repeat calculations in columns labelled (ii) for the same period using the updated methods and datasets to see how methodological and dataset updates alone would change previous assessments. Assessments for the updated periods are reported in columns labelled (iii). * Updated GMST observations, quoted from Sect. 7 of this update, are marked with an asterisk, with "*very likely*" ranges given in brackets. ** In AR6 WGI, best-estimate values were not provided for warming attributable to well-mixed GHGs, other human forcings and natural forcings (though they did receive a "*likely*" range); for comparison, best estimates (marked with two asterisks) have been retrospectively calculated in an identical way to the best estimate that AR6 provided for anthropogenic warming (see discussion in Supplement Sect. S8.4.1). * The SR1.5 assessment drew only on GWI rounded to 0.1°C precision, whereas the repeat and updated calculations use the updated multi-method assessment approach.**

Estimates of warming attributable to multiple influences, in °C, relative to the 1850–1900 baseline period
Results are given as best estimates, with the *likely* range in brackets, and reported as Global Mean Surface Temperature (GMST).

Definition ➡	**(a) IPCC AR6 Attributable Warming Update**			**(b) IPCC SR1.5 Attributable Warming Update**		
	Value for decade (average of previous 10-year period)			*Value for single year (30-year mean centred on current year)*		
Period ➡	**(i) 2010-2019** *Quoted from AR6 Chapter 3 Sect. 3.3.1.1.2 Table 3.1 for attributed warming, and Cross-chapter Box 2.3 Table 1 for observed warming*	**(ii) 2010-2019** *Repeat calculation using the updated methods and datasets*	**(iii) 2015-2024** *Updated value using updated methods and datasets*	**(i) 2017** *Quoted from SR1.5 Chapter 1 Sect. 1.2.1.3*	**(ii) 2017** *Repeat calculation using the updated methods and datasets*	**(iii) 2024** *Updated value using updated methods and datasets*
Component ⬇️						
Observed	1.06 [0.92 to 1.17]	1.07 [0.89 to 1.22] *	1.24 [1.11 to 1.35] *	-	-	1.52 [1.39 to 1.65]
Anthropogenic	1.07 [0.8 to 1.3]	1.09 [0.9 to 1.3]	1.22 [1.0 to 1.5]	1.0 [0.8 to 1.2] ***	1.13 [0.9 to 1.3]	1.36 [1.1 to 1.7]
Well-mixed GHGs	1.40** [1.0 to 2.0]	1.40 [1.0 to 1.9]	1.51 [1.0 to 2.0]	N/A	1.45 [1.0 to 1.9]	1.62 [1.1 to 2.1]
Other human forcings	-0.32** [-0.8 to 0.0]	-0.30 [-0.8 to 0.1]	-0.28 [-0.8 to 0.1]	N/A	-0.31 [-0.8 to 0.1]	-0.26 [-0.8 to 0.1]

Natural forcings	0.03** [-0.1 to 0.1]	0.05 [-0.1 to 0.2]	0.05 [-0.1 to 0.2]	N/A	0.05 [-0.1 to 0.2]	0.04 [-0.1 to 0.2]

The repeat calculations for attributable warming in 2010–2019 exhibit good correspondence with the results in AR6 WGI for the same period (see also Supplement, Sect. S8). The repeat calculation for the level of attributable anthropogenic warming in 2017 is about 0.1 ºC larger than the estimate provided in SR1.5 for the same period, resulting from changes in methods and observational data (see AR6 WGI Chapter 2 Box 2.3). The updated results for warming contributions in 2024 are higher than in 2017 due also to 7 additional years of increasing anthropogenic forcing. Note also that the SR1.5 assessment only used the GWI method, whereas these annual updates apply the full AR6 multi-method assessment (see Supplement Sect. S8.4 for details and rationale).

In this 2025 update, we assess the 2015–2024 decade average human induced-warming at 1.22 [1.0 to 1.5] °C, which is 0.15°C above the AR6 assessment for 2010–2019. The single year average human-induced warming is assessed to be 1.36 [1.1 to 1.7] °C in 2024 relative to 1850–1900. In general, these forced warming levels have evolved steadily and predictably in line with the current warming rate within uncertainty. The uncertainty range for the single-year level of anthropogenic warming already included 1.5 °C in previous years' assessments, and for the first time this year also lies at the edge of the uncertainty range for the (lagged) decade mean definition. The single-year anthropogenic warming best estimate is well below the observed best estimate for 2024 (1.52 °C, see Sect. 7), but note that the best estimate and lower uncertainty for observed warming lies within the uncertainty for single-year anthropogenic warming from each of the three attribution methods (see Supplement Table S5), whereas the upper uncertainty range of observed warming lies above the range for anthropogenic warming for the two attribution methods that fully exclude internal variability.

The best estimates for decade-average and single-year human-induced warming are 0.04 °C and 0.05 °C respectively above the value estimated in the previous update for the year 2023 (Forster et al., 2024), but should not be interpreted as a substantive increase in the rate of forced anthropogenic warming, as the rate increase is well within uncertainty ranges (Sect. 8.3).

AR6 found that, averaged for the 2010–2019 period, essentially all observed global surface temperature change was human-induced, with solar and volcanic drivers and internal climate variability making a negligible contribution. This conclusion remains the same for the 2015–2024 period. Generally, whatever methodology is used, on a global scale, the best estimate of the current level of human-induced warming is (within uncertainty) similar to the observed global surface temperature change (Table 6).

8.3 Rate of human-induced global warming

Estimates of the human-induced warming rate follow the same methodology as in the previous year's update (a rolling 10-year linear trend in attributed anthropogenic warming). A full description of the approach can be found in the Supplement Sect. S8.5. The rate of increase in attributed anthropogenic warming over time is distinct from the rate of increase in the observed global surface temperature, which is also affected by internal variability such as El Niño and natural forcings such as volcanic activity (see discussions in Sect. 7.2). The rate of anthropogenic warming we estimate here is driven by the rate of change of anthropogenic ERF (Sect. 5), with variations in the climate forcing trend over time correlating with variations in the rate of attributed warming (Fig. 10).

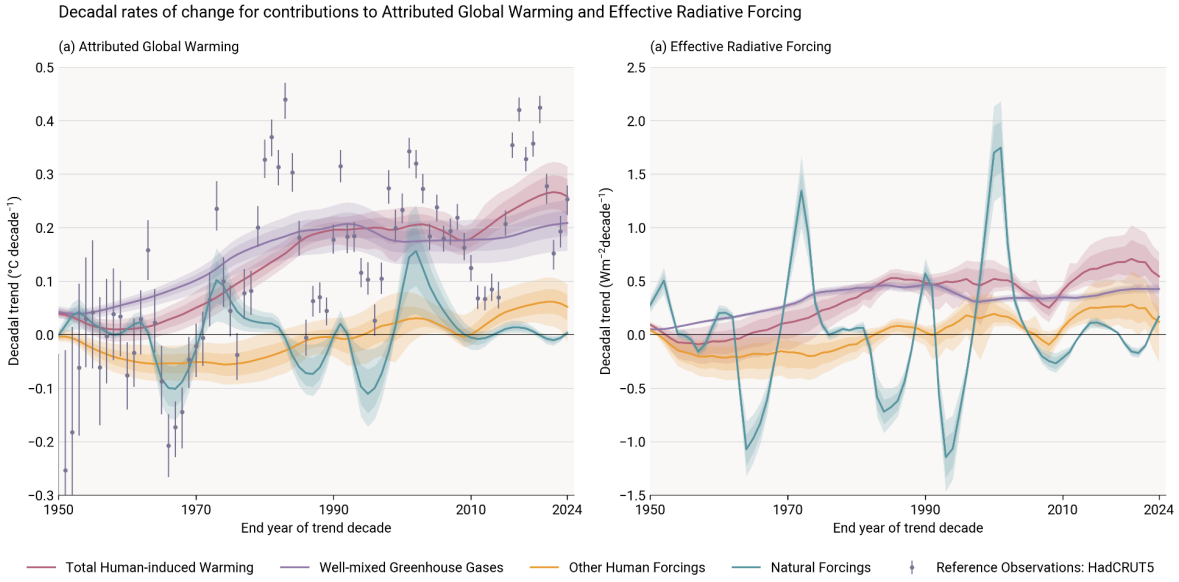

Figure 10 Rates of (a) attributable warming (global mean surface temperature (GMST)) and (b) effective radiative forcing. The attributable warming rate time-series are calculated using the Global Warming Index method with full ensemble uncertainty. The observed GMST rates included for reference are also calculated with uncertainty from the HadCRUT5 ensemble, and, for consistency with the attributed warming rates, do not include standard regression error, which, for observed warming, would increase the size of the error bars. The effective radiative forcing rates are calculated using a representative 1000-member ensemble of the forcings provided in Sect. 5 of this paper. The depicted rates are the decadal rates, with the end year of the decade in question being the value given on the time axis.

Estimates for the trend derived from the three warming attribution methodologies are presented in Table 7, with results for individual attribution methods detailed in the Supplement Table S6. The GWI (based on observed warming and forcing) and KCC (based on CMIP simulations) methodologies report results that are in close agreement, while estimates derived with the ROF method (also based on CMIP simulations) are more strongly influenced by residual internal variability that remains in the anthropogenic warming signal due to the limitations in size of the available

CMIP ensemble. The median result is presented at 0.01 °C/decade precision for the overall multi-method rate of warming assessment.

An overall best estimate attributed rate of human-induced warming of 0.27 °C/decade is found for the decade 2015–2024. This increased rate relative to the 0.2 °C/decade AR6 assessment is broken down in the following way: (i) 0.03 °C/decade from changing the rounding precision (updating the AR6 2010-2019 warming rate assessment from 0.2 to 0.23 °C/decade), (ii) 0.03 °C/decade is due to methodological and dataset updates (updating the 2010–2019 warming rate from 0.23 °C/decade to 0.26 °C/decade; including the effect of adding 5 additional observed years to the attribution over the entire historical period), and (iii) 0.01 °C/decade due to a real increase in rate for the 2015–2024 period since the 2010–2019 period (updating 0.26 °C/decade for 2010–2019 to 0.27 °C/decade for 2015–2024), consistent with increased GHG emissions over the last decade. The spread of rates across the three attribution methods remains similar to their spread in AR6, and previous updates of this work, and hence does not support a decrease in the headline uncertainty range. However, as previous assessments suggested, we update the uncertainty range for the rate of human-induced warming from [0.1–0.3] °C/decade in AR6 to [0.2–0.4] °C/decade to better reflect the closer agreement of the 5% floors and the larger spread in the 95% ceilings of the three methods, and higher rate from the ROF method. The rate of human-induced warming for the 2015-2024 decade is concluded to be 0.27 °C/decade with a range of [0.2–0.4] °C/decade). This agrees with the decadal trend in observed warming of 0.26 °C per decade (also calculated as a linear trend through 10-year periods - see Sect. 7.1). It is important to note, however, that internal variability leads to the decadal rates of observed warming being far less stable than for anthropogenic warming, and the very close correspondence between the two this year is somewhat incidental (see Fig. 10).

Table 7 Updates to the IPCC AR6 rate of human-induced warming. Results for each method are given in the Supplement Table S6; assessment results are given as a best estimate with *likely* range in brackets. Results from AR6 WGI (Ch.3 Sect. 3.3.1.1.2 Table 3.1) are quoted in column (i), and compared with a repeat calculation using the updated methods and datasets in column (ii), and finally updated for the 2015-2024 period in column (iii). The AR6 assessment result was identical to the SR1.5 assessment result, though the latter was based on a different set of studies and timeframes. * Note that for clarity and ease of comparison with this year's updated assessment, the assessed rate in column (i) both quotes the assessment from AR6 and retrospectively applies the median approach adopted in this paper. The observed rates are calculated using the multi-dataset observed temperature dataset from Sect. 7; no ensemble is available for this, hence the absence of an uncertainty range.

Estimates of anthropogenic warming rate, in °C per decade Results are given as best estimates, with brackets giving the *likely* range for the assessments, and 5-95% uncertainty for the individual methods			
Definition ➡	**IPCC AR6 Anthropogenic Warming Rate Update** *Linear trend in anthropogenic warming over the trailing 10-year period*		
Period ➡	**(i) 2010-2019** *Quoted from AR6 Chapter 3 Sect. 3.3.1.1.2 Table 3.1*	**(ii) 2010-2019** *Repeat calculation using the updated methods and datasets*	**(iii) 2015-2024** *Updated value using updated methods and datasets*
Anthropogenic Warming Rate Assessment	Quoted from AR6: 0.2 [0.1 to 0.3]	0.26 [0.2 to 0.4]	0.27 [0.2 to 0.4]

	Using the median approach: 0.23 [0.1 to 0.3] *		
Observed		0.37	0.26

9 Remaining Carbon Budget

AR5 (IPCC, 2013) assessed that long-term global surface temperature increase caused by CO_2 emissions is close to linearly proportional to the total amount of cumulative CO_2 emissions (Collins et al., 2013). The most recent AR6 report reaffirmed this assessment and highlights that this near-linear relationship also holds between cumulative CO_2 emissions and maximum global surface temperature increase caused by CO_2 (Canadell et al., 2021). This near-linear relationship implies that for keeping global warming below a specified temperature level, one can estimate the total amount of CO_2 that can ever be emitted. When expressed relative to a recent reference period, this is referred to as the remaining carbon budget (Rogelj et al., 2018).

AR6 assessed the remaining carbon budget (RCB) in Chap. 5 of its WGI report (Canadell et al., 2021) for warming limits ranging from 1.3 to 2.4 °C relative to the 1850-1900 period (see Table 5.8 in Canadell et al., 2021). A selection of these (1.5, 1.7, and 2 °C) were also reported in its Summary for Policymakers (Table SPM.2, IPCC, 2021b). These RCB values are updated in this section using the same method as last year (Forster et al., 2024). Data for four warming limits (1.5, 1.6, 1.7 and 2 °C) are included in Table 8 while figures for more values are included in the Supplement Sect. S9.

The RCB is estimated by application of the WGI AR6 method described in Rogelj et al. (2019), which involves the combination of the assessment of five factors: (i) the amount of human-induced warming for the most recent decade (given in Sect. 8), (ii) the transient climate response to cumulative emissions of CO_2 (TCRE), which quantifies the linear proportionality between cumulative CO_2 emissions and CO_2-induced warming (iii) the zero emissions commitment (ZEC), representing the expected amount of additional (at present unrealized) warming caused by past CO_2 emissions (iv) the temperature contribution of future non-CO_2 emissions and (v) an adjustment term for Earth system feedbacks that are otherwise not captured through the other factors. AR6 WGI reassessed all five terms (Canadell et al., 2021). Lamboll et al. (2023) further considered the temperature contribution of non-CO_2 emissions and integrated different uncertainties, while Rogelj and Lamboll (2024) clarified the reductions in non-CO_2 emissions that are assumed in the RCB estimation.

The RCB for 1.5, 1.6, 1.7 and 2 °C warming levels is re-assessed based on the most recent available data. Estimated RCBs are reported in Table 8. They are expressed relative to the start of 2025 for estimates based on the 2015–2024

human-induced warming update (Sect. 8). Based on the variation in non-CO_2 emissions across the scenarios in AR6 WGIII scenario database, the estimated RCB values can be higher or lower by around 200 $GtCO_2$ depending on how successful non-CO_2 emissions reductions are (Lamboll et al., 2023; Rogelj and Lamboll, 2024). Notably, RCB estimates consider the subset of non-CO_2 emission scenarios in the AR6 WGIII database that are aligned with a global transition to net zero CO_2 emissions (Lamboll et al., 2023; Rogelj and Lamboll, 2024). These estimates assume median reductions in non-CO_2 emissions between 2020–2050 of CH_4 (about 50 %), N_2O (about 20 %) and SO_2 (about 80 %) (see Supplement, Sect. S9 and Table S7 and (Rogelj and Lamboll, 2024)). If these non-CO_2 GHG emission reductions are not achieved, the RCB for all temperature targets would be smaller than the values reported here in Table 8 (see Lamboll et al., 2023, Rogelj and Lamboll, 2024).

Compared to RCB values reported in AR6, our estimates here are smaller owing to several factors. First, AR6 budgets were expressed from 2020 onwards, and approximately 200 $GtCO_2$ have been emitted between 2020 and 2024. Second, we use updated physical models of non-CO_2 forcing which lead to an increased estimate of the importance of aerosols that are expected to decline with time in low emissions pathways (Rogelj et al., 2014; Rogelj and Lamboll, 2024). This decreased negative forcing from aerosols is expected to cause additional net non-CO_2 warming because more non-CO_2 GHG warming is being unmasked and this decreases the RCB (Lamboll et al., 2023) by slightly over 100 $GtCO_2$. There was also a small reduction in the budget (about 10 $GtCO_2$) from using the newer AR6 scenario set. Finally, the updated warming estimate reported in Sect. 8 is slightly increased due to the high observed temperatures in the last few years, which resulted in a further reduction of the budget by around 40 $GtCO_2$, relative to values reported in last year's assessment (Forster et al. 2024). This gives a total reduction in RCB values estimated from the beginning of 2025 of ~370 $GtCO_2$ compared to the values from 2020 reported in AR6.

Table 8 Updated estimates of the remaining carbon budget for 1.5, 1.6, 1.7 and 2.0 °C, for five levels of likelihood, considering only uncertainty in TCRE. Estimates are expressed relative to the start of 2024. The probability includes only the uncertainty in how the Earth immediately responds to CO_2 emissions (TCRE), not long-term committed warming or uncertainty in the climate response to other non-CO_2 emissions. All values are rounded to the nearest 10 $GtCO_2$. Additional values can be found in the Supplement Tables S7 and S8.

Temperature (°C)	Estimated remaining carbon budgets from the beginning of 2025 ($GtCO_2$)				
Avoidance probability:	17%	33%	50%	67%	83%
1.5	320	200	130	80	30
1.6	620	420	310	240	160
1.7	910	640	490	390	290

2.0	1790	1310	1050	870	690

This year's update of the 1.5 °C budget uses the historical warming level for the 2015-2024 period of 1.24 °C, with 0.11 °C future contribution of non-CO_2 warming. Assuming a median TCRE estimate of 0.45 °C per 1000 $GtCO_2$ this gives around 340 $GtCO_2$ from the midpoint of the period, from which we subtract around 210 $GtCO_2$ (204 $GtCO_2$ that were already emitted from the middle until the end of the 2015-2024 period, and 7 $GtCO_2$ that represents the median estimate of the impact of Earth systems feedbacks such as permafrost feedback that would otherwise not be covered). The same method is used to calculate budgets for the other warming levels.

The values in Table 8 are all greater than zero, implying that we have not yet emitted the amount of CO_2 that would commit us to these levels of warming. However, including the uncertainty in ZEC (as in the Supplement Table S8), non-CO_2 emission and forcing uncertainty, and underrepresented Earth-system feedbacks results in negative RCB estimates for limiting warming to low temperature limits with high likelihood. A negative RCB for a specific temperature limit would mean that the world is already committed to this amount of warming, and that net negative emissions would therefore be required to return to the temperature limit after a period of overshoot. The assumption behind such a calculation is that we can treat the warming impact of positive and negative net emissions as approximately symmetric. While the claim of symmetry is likely valid for small emissions values, some model studies have shown that it holds less well for reversal of larger emissions (Canadell et al., 2021, Zickfeld et al., 2021, Vakilifard et al., 2022, Pelz et al., 2025) As such, larger exceedances of the RCB for a particular temperature target would decrease the likelihood that the temperature target could still be achieved by an equivalent amount of net negative emissions.

Note that the 50 % RCB estimate of 130 $GtCO_2$ would be be exhausted in a little more than 3 years if global CO_2 emissions remain at 2024 levels (42 $GtCO_2$/yr, see Table 1). This is not expected to correspond exactly to the time that 1.5 °C global warming level is reached due to uncertainty associated with committed warming from past CO_2 emissions (the ZEC) as well as ongoing warming and cooling contributions from non-CO_2 emissions. For comparison, our estimate of 2024 anthropogenic warming (1.36 °C) and the recent rate of increase (0.27 °C/decade) would suggest that continued emissions at current levels would cause human-induced global warming to reach 1.5°C in approximately 5 years.

10 Indicator of climate and weather extremes: land average maximum temperatures

Changes in climate and weather extremes are among the most visible effects of human-induced climate change. Within AR6 WGI, a full chapter was dedicated to the assessment of past and projected changes in extremes on continents (Seneviratne et al., 2021), and the chapter on ocean, cryosphere and sea level changes also provided assessments on changes in marine heatwaves (Fox-Kemper et al., 2021). Global indicators related to climate extremes include averaged changes in climate extremes, for example, the mean increase of annual minimum and maximum temperatures

on land (AR6 WGI Chap. 11, Fig. 11.2, Seneviratne et al., 2021) or the area affected by certain types of extremes (AR6 WGI Chap. 11, Box 11.1, Fig. 1, Seneviratne et al., 2021; Sippel et al., 2015).

The presented climate indicator for changes in temperature extremes consists of land average maximum temperatures for any single day in a year (TXx) (excluding Antarctica). Fig. 11 updates the land mean TXx shown in Forster et al. (2023, 2024), originally based on Fig. 11.2 from Seneviratne et al. (2021). Three datasets are analyzed: HadEX3 (Dunn et al., 2020), Berkeley Earth Surface Temperature (building off Rohde et al., 2013), and the fifth-generation ECMWF atmospheric reanalysis of the global climate (ERA5; Hersbach et al., 2020). HadEX3 is static and has not received any updates. Berkeley Earth has been extended and updated compared to Forster et al. (2024), resulting in TXx differences for most years (less than 0.1°C), and now includes data for 2023. Of the three datasets, only ERA5 covers the whole of 2024 at the present time. TXx is calculated by averaging the annual maximum temperature over all available land grid points (excluding Antarctica) and then converted to anomalies with respect to a base period of 1961–1990. To express the TXx as anomalies with respect to 1850–1900, we add an offset of 0.51 °C to all three datasets. See Supplement Sect. S10 for details on the data selection, averaging and offset computation.

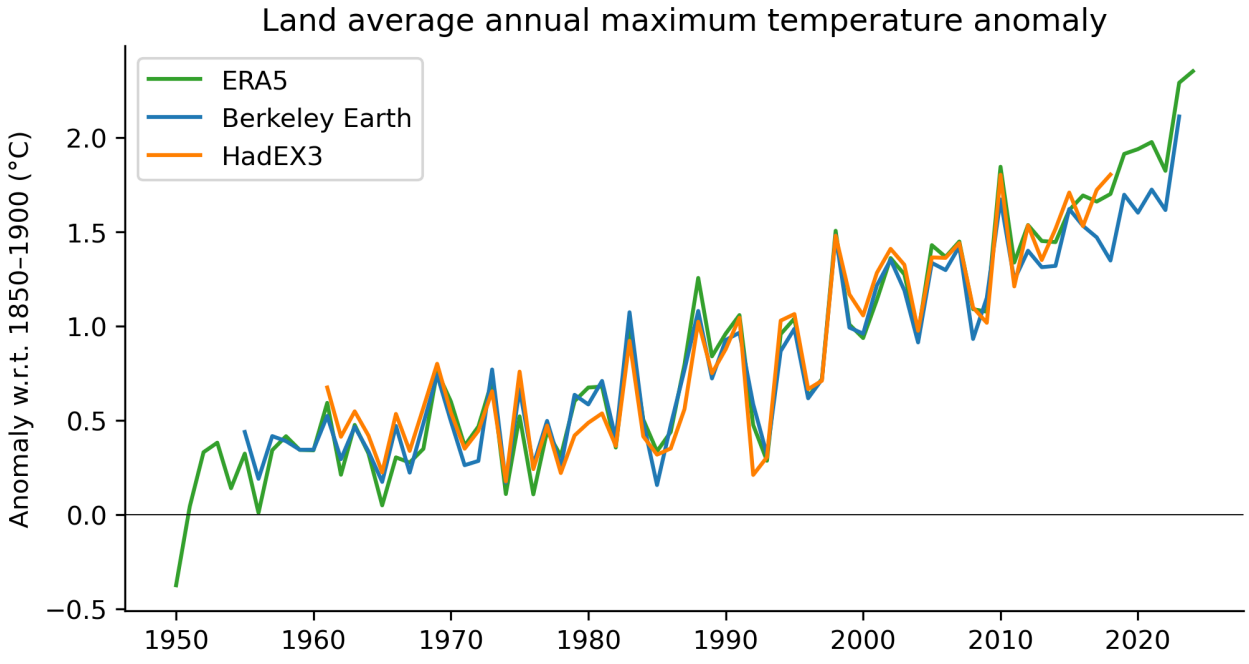

Figure 11 Time series of observed temperature anomalies for land average annual maximum temperature (TXx) for ERA5 (1950–2024), Berkeley Earth (1955–2023) and HadEX3 (1961–2018), with respect to 1850–1900. The datasets have different spatial coverage and are not coverage-matched. All anomalies are calculated relative to 1961–1990, and an offset of 0.51 °C is added to obtain TXx values relative to 1850–1900. Note that while the HadEX3 numbers are the same as shown in Seneviratne et al. (2021) Fig. 11.2, these numbers were not specifically assessed.

Our climate has warmed rapidly in the last few decades (Sect. 7), which also manifests in changes in the occurrence and intensity of climate and weather extremes. From about 1980 onwards, all datasets point to a strong TXx increase,

which coincides with the transition from global dimming, associated with aerosol increases, to brightening, associated with aerosol decreases (Wild et al., 2005, Sect. 4). The ERA5 based TXx warming estimate w.r.t. 1850–1900 for 2024 is at 2.35 °C; an increase of 0.05 °C compared to 2023, and thus even warmer than the previous record in 2023. On longer time scales, land average TXx has warmed 0.49 °C in the past 10 years (comparing the decades 2015–2024 to 2005–2014) and 1.90 °C with respect to pre-industrial conditions (Table 9). Since the offset relative to our pre-industrial baseline period is calculated over 1961–1990, temperature anomalies align by construction over this period but can diverge afterwards.

Table 9 Anomalies of land average annual maximum temperature (TXx) for recent decades based on HadEX3, Berkeley Earth, and ERA5, with respect to 1850–1900. All anomalies are calculated relative to 1961–1990, and an offset of 0.51 °C is added to obtain TXx values relative to 1850–1900.

	HadEX3	Berkeley Earth	ERA5
2000–2009	1.23	1.18	1.21
2005–2014	1.37	1.31	1.4
2009–2018	1.52	1.41	1.54
2011–2020	-	1.45	1.63
2013–2022	-	1.52	1.72
2014–2023	-	1.6	1.81
2015–2024	-	-	1.9

11 Global land precipitation

Anthropogenic radiative forcings modify the Earth's energy budget and subsequently drive substantial and widespread changes in the global water cycle including precipitation, evaporation, atmospheric moisture, and runoff (Forster et al., 2021, Douville et al., 2021; Gulev et al. 2021). AR6 Chapter 8 assessed that human-caused climate change has driven detectable changes in the global water cycle since the mid-20th century with high confidence, including an overall increase in atmospheric moisture (7% per 1 °C of warming), precipitation intensity (1-3% per 1 °C of warming) and increased terrestrial evapotranspiration (Douville et al., 2021).

In AR6, global land precipitation was highlighted as one of the large-scale indicators of climate change rather than global precipitation since land precipitation has greater societal relevance and in situ precipitation records over land extend back to the early to mid-20th century quasi-globally except Antarctica and parts of Africa and South America (Gulev et al., 2021; Lee et al., 2021; Douville et al., 2021). AR6 assessed that global land precipitation has likely increased since the middle of the 20th century with a faster increase since the 1980s with large interannual variability

and regional heterogeneity. The observed Northern Hemispheric land summer monsoon precipitation experienced a significant decline during 1901-2014, which has been attributed to the dominant influence of anthropogenic aerosols (Cao et al., 2022). Here, we include an update of global land precipitation change since AR6 (i.e., from 2020 to 2024).

Figure 12 shows annual global land precipitation anomaly relative to 1991-2020, following the current WMO climatology reference, obtained from GPCC V2020 (Schamm et al., 2014), CRU TS 4.08 (Harris et al., 2020), GPCP V.2.3 (Adler et al., 2018), and GHCN V4 (Menne et al., 2018) observed datasets. The change of reference period to 1991-2020 affects the perceived evolution compared to Figure 2.15c in AR6 WGI which had a 1981-2010 reference period. There is little consistency among datasets due to differences in input data, completeness of records, period of covered, and the gridding procedures applied (Sun et al., 2018; Nogueira, 2020). While the globally averaged land surface specific humidity has continuously increased (Dunn et al., 2024), global land precipitation has exhibited considerable interannual to interdecadal variability (Fig, 12). There was a positive anomaly in global land precipitation in 2024 but a negative anomaly in 2023. The former was contributed to by above-normal precipitation over the Asian and Australian monsoon region, likely associated with La Nina conditions, but was offset by dry conditions over South America and the southern part of Africa. The latter was driven by below normal precipitation over South Asia, Maritime Continents, the southern part of North America and the northern part of South America, due to El Niño conditions, with a corresponding increase in precipitation over the ocean (Adler and Gu, 2024).

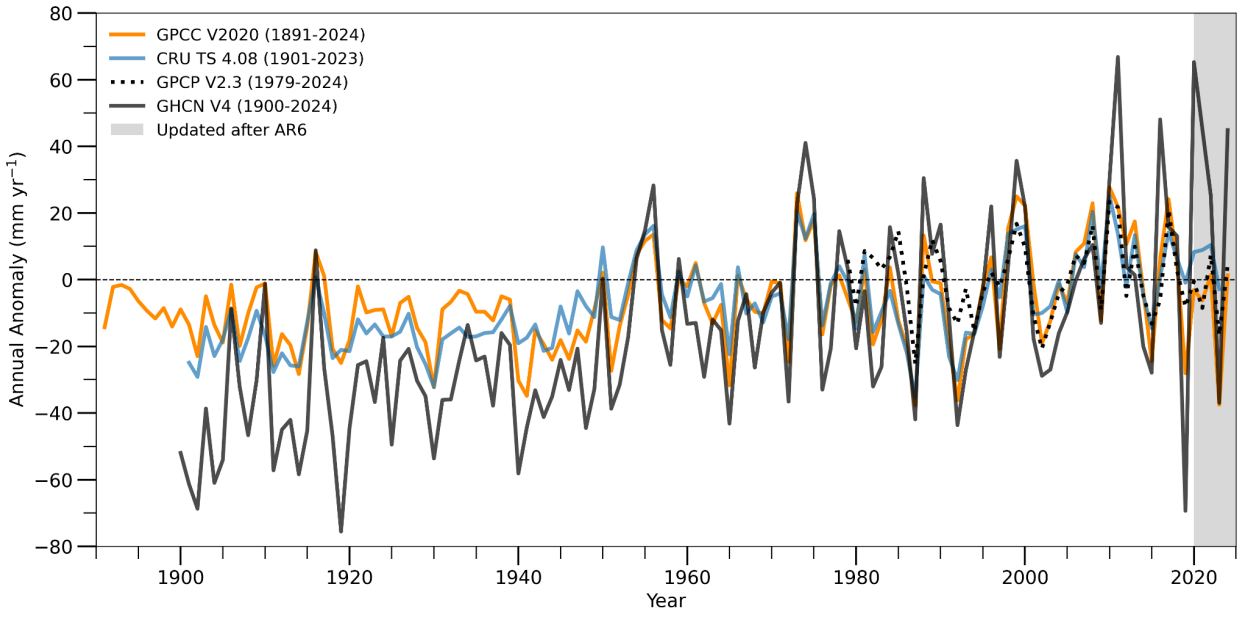

Figure 12 Time series of annual global land precipitation (mm yr^{-1}) from 1891 to date relative to a 1991-2020 climatology obtained from GPCP V2020, CRU TS 4.08, GPCP V2.3, and GHCN V4 (note that different products commence at distinct times). Annual global land precipitation for each observed data is estimated following the AR6 method except the period of climatology and updated from 2020 to 2024. In AR6, the reference period of the climatology was from 1981 to 2010.

12 Global mean sea-level rise

Global mean sea-level rise (GMSLR) is included in this annual update of AR6 for the first time. GMSLR is primarily driven by: (i) thermal expansion as the ocean warms; and (ii) increases in ocean mass associated with the addition of water or ice from land-based reservoirs, including glaciers and ice sheets (Fox-Kemper et al., 2021). Most of these processes are directly linked to changes in the global Earth energy inventory (Sect. 6). Sea-level rise can have large consequences for coastal ecosystems, safety and management, as it increases the baseline for sea-level extremes arising from short-term phenomena such as storm surges, waves and tides.

Observed GMSLR was assessed in IPCC AR6 WG1, in Chapter 2 (their Section 2.3.3.3, Gulev et al., 2021) and Chapter 9 (their Section 9.6.1 and Cross-Chapter Box 9.1, Fox-Kemper et al., 2021) on the basis of tide gauge reconstructions (up to 1993) and satellite altimeter observations (1993-2018). The assessment of GMSLR from tide gauge reconstructions used the ensemble approach presented by Palmer et al. (2021), which quantifies an ensemble and its uncertainties by combining an estimate of the structural uncertainty (informed by the ensemble spread) with an estimate of the internal uncertainty across the ensemble (i.e. the parametric uncertainty of each of the members in the ensemble). The members included in the tide gauge ensemble, which informed the total sea-level change estimate for the period 1901-1992, were reconstructions from Church and White (2011), Dangendorf et al (2019), Frederikse et al. (2020) and Hay et al. (2015). For the satellite period, from 1993 to 2018, AR6 used the estimate of the WCRP Global Sea Level Budget Group (2018), which was constructed from satellite-based GMSLR time series from six groups (AVISO/CNES, CSIRO, NASA/GSFC, NOAA, SL_cci/ESA and University of Colorado). Based on this information, AR6 concluded that GMSLR increased by 0.20 [0.15 to 0.25] m over the period 1901 to 2018, with a rate of 1.73 [1.28 to 2.17] mm yr^{-1} (*high confidence*). Periods closer to the present showed an accelerating GMSLR, with a rate of 2.3 [1.6 to 3.1] mm yr^{-1} over the period 1971–2018 increasing to 3.7 [3.2 to 4.2] mm yr^{-1} over the period 2006–2018 (*high confidence*).

Here, we extend the AR6 GMSLR time series, which ended in 2018, closer to the present day. We use the same tide gauge-based ensemble estimate as in AR6 for the period up to 1993. We do note that two new reconstructions have been published recently, both providing rates in line with the AR6 assessment rates given above. The new GMSLR reconstruction by Dangendorf et al. (2024) uses a Kalman-smoother and adjusted estimates of the contributions of glacial isostatic adjustment, barystatic and sterodynamic changes to sea-level change and finds a trend of 1.50 ± 0.20 mm/yr for the period 1900-2021. The new reconstruction by Wang et al. (2024) uses an updated vertical land motion correction and considers barystatic fingerprints and sterodynamic patterns from CMIP6 models and finds a trend of 1.6 ± 0.2 mm/yr over 1900-2019.

The satellite record now provides observations up to the end of 2024, for three out of the six satellite data products used for the WCRP estimate used in AR6. The three records available to the end of 2024 are from NASA (2025), NOAA (2025) and AVISO (2025). All data was downloaded on 19 February 2025. We use the global mean time series based on the reference missions, with seasonal signals removed and corrected for glacial isostatic adjustment. We first compute annual averages and then an ensemble average time series, which is spliced to the AR6 GMSLR record ending in 2018. For consistency, we retain the uncertainties from the six-member WCRP ensemble and propagate them over the period 2019-2024. We note that reprocessing of the altimetry record is periodically required to account for new insights on instrument drift, retracking and geophysical corrections to the altimetry missions. This reprocessing may lead to small differences in the satellite altimeter record and the associated assessment of GMSLR in future iterations of IGCC.

Over the period 2019 to 2024 global mean sea level has increased by 26.1 [19.8 to 32.4] mm. When combining the AR6 estimate up to 2018 with the satellite time series for 2019-2024, we find a total GMSLR of 228.0 [176.4 to 279.6] mm for the period 1901-2024, which translates to an average rate of 1.85 [1.43 to 2.27] mm yr^{-1} (Table 10, Fig. 13). The rate increase associated with extending the time series by just 6 years, as well as the increasing rates over consecutive 20-yr periods (Fig. 13b), indicate a continuing acceleration of GMSLR. This is in line with the assessments of AR6 (Fox-Kemper et al., 2021), SROCC (Oppenheimer et al., 2019) and AR5 (Church et al., 2013) that sea-level change has been accelerating over the course of the 20th and early 21st centuries, and consistent with the observed acceleration in some components of the Earth heat inventory (see Sect. 6).

Table 10 Observed global mean sea-level rise (GMSLR) as presented in IPCC AR6, table 9.5 (Fox-Kemper et al., 2021) compared with the extended time series in this study. Values are expressed as the total change (Δ) in the annual mean over each period (mm) along with the equivalent rate calculated as the total change divided by the number of years (mm yr^{-1}). Uncertainties represent the *very likely* range.

Observed GMSLR		**IPCC AR6**	**This study**
Start year		**End year 2018**	**End year 2024**
1901	**Δ(mm)**	201.9 [150.3 to 253.5]	228.0 [176.4 to 279.6]
	mm yr^{-1}	1.73 [1.28 to 2.17]	1.85 [1.43 to 2.27]
1971	**Δ(mm)**	109.6 [72.8 to 146.4]	135.8 [99.0 to 172.5]
	mm yr^{-1}	2.33 [1.55 to 3.12]	2.56 [1.87 to 3.26]
1993	**Δ(mm)**	81.2 [72.1 to 90.2]	107.3 [98.2 to 116.4]
	mm yr^{-1}	3.25 [2.88 to 3.61]	3.46 [3.17 to 3.75]
2006	**Δ(mm)**	44.3 [38.6 to 50.0]	70.4 [64.7 to 76.1]

	mm yr^{-1}	3.69 [3.21 to 4.17]	3.91 [3.59 to 4.23]

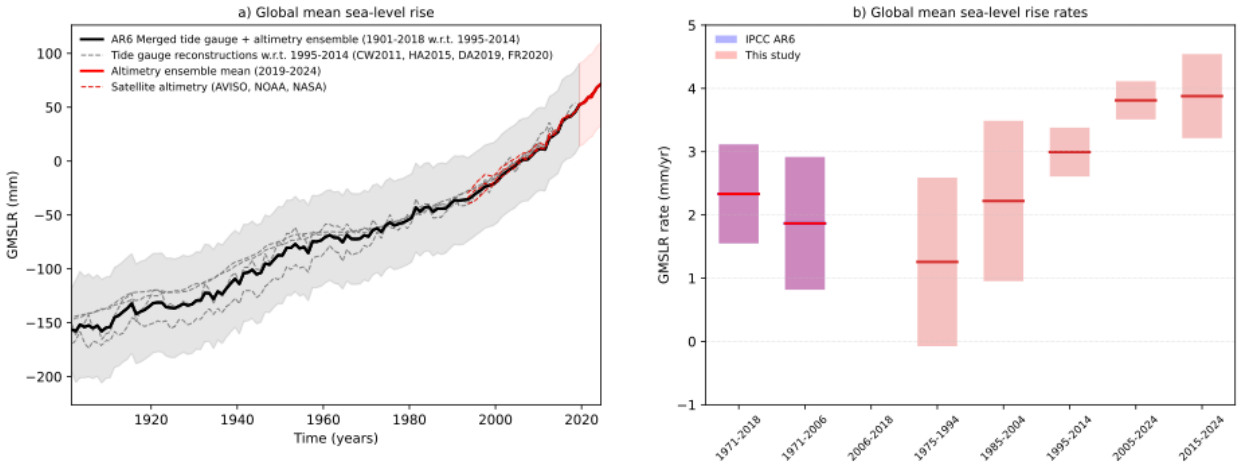

Figure 13 (a) Global mean sea-level rise time series 1901-2024 (mm). The GMSLR ensemble from AR6 in black, w.r.t. the period 1995-2014; the updated satellite altimetry ensemble in red, w.r.t. the AR6 ensemble in 2018. Individual time series are shown in dashed lines. (b) GMSLR rates (mm yr-1) for different periods. Uncertainties in a) show the *likely* range and in b) the *very likely* range, computed relative to 1901, including estimates of both structural uncertainty and parametric uncertainty (Palmer et al., 2021).

13 Code, data availability and visualisations

We publish a set of selected key indicators of global climate change via Climate Change Tracker (https://climatechangetracker.org/, Climate Change Tracker, 2025), a platform which aims to provide reliable, user-friendly, high-quality interactive dashboards, visualisations, data, and easily accessible insights of this paper.

With Climate Change Tracker we aim to reach a wider public audience, including policymakers involved in UNFCCC negotiations, and decision makers working in climate change mitigation and adaptation. Climate Change Tracker plans to update significant indicators multiple times throughout the year, providing an up-to-date picture of the indicators of climate change. Within the dashboards, all data is traceable to the underlying sources. Fig. 14 presents a screenshot of the IGCC dashboard.

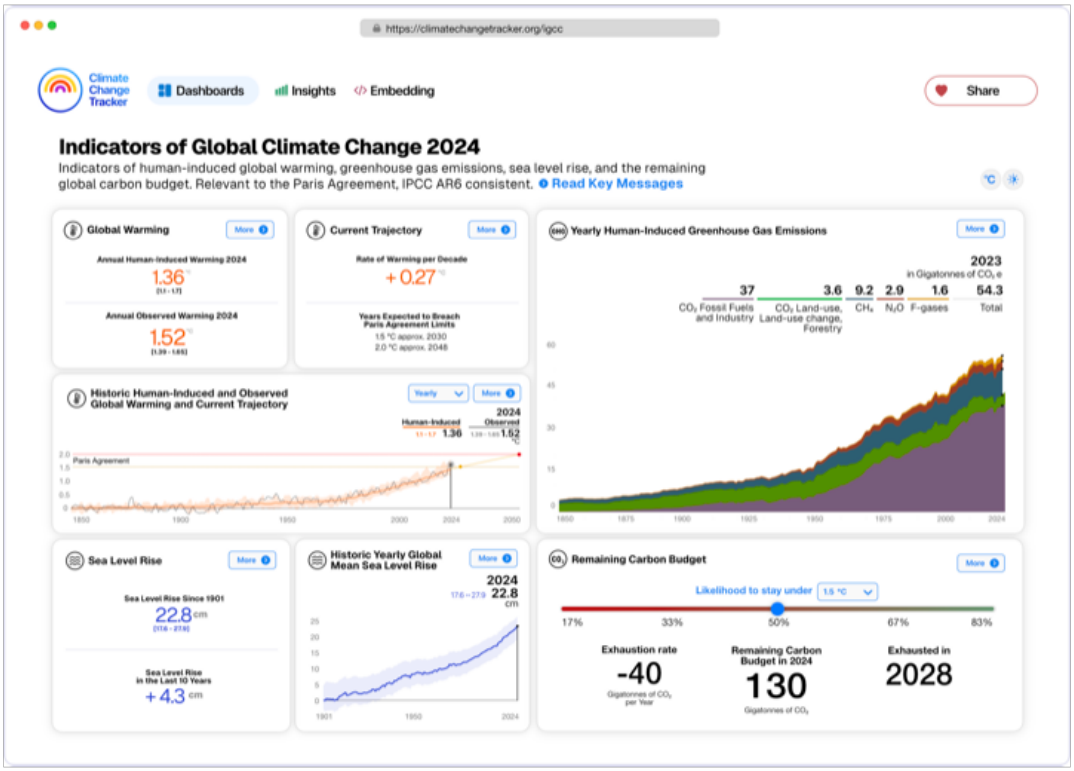

Figure 14 Screenshot of the IGCC dashboard, (https://climatechangetracker.org/, Climate Change Tracker, 2025).

The carbon budget calculation is available from https://github.com/Rlamboll/AR6CarbonBudgetCalc/tree/v1.0.3 (Lamboll and Rogelj, 2025). The code and data used to produce other indicators are available in repositories under https://github.com/ClimateIndicator/data/tree/v2025.06.11 (Smith et al., 2025b). All data are available from https://doi.org/10.5281/zenodo.15639576 (Smith et al., 2025a). Data are provided under the CC-BY 4.0 License.

HadEX3 [3.0.4] data were obtained from https://catalogue.ceda.ac.uk/uuid/115d5e4ebf7148ec941423ec86fa9f26 (Dunn et al., 2023) on 5 April 2023 and are © British Crown Copyright, Met Office, 2022, provided under an Open Government Licence; http://www.nationalarchives.gov.uk/doc/open-government-licence/version/2/ (last access: 2 June 2023).

14 Discussion and conclusions

The third year of the Indicators of Global Climate Change (IGCC) initiative has built on previous years' efforts to provide a comprehensive update of the climate change indicators required to estimate the human-induced warming

and the remaining carbon budget. Table 11 and Fig. 15 present a summary of the headline indicators from each section compared to those given in the AR6 assessment. Table 11 also summarises methodological updates.

Table 11 Summary of headline results and methodological updates from the Indicators of Global Climate Change (IGCC) initiative.

Climate Indicator	AR6 2021 assessment	This 2024 assessment	Explanation of changes	Methodological updates since AR6
GHG emissions **AR6 WGIII Chapter 2: Dhakal et al. (2022); see also Minx et al. (2021)**	**2010-2019 average:** **55.9 ± 6 $GtCO_2e$**	**2010-2019 average:** **52.9 ± 5.4 $GtCO_2e$** **2014-2023 average:** **53.6 ± 5.2 $GtCO_2e$**	**Average emissions in the past decade grew at a slower rate than in the previous decade. The change from AR6 is due to a systematic downward revision in CO_2-LULUCF and CH_4 estimates. Real-world emissions have slightly increased.**	**CO_2-LULUCF emissions revised down. CO_2 GCB Fossil Fuel and Industry emissions used instead of EDGAR. PRIMAP-hist TP used in place of EDGAR for CH_4 and N_2O emissions, atmospheric measurements taken for F-gas emissions. These changes reduce estimates by around 3 $GtCO_2e$ (Sect. 2).**
GHG concentrations **AR6 WGI Chapter 2: Gulev et al. (2021)**	**2019:** **CO_2, 410.1 [± 0.36] ppm** **CH_4, 1866.3 [± 3.2] ppb** **N_2O, 332.1 [± 0.7] ppb**	**2024:** **CO_2, 422.8 [±0.4] ppm** **CH_4, 1929.7 [±3.3] ppb** **N_2O, 337.9 [±0.4] ppb**	**Increases caused by continued GHG anthropogenic emissions**	**Updates based on NOAA data and AGAGE (Sect. 3)**
Effective radiative forcing change since 1750 **AR6 WGI Chapter 7: Forster et al. (2021)**	**2019:** **2.72 [1.96 to 3.48] W m^{-2}**	**2024:** **2.97 [2.05 to 3.77] W m^{-2}**	**Trend since 2019 is caused by increases in GHG concentrations and reductions in aerosol precursors.**	**Follows AR6 with minor update to aerosol precursor treatment and emissions dataset that revises 2019 ERF estimate relative to 1750 downwards (more negative) by 0.09 W m^{-2}. Added this year is a new method to estimate the ERF from land use surface reflection and irrigation to avoid scaling with cumulative emissions. This**

				does not materially affect the ERF. (Sect. 5)
Earth's energy imbalance **AR6 WGI Chapter 7: Forster et al. (2021)**	**2006-2018 average:** **0.79 [0.52 to 1.06] W m^{-2}**	**2012-2024 average:** **0.99 [0.70 to 1.28] W m^{-2}**	**A 25% increase in energy imbalance estimated based on increased rate of ocean heating.**	**Ocean heat content timeseries extended from 2018 to 2024 using all of the 5 AR6 datasets. Other heat inventory terms updated following von Schuckmann et al. (2023a). Ocean heat content uncertainty is used as a proxy for total uncertainty. Further details in Sect. 6.**
Global mean surface temperature change since 1850-1900 **AR6 WGI Chapter 2: Gulev et al. (2021)**	**2011-2020 average:** **1.09 [0.95 to 1.20] °C**	**2015-2024 average:** **1.24 [1.11 to 1.35] °C**	**An increase of 0.15 °C within four years, indicating a high decadal rate of change which may in part be internal variability.**	**Methods match four datasets used in AR6. Individual datasets have updated historical data, but these changes are not materially affecting results. (Sect. 7).**
Human induced global warming since preindustrial **AR6 WGI Chapter 3: Eyring et al. (2021)** **SR1.5 Chapter 1**	**2010-2019 decade average:** **1.07 [0.8 to 1.3] °C** **2017 single year: 1.0 [0.8 to 1.2] °C**	**2015-2024 decade average:** **1.22 [1.0 to 1.5] °C** **2024 single year: 1.36 [1.1 to 1.7] °C**	**An increase of 0.15 °C within five years, indicating a high decadal rate of change (broadly consistent with warming projections). The decadal warming rate increased slightly between 2019 and 2024. One of the three AR6 methods is diverging.**	**The three methods for the basis of the AR6 assessment are retained, but each has new input data (Sect. 8)**

Remaining carbon budget for 50% likelihood of limiting global warming to 1.5 °C **AR6 WGI Chapter 5: Canadell et al. (2021)**	**From the start of 2020:** **500 $GtCO_2$**	**From the start of 2025:** **130 $GtCO_2$**	**The 1.5 °C budget is becoming very small. The RCB can exhaust before the 1.5 °C threshold is reached due to having to allow for future non-CO_2 warming.**	**Emulator and scenario change has reduced budget since 2020 by 100 $GtCO_2$ (Sect. 9)**
Land average maximum temperature change compared to pre-industrial. **AR6 WGI Chapter 11: Seneviratne et al., 2021**	**2009-2018 average:** **1.55 °C**	**2015-2024 average:** **1.90 °C**	**Rising at a substantially faster rate compared to global mean surface temperature**	**HadEX3 data used in AR6 replaced with ERA reanalysis data employed in this report which is more updatable going forward. Adds 0.01 °C to estimate (Sect. 10)**
Global land precipitation compared to preindustrial (Douville et al., 2021)	**Likely increased since the middle of the 20th century with a faster increase since the 1980s with large interannual variability**	**Large interannual variability associated with El Niño dominates the record in recent years, making long-term trend less clear**	**2023 exhibited a negative anomaly relative to preindustrial due to El Niño conditions**	**The four datasets used in AR6 have been extended (Sect. 11)**
Global mean sea-level rise since 1901 **(Gulev et al., 2021; Fox-Kemper et al., 2021)**	**1901 to 2018 change** **201.9 [150.3 to 253.5] mm** **at a rate of** **1.73 [1.28 to 2.17] mm yr^{-1}**	**1901 to 2024 change** **228.0 [176.4 to 279.6] mm** **at a rate of** **1.85 [1.43 to 2.27] mm yr^{-1}**	**Sea-level rise continues to accelerate.**	**AR6 data extended with three of the six datasets from AR6, using latest satellite data (Sect. 12).**

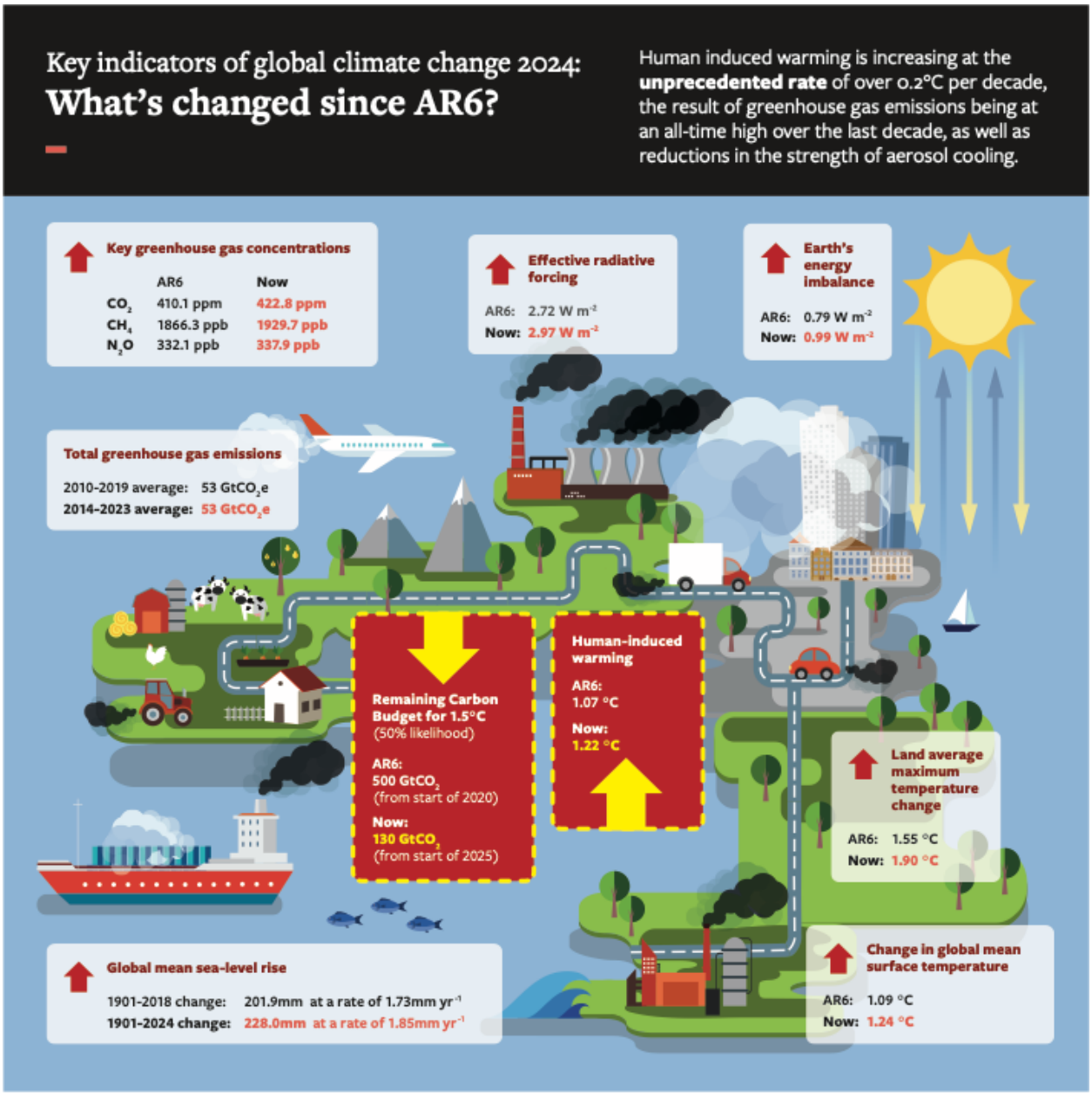

Figure 15 Infographic for the best estimate of headline indicators assessed in this paper.

Last year (2024) witnessed global surface temperatures more likely than not exceeding 1.5 °C above preindustrial levels which has widely been reported in the press. Sects. 7 and 8. show that such high levels of global temperature anomalies are typical of what we expect from current best estimates of human induced warming, modulated by internal climate variability.

The overview of key indicators of the state of global climate indeed highlights the multiple fingerprints of the 2023-2024 El-Nino event regarding peak global surface temperature (Section 7.2), regional dry anomalies in land precipitation (Section 11), and their implications for reduced land carbon sinks and the record growth rate of atmospheric CO_2 concentrations in 2024 (Section 3).

The overall increase in land maximum temperatures (Section 10), closely related to global warming levels, drives increasing trends in potential evapotranspiration, decreasing trends in soil moisture (Seo et al., 2025), contributing to the increased rate of global mean sea-level rise (Section 12).

Methane and biomass emissions had a strong component of change related to climate feedbacks (Sects. 2 and 3). Such changes will become increasingly important over this century, even if the direct human influence declines. This year, we explored different inventory choices in Sect. 2. In future years a more consistent approach to attribution of atmospheric emissions, concentration change and radiative forcing should be developed, so it can be assessed in AR7.

It is hoped that this update can support the science community in its collection and provision of reliable and timely global climate data. In future years we are particularly interested in improving SLCF updating methods to get a more accurate estimate of short-term ERF changes. The work also highlights the importance of high-quality metadata to document changes in methodological approaches over time. This year we have extended the datasets with land precipitation and global mean sea level rise. In future years we hope to improve the robustness of the indicators presented here and could update other AR6 assessments. Parallel efforts could explore how we might update indicators of regional climate extremes and their attribution, which are particularly relevant for supporting actions on adaptation and loss and damage.

Generally, scientists and scientific organisations have an important role as “watchdogs” to critically inform evidence-based decision-making. This annual update traced to IPCC methods can provide a reliable, timely source of trustworthy information, IGCC and the complimentary updates of the State of the Climate (BAMS) and State of Global Climate (WMO) reports, very much rely on continued support for high quality global monitoring networks of atmospheric and climate data, and also on open data sources that are regularly updated and easily accessed.

This is a critical decade: human-induced global warming rates are at their highest historical level, and 1.5 °C global warming might be expected to be reached or exceeded in around 5 years in the absence of cooling from major volcanic eruptions (Sects. 8 and 9). Yet this is also the decade when global GHG emissions could be expected to peak and begin to substantially decline. The indicators of global climate change presented here show that the Earth's energy imbalance has increased to around 1.0 $W\,m^{-2}$, averaged over the last 12 years (Sect. 5), which represents a 25% increase on the value assessed for 2006-2018 by AR6. This also has implications for the committed response of slow components in the climate system (glaciers, deep ocean, ice sheets) and committed long-term sea-level rise (through ocean thermal expansion and land-based ice melt/loss), to be addressed further in future updates. However, rapid and

stringent GHG emission decreases such as those committed to at COP28 could halve warming rates over the next 20 years (McKenna et al., 2021). Table 1 shows that global GHG emissions are at a long-term high, yet there are signs that their rate of increase has slowed. Depending on the societal choices made in this critical decade, a continued series of these annual updates could track an improving trend for some of the indicators herein discussed.

Supplement

The supplement related to this article is available online.

Author contributions

PMF, CS, MA, PF, JR and AP developed the concept of an annual update in discussions with the wider IPCC community over many years. CS led the work of the data repositories. VMD, PZ, SS, CS, SIS, VN, AP, NPG, GPP, BT, MDP, KvS, JR, PF, MA, JCM, XZ, RAB, CB, CC, SB and PT provided important IPCC and UNFCCC framing. PMF coordinated the production of the manuscript with support from DR. WFL led Sect. 2 with contributions from PF, GPP, JG, JP, JCM and RA. CS led Sect. 3 with inputs from JM, PK, LW, PMF and MR. SS led Sect. 4 with inputs from VK, CS, GvdW, LAR and MG. CS led Sect. 5 with contributions from CW, TG, SS, VN and GvdW. KvS and MDP led Sect. 6 with contributions from LC, MI, JR, REK, AS, CMD, DPM and SEW. BT, CC and ZH led Sect. 7 with contributions from PT, CM, CK, JK, RR, RV, AL and LC. TW led Sect. 8 with contributions and calculations from AR, NPG, SJ, CS and MA. RL led Sect. 9 with contributions from JR and HDM. Sect. 10 was led by MH, with contributions from SIS, and XZ. JYL, JEY, and RK led Sect. 11 with contributions from VMD, PT, and KvS. AS led Sect. 12 with contributions from MDP. All authors either edited or commented on the manuscript. DR, AB and JAB coordinated the data visualisation effort.

Competing interests

The contact author has declared that none of the authors has any competing interests.

Disclaimer

Publisher’s note: Copernicus Publications remains neutral with regard to jurisdictional claims in published maps and institutional affiliations.

Acknowledgements

This research has been supported by the European Union's Horizon Europe research and innovation programme under Grant Agreement Nos. 820829, 101081395, 101081661 and 821003, the H2020 European Research Council (grant no. 951542), the Natural Environment Research Council (NE/X00452X/1) and the Engineering and Physical Research Council (EP/V000772/1). Matthew Palmer, Colin Morice, Rachel Killick and Richard Betts were supported by the Met Office Hadley Centre Climate Programme funded by DSIT. Peter Thorne was supported by Co-Centre award

number 22/CC/11103. The Co-Centre award is managed by Research Ireland Northern Ireland's Department of Agriculture, Environment and Rural Affairs (DAERA) and UK Research and Innovation (UKRI), and supported via UK's International Science Partnerships Fund (ISPF), and the Irish Government's Shared Island initiative. Analyses and visualizations for concentrations of Short Lived Climate Forcers used in this paper were produced with the Giovanni online data system, developed and maintained by the NASA GES DISC (as available in February 2025). June-Yi Lee and Jung-Eun Yun were supported by the National Research Foundation of Korea (NRF) grant funded by the Korea government (MSIT) (No. RS-2024-00416848). Aimée Slangen was supported by the research programme ENW-Vidi (DARSea, project number VI.Vidi.2023.058) funded by the Dutch Research Council (NWO). We thank Xin Lan for assistance with compiling the GHG concentration data.

References

Acker, J. G. and Leptoukh, G.: Online analysis enhances use of NASA Earth science data, EoS Transactions, 88, 14–17, https://doi.org/10.1029/2007EO020003, 2007.

Adler, R. F. and Gu, G.: Global precipitation for the year 2023 and how it relates to longer term variations and trends, Atmosphere, 15, 535, 2024.

Adler, R. F., Sapiano, M. R. P., Huffman, J., Wang, J.-J., Gu G., Bolvin, D., Chiu, L., Schneider, U., Becker, A., Nelkin, E., Xie, P., Ferrarok R., and Shin, D.-B.: The global precipitation climatology project (GPCP) monthly analysis (new version 2.3) and a review of 2017 global precipitation. Atmosphere, 9, 138, https://doi.org/10.3390/atmos9040138, 2018.

Allan ,R.P. and Merchant, C.J.: Reconciling Earth's growing energy imbalance with ocean warming, Environ. Res. Lett, 20 04402, https://doi.org/10.1088/1748-9326/adb448, 2025.

Allen, M. R., O. P. Dube, W. Solecki, F. Aragón-Durand, W. Cramer, S. Humphreys, M. Kainuma, J. Kala, N. Mahowald, Y. Mulugetta, R. Perez, M. Wairiu, and K. Zickfeld, 2018: Framing and Context. In: Global Warming of 1.5°C. An IPCC Special Report on the impacts of global warming of 1.5°C above pre-industrial levels and related global greenhouse gas emission pathways, in the context of strengthening the global response to the threat of climate change, sustainable development, and efforts to eradicate poverty [Masson-Delmotte, V., P. Zhai, H.-O. Pörtner, D. Roberts, J. Skea, P.R. Shukla, A. Pirani, W. Moufouma-Okia, C. Péan, R. Pidcock, S. Connors, J.B.R. Matthews, Y. Chen, X. Zhou, M.I. Gomis, E. Lonnoy, T. Maycock, M. Tignor, and T. Waterfield (eds.)], Cambridge University Press, Cambridge, UK and New York, NY, USA, 49-92, https://doi.org/10.1017/9781009157940.003, 2018.

Allen, M. R., Frame, D. J., Friedlingstein, P., Gillett, N. P., Grassi, G., Gregory, J. M., Hare, W., House, J., Huntingford, C., Jenkins, S., Jones, C. D., Knutti, R., Lowe, J. A., Matthews, H. D., Meinshausen, M., Meinshausen, N., Peters, G. P., Plattner, G.-K., Raper, S., Rogelj, J., Stott, P. A., Solomon, S., Stocker, T. F., Weaver, A. J., and Zickfeld, K.: Geological Net Zero and the need for disaggregated accounting for carbon sinks, Nature, 638, 343–350, https://doi.org/10.1038/s41586-024-08326-8, 2025.

Allison, L. C., Palmer, M. D., Allan, R. P., Hermanson, L., Liu, C., and Smith, D. M.: Observations of planetary heating since the 1980s from multiple independent datasets, Environ. Res. Commun., 2, 101001, https://doi.org/10.1088/2515-7620/abbb39, 2020.

AVISO: Mean sea-level product, https://www.aviso.altimetry.fr/en/data/products/ocean-indicators-products/mean-sea-level/data-acces.html, [data set], accessed 19 February 2025, 2025.

Barnes, C., Boulanger, Y., Keeping, T., Gachon, P., Gillett, N., Haas, O., Wang, X., Roberge, F., Kew, S., Heinrich, D., Singh, R., Vahlberg, M., Van Aalst, M., Otto, F., Kimutai, J., Boucher, J., Kasoar, M., Zachariah, M., and Krikken, F.: Climate change more than doubled the likelihood of extreme fire weather conditions in Eastern Canada, Imperial College London, https://doi.org/10.25561/105981, 2023.

Basu, S., Lan, X., Dlugokencky, E., Michel, S., Schwietzke, S., Miller, J. B., Bruhwiler, L., Oh, Y., Tans, P. P., Apadula, F., Gatti, L. V., Jordan, A., Necki, J., Sasakawa, M., Morimoto, S., Di Iorio, T., Lee, H., Arduini, J., and Manca, G.: Estimating emissions of methane consistent with atmospheric measurements of methane and δ 13 C of methane, Atmos. Chem. Phys., 22, 15351–15377, https://doi.org/10.5194/acp-22-15351-2022, 2022.

Bellouin, N., Davies, W., Shine, K. P., Quaas, J., Mülmenstädt, J., Forster, P. M., Smith, C., Lee, L., Regayre, L., Brasseur, G., Sudarchikova, N., Bouarar, I., Boucher, O., and Myhre, G.: Radiative forcing of climate change from the Copernicus reanalysis of atmospheric composition, Earth Syst. Sci. Data, 12, 1649–1677, https://doi.org/10.5194/essd-12-1649-2020, 2020.

Betts, R. A., Belcher, S. E., Hermanson, L., Klein Tank, A., Lowe, J. A., Jones, C. D., Morice, C. P., Rayner, N. A., Scaife, A. A., and Stott, P. A.: Approaching 1.5 °C: how will we know we've reached this crucial warming mark?, Nature, 624, 33–35, https://doi.org/10.1038/d41586-023-03775-z, 2023.

Bond, T. C., Doherty, S. J., Fahey, D. W., Forster, P. M., Berntsen, T., DeAngelo, B. J., Flanner, M. G., Ghan, S., Kärcher, B., Koch, D., Kinne, S., Kondo, Y., Quinn, P. K., Sarofim, M. C., Schultz, M. G., Schulz, M., Venkataraman, C., Zhang, H., Zhang, S., Bellouin, N., Guttikunda, S. K., Hopke, P. K., Jacobson, M. Z., Kaiser, J. W., Klimont, Z., Lohmann, U., Schwarz, J. P., Shindell, D., Storelvmo, T., Warren, S. G., and Zender, C. S.: Bounding the role of black carbon in the climate system: A scientific assessment, J. Geophys. Res.-Atmos., 118, 5380–5552, https://doi.org/10.1002/jgrd.50171, 2013.

Bun, R., Marland, G., Oda, T., See, L., Puliafito, E., Nahorski, Z., Jonas, M., Kovalyshyn, V., Ialongo, I., Yashchun, O., and Romanchuk, Z.: Tracking unaccounted greenhouse gas emissions due to the war in Ukraine since 2022, Science of The Total Environment, 914, 169879, https://doi.org/10.1016/j.scitotenv.2024.169879, 2024.

Burton, C., Lampe, S., Kelley, D. I., Thiery, W., Hantson, S., Christidis, N., Gudmundsson, L., Forrest, M., Burke, E., Chang, J., Huang, H., Ito, A., Kou-Giesbrecht, S., Lasslop, G., Li, W., Nieradzik, L., Li, F., Chen, Y., Randerson, J., Reyer, C. P. O., and Mengel, M.: Global burned area increasingly explained by climate change, Nat. Clim. Chang., 14, 1186–1192, https://doi.org/10.1038/s41558-024-02140-w, 2024.

Canadell, J.G., P. M. S. Monteiro, M. H. Costa, L. Cotrim da Cunha, P. M. Cox, A.V. Eliseev, S. Henson, M. Ishii, S. Jaccard, C. Koven, A. Lohila, P. K. Patra, S. Piao, J. Rogelj, S. Syampungani, S. Zaehle, and K. Zickfeld: Global

Carbon and other Biogeochemical Cycles and Feedbacks. In Climate Change 2021: The Physical Science Basis. Contribution of Working Group I to the Sixth Assessment Report of the Intergovernmental Panel on Climate Change [Masson-Delmotte, V., P. Zhai, A. Pirani, S.L. Connors, C. Péan, S. Berger, N. Caud, Y. Chen, L. Goldfarb, M.I. Gomis, M. Huang, K. Leitzell, E. Lonnoy, J.B.R. Matthews, T.K. Maycock, T. Waterfield, O. Yelekçi, R. Yu, and B. Zhou (eds.)]. Cambridge University Press, Cambridge, United Kingdom and New York, NY, USA, pp. 673–816, https://doi.org/10.1017/9781009157896.007, 2021.

Cao, J., Wang, H., Wang, B., Zhao, H., Wang, C., and Zhu, X.: Higher sensitivity of Northern Hemisphere monsoon to anthropogenic aerosol than greenhouse gases, Geophys Res. Lett., 49, e2022GL100270. https://doi.org/10.1029/2022GL100270, 2022.

Cattiaux, J., Ribes, A., and Cariou, E.: How Extreme Were Daily Global Temperatures in 2023 and Early 2024?, Geophysical Research Letters, 51, e2024GL110531, https://doi.org/10.1029/2024GL110531, 2024.

Cheng, L., Abraham, J., Hausfather, Z., and Trenberth, K. E.: How fast are the oceans warming?, Science, 363, 128–129, https://doi.org/10.1126/science.aav7619, 2019.

Cheng, L., Von Schuckmann, K., Abraham, J. P., Trenberth, K. E., Mann, M. E., Zanna, L., England, M. H., Zika, J. D., Fasullo, J. T., Yu, Y., Pan, Y., Zhu, J., Newsom, E. R., Bronselaer, B., and Lin, X.: Past and future ocean warming, Nat. Rev. Earth. Environ., 3, 776–794, https://doi.org/10.1038/s43017-022-00345-1, 2022.

Church, J. A., White, N. J., Konikow, L. F., Domingues, C. M., Cogley, J. G., Rignot, E., Gregory, J. M., Van Den Broeke, M. R., Monaghan, A. J., and Velicogna, I.: Revisiting the Earth's sea-level and energy budgets from 1961 to 2008: SEA-LEVEL AND ENERGY BUDGETS, Geophys. Res. Lett., 38, n/a-n/a, https://doi.org/10.1029/2011GL048794, 2011.

Climate Change Tracker, https://climatechangetracker.org/igcc, accessed 20.05.2025, 2025.

Collins, M., Knutti, R., Arblaster, J., Dufresne, J.-L., Fichefet, T., Friedlingstein, P., Gao, X., Gutowski, W.J., Johns, T., Krinner, G., Shongwe, M., Tebaldi, C., Weaver, A.J. & Wehner, M.: Long-term Climate Change: Projections, Commitments and Irreversibility. In: V.B. Stocker T.F., .D. Qin, G.K. Plattner, M. Tignor, S.K. Allen, J. Boschung, A. Nauels, Y. Xia & P.M. Midgley (eds.). Climate Change 2013: The Physical Science Basis. Contribution of Working Group I to the Fifth Assessment Report of the Intergovernmental Panel on Climate Change. Cambridge, United Kingdom and New York, NY, USA, Cambridge University Press. pp. 1029–1136, 2013.

Crippa, M., Guizzardi, D., Schaaf, E., Monforti-Ferrario, F., Quadrelli, R., Risquez Martin, A., Rossi, S., Vignati, E., Muntean, M., Brandao De Melo, J., Oom, D., Pagani, F., Banja, M., Taghavi-Moharamli, P., Köykkä, J., Grassi, G., Branco, A., and San-Miguel, J.: GHG emissions of all world countries – 2023, Publications Office of the European Union, https://doi.org/doi/10.2760/953322, 2023.

Cuesta-Valero, F. J., Beltrami, H., García-García, A., Krinner, G., Langer, M., MacDougall, A., Nitzbon, J., Peng, J., von Schuckmann, K., Seneviratne, S., Thiery, W., Vanderkelen, I., Wu, T.: GCOS EHI 1960-2020 Continental Heat Content (Version 2), World Data Center for Climate (WDCC) at DKRZ, https://doi.org/10.26050/WDCC/GCOS_EHI_1960-2020_CoHC_v2, 2023.

Dangendorf, S., Hay, C., Calafat, F. M., Marcos, M., Piecuch, C. G., Berk, K., and Jensen, J.: Persistent acceleration in global sea-level rise since the 1960s, Nat. Clim. Chang., 9, 705–710, https://doi.org/10.1038/s41558-019-0531-8, 2019.

Dangendorf, S., Sun, Q., Wahl, T., Thompson, P., Mitrovica, J. X., and Hamlington, B.: Probabilistic reconstruction of sea-level changes and their causes since 1900, Earth Syst. Sci. Data, 16, 3471–3494, https://doi.org/10.5194/essd-16-3471-2024, 2024.

Deng, Z., Ciais, P., Tzompa-Sosa, Z. A., Saunois, M., Qiu, C., Tan, C., Sun, T., Ke, P., Cui, Y., Tanaka, K., Lin, X., Thompson, R. L., Tian, H., Yao, Y., Huang, Y., Lauerwald, R., Jain, A. K., Xu, X., Bastos, A., Sitch, S., Palmer, P. I., Lauvaux, T., d'Aspremont, A., Giron, C., Benoit, A., Poulter, B., Chang, J., Petrescu, A. M. R., Davis, S. J., Liu, Z., Grassi, G., Albergel, C., Tubiello, F. N., Perugini, L., Peters, W., and Chevallier, F.: Comparing national greenhouse gas budgets reported in UNFCCC inventories against atmospheric inversions, Earth System Science Data, 14, 1639–1675, https://doi.org/10.5194/essd-14-1639-2022, 2022.

Deng, Z., Zhu, B., Davis, S. J., Ciais, P., Guan, D., Gong, P., and Liu, Z.: Global carbon emissions and decarbonization in 2024, Nat Rev Earth Environ, 6, 231–233, https://doi.org/10.1038/s43017-025-00658-x, 2025.

Denier van der Gon, H., Gauss, M., Granier, C., Arellano, S., Benedictow, A., Darras, S., Dellaert, S., Guevara, M., Jalkanen, J.-P., Krueger, K., Kuenen, J., Liaskoni, M., Liousse, C., Markova, J., Prieto Perez, A., Quack, B., Simpson, D., Sindelarova, K., and Soulie, A.: Documentation of CAMS emission inventory products, https://doi.org/10.24380/Q2SI-TI6I, 2023.

Dhakal, S., J. C. Minx, F. L. Toth, A. Abdel-Aziz, M. J. Figueroa Meza, K. Hubacek, I. G. C. Jonckheere, Yong-Gun Kim, G. F. Nemet, S. Pachauri, X. C. Tan, T. Wiedmann: Emissions Trends and Drivers. In IPCC, 2022: Climate Change 2022: Mitigation of Climate Change. Contribution of Working Group III to the Sixth Assessment Report of the Intergovernmental Panel on Climate Change [P.R. Shukla, J. Skea, R. Slade, A. Al Khourdajie, R. van Diemen, D. McCollum, M. Pathak, S. Some, P. Vyas, R. Fradera, M. Belkacemi, A. Hasija, G. Lisboa, S. Luz, J. Malley, (eds.)]. Cambridge University Press, Cambridge, UK and New York, NY, USA, https://doi.org/10.1017/9781009157926.004, 2022.

Douville, H., K. Raghavan, J. Renwick, R.P. Allan, P.A. Arias, M. Barlow, R. Cerezo-Mota, A. Cherchi, T.Y. Gan, J. Gergis, D. Jiang, A. Khan, W. Pokam Mba, D. Rosenfeld, J. Tierney, and O. Zolina: Water Cycle Changes. In Climate Change 2021: The Physical Science Basis. Contribution of Working Group I to the Sixth Assessment Report of the Intergovernmental Panel on Climate Change [Masson-Delmotte, V., P. Zhai, A. Pirani, S.L. Connors, C. Péan, S. Berger, N. Caud, Y. Chen, L. Goldfarb, M.I. Gomis, M. Huang, K. Leitzell, E. Lonnoy, J.B.R. Matthews, T.K. Maycock, T. Waterfield, O. Yelekçi, R. Yu, and B. Zhou (eds.)]. Cambridge University Press, Cambridge, United Kingdom and New York, NY, USA, pp. 1055–1210, https://doi.org/10.1017/9781009157896.010, 2021.

Droste, E. S., Adcock, K. E., Ashfold, M. J., Chou, C., Fleming, Z., Fraser, P. J., Gooch, L. J., Hind, A. J., Langenfelds, R. L., Leedham Elvidge, E. C., Mohd Hanif, N., O'Doherty, S., Oram, D. E., Ou-Yang, C.-F., Panagi, M., Reeves, C. E., Sturges, W. T., and Laube, J. C.: Trends and emissions of six perfluorocarbons in the Northern Hemisphere and Southern Hemisphere, Atmos. Chem. Phys., 20, 4787–4807, https://doi.org/10.5194/acp-20-4787-2020, 2020.

Dunn, R. J. H., Alexander, L. V., Donat, M. G., Zhang, X., Bador, M., Herold, N., Lippmann, T., Allan, R., Aguilar, E., Barry, A. A., Brunet, M., Caesar, J., Chagnaud, G., Cheng, V., Cinco, T., Durre, I., Guzman, R., Htay, T. M., Wan Ibadullah, W. M., Bin Ibrahim, M. K. I., Khoshkam, M., Kruger, A., Kubota, H., Leng, T. W., Lim, G., Li-Sha, L., Marengo, J., Mbatha, S., McGree, S., Menne, M., Milagros Skansi, M., Ngwenya, S., Nkrumah, F., Oonariya, C., Pabon-Caicedo, J. D., Panthou, G., Pham, C., Rahimzadeh, F., Ramos, A., Salgado, E., Salinger, J., Sané, Y., Sopaheluwakan, A., Srivastava, A., Sun, Y., Timbal, B., Trachow, N., Trewin, B., Schrier, G., Vazquez-Aguirre, J., Vasquez, R., Villarroel, C., Vincent, L., Vischel, T., Vose, R., and Bin Hj Yussof, M. N.: Development of an updated global land in situ-based data set of temperature and precipitation extremes: HadEX3, J. Geophys. Res.-Atmos., 125, e2019JD032263, https://doi.org/10.1029/2019JD032263, 2020.

Dunn, R. J. H., Donat, M. G., and Alexander, L. V.: Comparing extremes indices in recent observational and reanalysis products, Front. Clim., 4, 98905, https://doi.org/10.3389/fclim.2022.989505, 2022.

Dunn, R.J.H., Alexander, L., Donat, M., Zhang, X., Bador, M., Herold, N., Lippmann, T., Allan, R.J., Aguilar, E., Aziz, A., Brunet, M., Caesar, J., Chagnaud, G., Cheng, V., Cinco, T., Durre, I., de Guzman, R., Htay, T.M., Wan Ibadullah, W.M., Bin Ibrahim, M.K.I., Khoshkam, M., Kruge, A., Kubota, H., Leng, T.W., Lim, G., Li-Sha, L., Marengo, J., Mbatha, S., McGree, S., Menne, M., de los Milagros Skansi, M., Ngwenya, S., Nkrumah, F., Oonariya, C., Pabon-Caicedo, J.D., Panthou, G., Pham, C., Rahimzadeh, F., Ramos, A., Salgado, E., Salinger, J., Sane, Y., Sopaheluwakan, A., Srivastava, A., Sun, Y., Trimbal, B., Trachow, N., Trewin, B., van der Schrier, G., Vazquez-Aguirre, J., Vasquez, R., Villarroel, C., Vincent, L., Vischel, T., Vose, R., Bin Hj Yussof, and M.N.A.: HadEX3: Global land-surface climate extremes indices v3.0.4 (1901-2018), NERC EDS Centre for Environmental Data Analysis [data set], https://dx.doi.org/10.5285/115d5e4ebf7148ec941423ec86fa9f26, 2023.

Dunn, R. J. H., Blannin, J., Gobron, N., Miller, J. B. and Willett, K. M. eds: Global climate [in "State of the Climate in 2023"]. Bull. Amer. Meteor. Soc., 105, S12-S155, https://doi.org/10.1175/BAMS-D-24-0116.1, 2024.

Dutton, G.S., B. D. Hall, S.A. Montzka, J. D. Nance, S. D. Clingan, K. M. Petersen, Combined Atmospheric Chloroflurocarbon-12 Dry Air Mole Fractions from the NOAA GML Halocarbons Sampling Network, 1977-2024, Version: 2024-03-07, https://doi.org/10.15138/PJ63-H440, 2024.

ECCAD: CAMS database version 6.2 (v6.2), https://permalink.aeris-data.fr/CAMS-GLOB-ANT, [data set], accessed 20 April 2025, 2025.

Eyring, V., N. P. Gillett, K.M. Achuta Rao, R. Barimalala, M. Barreiro Parrillo, N. Bellouin, C. Cassou, P. J. Durack, Y. Kosaka, S. McGregor, S. Min, O. Morgenstern, and Y. Sun: Human Influence on the Climate System. In Climate Change 2021: The Physical Science Basis. Contribution of Working Group I to the Sixth Assessment Report of the Intergovernmental Panel on Climate Change[Masson-Delmotte, V., P. Zhai, A. Pirani, S.L. Connors, C. Péan, S. Berger, N. Caud, Y. Chen, L. Goldfarb, M.I. Gomis, M. Huang, K. Leitzell, E. Lonnoy, J.B.R. Matthews, T.K. Maycock, T. Waterfield, O. Yelekçi, R. Yu, and B. Zhou (eds.)]. Cambridge University Press, Cambridge, United Kingdom and New York, NY, USA, pp. 423–552, http://doi:10.1017/9781009157896.005, 2021.

Feron, S., Malhotra, A., Bansal, S., Fluet-Chouinard, E., McNicol, G., Knox, S. H., Delwiche, K. B., Cordero, R. R., Ouyang, Z., Zhang, Z., Poulter, B., and Jackson, R. B.: Recent increases in annual, seasonal, and extreme methane fluxes driven by changes in climate and vegetation in boreal and temperate wetland ecosystems, Global Change Biology, 30, e17131, https://doi.org/10.1111/gcb.17131, 2024.

Forster, P. M., Forster, H. I., Evans, M. J., Gidden, M. J., Jones, C. D., Keller, C. A., Lamboll, R. D., Le Quéré, C., Rogelj, J., Rosen, D., Schleussner, C. F., Richardson, T. B., Smith, C. J. and Turnock, S. T.: Current and future global climate impacts resulting from COVID-19, Nature Clim. Chang, 10, 913–919, https://doi.org/10.1038/s41558-020-0883-0, 2020.

Forster, P., T. Storelvmo, K. Armour, W. Collins, J.-L. Dufresne, D. Frame, D.J. Lunt, T. Mauritsen, M.D. Palmer, M. Watanabe, M. Wild, and H. Zhang, 2021: The Earth's Energy Budget, Climate Feedbacks, and Climate Sensitivity. In Climate Change 2021: The Physical Science Basis. Contribution of Working Group I to the Sixth Assessment Report of the Intergovernmental Panel on Climate Change [Masson-Delmotte, V., P. Zhai, A. Pirani, S.L. Connors, C. Péan, S. Berger, N. Caud, Y. Chen, L. Goldfarb, M.I. Gomis, M. Huang, K. Leitzell, E. Lonnoy, J.B.R. Matthews, T.K. Maycock, T. Waterfield, O. Yelekçi, R. Yu, and B. Zhou (eds.)]. Cambridge University Press, Cambridge, United Kingdom and New York, NY, USA, pp. 923–1054, https://doi.org/10.1017/9781009157896.009, 2021.

Forster, P., Smith, C., Walsh, T., Lamb, W., Lamboll, R., Hauser, M., Ribes, A., Rosen, D., Gillett, N., Palmer, M., Rogelj, J., von Schuckmann, K., Seneviratne, S., Trewin, B., Zhang, X., Allen, M., Andrew, R., Birt, A., Borger, A., Boyer, T., Broersma, J., Cheng, L., Dentener, F., Friedlingstein, P., Gutiérrez, J., Gütschow, J., Hall, B., Ishii, M., Jenkins, S., Lan, X., Lee, J.-Y., Morice, C., Kadow, C., Kennedy, J., Killick, R., Minx, J., Naik, V., Peters, G., Pirani, A., Pongratz, J., Schleussner, C.-F., Szopa, S., Thorne, P., Rohde, R., Rojas Corradi, M., Schumacher, D., Vose, R., Zickfeld, K., Masson-Delmotte, V., and Zhai, P.: Indicators of Global Climate Change 2022: annual update of large-scale indicators of the state of the climate system and human influence, Earth System Science Data, 15, 2295–2327, https://doi.org/10.5194/essd-15-2295-2023, 2023.

Forster, P. M., Smith, C., Walsh, T., Lamb, W. F., Lamboll, R., Hall, B., Hauser, M., Ribes, A., Rosen, D., Gillett, N. P., Palmer, M. D., Rogelj, J., Von Schuckmann, K., Trewin, B., Allen, M., Andrew, R., Betts, R. A., Borger, A., Boyer, T., Broersma, J. A., Buontempo, C., Burgess, S., Cagnazzo, C., Cheng, L., Friedlingstein, P., Gettelman, A., Gütschow, J., Ishii, M., Jenkins, S., Lan, X., Morice, C., Mühle, J., Kadow, C., Kennedy, J., Killick, R. E., Krummel, P. B., Minx, J. C., Myhre, G., Naik, V., Peters, G. P., Pirani, A., Pongratz, J., Schleussner, C.-F., Seneviratne, S. I., Szopa, S., Thorne, P., Kovilakam, M. V. M., Majamäki, E., Jalkanen, J.-P., Van Marle, M., Hoesly, R. M., Rohde, R., Schumacher, D., Van Der Werf, G., Vose, R., Zickfeld, K., Zhang, X., Masson-Delmotte, V., and Zhai, P.: Indicators of Global Climate Change 2023: annual update of key indicators of the state of the climate system and human influence, Earth Syst. Sci. Data, 16, 2625–2658, https://doi.org/10.5194/essd-16-2625-2024, 2024.

Fox-Kemper, B.,Fox-Kemper, B., H. T. Hewitt, C. Xiao, G. Aðalgeirsdóttir, S.S. Drijfhout, T. L. Edwards, N. R. Golledge, M. Hemer, R. E. Kopp, G. Krinner, A. Mix, D. Notz, S. Nowicki, I. S. Nurhati, L. Ruiz, J.-B. Sallée, A. B. A. Slangen, and Y. Yu: Ocean, Cryosphere and Sea Level Change. In Climate Change 2021: The Physical Science Basis. Contribution of Working Group I to the Sixth Assessment Report of the Intergovernmental Panel on Climate

Change [Masson-Delmotte, V., P. Zhai, A. Pirani, S.L. Connors, C. Péan, S. Berger, N. Caud, Y. Chen, L. Goldfarb, M.I. Gomis, M. Huang, K. Leitzell, E. Lonnoy, J. B. R. Matthews, T. K. Maycock, T. Waterfield, O. Yelekçi, R. Yu, and B. Zhou (eds.)]. Cambridge University Press, Cambridge, United Kingdom and New York, NY, USA, pp. 1211–1362, https://doi.org/10.1017/9781009157896.011, 2021.

Francey, R.J., L.P. Steele, R.L. Langenfelds and B.C. Pak, High precision long-term monitoring of radiatively-active trace gases at surface sites and from ships and aircraft in the Southern Hemisphere atmosphere, J. Atmos. Science, 56, 279-285 https://doi.org/10.1175/1520-0469(1999)056<0279:HPLTMO>2.0.CO;2, 1999.

Frederikse, T., Landerer, F., Caron, L., Adhikari, S., Parkes, D., Humphrey, V. W., Dangendorf, S., Hogarth, P., Zanna, L., Cheng, L., and Wu, Y.-H.: The causes of sea-level rise since 1900, Nature, 584, 393–397, https://doi.org/10.1038/s41586-020-2591-3, 2020.

Friedlingstein, P., O'Sullivan, M., Jones, M. W., Andrew, R. M., Hauck, J., Olsen, A., Peters, G. P., Peters, W., Pongratz, J., Sitch, S., Le Quéré, C., Canadell, J. G., Ciais, P., Jackson, R. B., Alin, S., Aragão, L. E. O. C., Arneth, A., Arora, V., Bates, N. R., Becker, M., Benoit-Cattin, A., Bittig, H. C., Bopp, L., Bultan, S., Chandra, N., Chevallier, F., Chini, L. P., Evans, W., Florentie, L., Forster, P. M., Gasser, T., Gehlen, M., Gilfillan, D., Gkritzalis, T., Gregor, L., Gruber, N., Harris, I., Hartung, K., Haverd, V., Houghton, R. A., Ilyina, T., Jain, A. K., Joetzjer, E., Kadono, K., Kato, E., Kitidis, V., Korsbakken, J. I., Landschützer, P., Lefèvre, N., Lenton, A., Lienert, S., Liu, Z., Lombardozzi, D., Marland, G., Metzl, N., Munro, D. R., Nabel, J. E. M. S., Nakaoka, S.-I., Niwa, Y., O'Brien, K., Ono, T., Palmer, P. I., Pierrot, D., Poulter, B., Resplandy, L., Robertson, E., Rödenbeck, C., Schwinger, J., Séférian, R., Skjelvan, I., Smith, A. J. P., Sutton, A. J., Tanhua, T., Tans, P. P., Tian, H., Tilbrook, B., van der Werf, G., Vuichard, N., Walker, A. P., Wanninkhof, R., Watson, A. J., Willis, D., Wiltshire, A. J., Yuan, W., Yue, X., and Zaehle, S.: Global carbon budget 2020, Earth Syst. Sci. Data, 12, 3269–3340, https://doi.org/10.5194/essd-12-3269-2020, 2020.

Friedlingstein, P., O'Sullivan, M., Jones, M. W., Andrew, R. M., Gregor, L., Hauck, J., Le Quéré, C., Luijkx, I. T., Olsen, A., Peters, G. P., Peters, W., Pongratz, J., Schwingshackl, C., Sitch, S., Canadell, J. G., Ciais, P., Jackson, R. B., Alin, S. R., Alkama, R., Arneth, A., Arora, V. K., Bates, N. R., Becker, M., Bellouin, N., Bittig, H. C., Bopp, L., Chevallier, F., Chini, L. P., Cronin, M., Evans, W., Falk, S., Feely, R. A., Gasser, T., Gehlen, M., Gkritzalis, T., Gloege, L., Grassi, G., Gruber, N., Gürses, Ö., Harris, I., Hefner, M., Houghton, R. A., Hurtt, G. C., Iida, Y., Ilyina, T., Jain, A. K., Jersild, A., Kadono, K., Kato, E., Kennedy, D., Klein Goldewijk, K., Knauer, J., Korsbakken, J. I., Landschützer, P., Lefèvre, N., Lindsay, K., Liu, J., Liu, Z., Marland, G., Mayot, N., McGrath, M. J., Metzl, N., Monacci, N. M., Munro, D. R., Nakaoka, S.-I., Niwa, Y., O'Brien, K., Ono, T., Palmer, P. I., Pan, N., Pierrot, D., Pocock, K., Poulter, B., Resplandy, L., Robertson, E., Rödenbeck, C., Rodriguez, C., Rosan, T. M., Schwinger, J., Séférian, R., Shutler, J. D., Skjelvan, I., Steinhoff, T., Sun, Q., Sutton, A. J., Sweeney, C., Takao, S., Tanhua, T., Tans, P. P., Tian, X., Tian, H., Tilbrook, B., Tsujino, H., Tubiello, F., van der Werf, G. R., Walker, A. P., Wanninkhof, R., Whitehead, C., Willstrand Wranne, A., et al.: Global Carbon Budget 2022, Earth Syst. Sci. Data, 14, 4811–4900, https://doi.org/10.5194/essd-14-4811-2022, 2022.

Friedlingstein, P., O'Sullivan, M., Jones, M. W., Andrew, R. M., Bakker, D. C. E., Hauck, J., Landschützer, P., Le Quéré, C., Luijkx, I. T., Peters, G. P., Peters, W., Pongratz, J., Schwingshackl, C., Sitch, S., Canadell, J. G., Ciais, P., Jackson, R. B., Alin, S. R., Anthoni, P., Barbero, L., Bates, N. R., Becker, M., Bellouin, N., Decharme, B., Bopp, L., Brasika, I. B. M., Cadule, P., Chamberlain, M. A., Chandra, N., Chau, T.-T.-T., Chevallier, F., Chini, L. P., Cronin, M., Dou, X., Enyo, K., Evans, W., Falk, S., Feely, R. A., Feng, L., Ford, D. J., Gasser, T., Ghattas, J., Gkritzalis, T., Grassi, G., Gregor, L., Gruber, N., Gürses, Ö., Harris, I., Hefner, M., Heinke, J., Houghton, R. A., Hurtt, G. C., Iida, Y., Ilyina, T., Jacobson, A. R., Jain, A., Jarníková, T., Jersild, A., Jiang, F., Jin, Z., Joos, F., Kato, E., Keeling, R. F., Kennedy, D., Klein Goldewijk, K., Knauer, J., Korsbakken, J. I., Körtzinger, A., Lan, X., Lefèvre, N., Li, H., Liu, J., Liu, Z., Ma, L., Marland, G., Mayot, N., McGuire, P. C., McKinley, G. A., Meyer, G., Morgan, E. J., Munro, D. R., Nakaoka, S.-I., Niwa, Y., O'Brien, K. M., Olsen, A., Omar, A. M., Ono, T., Paulsen, M., Pierrot, D., Pocock, K., Poulter, B., Powis, C. M., Rehder, G., Resplandy, L., Robertson, E., Rödenbeck, C., Rosan, T. M., Schwinger, J., Séférian, R., et al.: Global Carbon Budget 2023, Earth System Science Data, 15, 5301–5369, https://doi.org/10.5194/essd-15-5301-2023, 2023.

Friedlingstein, P., O'Sullivan, M., Jones, M. W., Andrew, R. M., Hauck, J., Landschützer, P., Le Quéré, C., Li, H., Luijkx, I. T., Olsen, A., Peters, G. P., Peters, W., Pongratz, J., Schwingshackl, C., Sitch, S., Canadell, J. G., Ciais, P., Jackson, R. B., Alin, S. R., Arneth, A., Arora, V., Bates, N. R., Becker, M., Bellouin, N., Berghoff, C. F., Bittig, H. C., Bopp, L., Cadule, P., Campbell, K., Chamberlain, M. A., Chandra, N., Chevallier, F., Chini, L. P., Colligan, T., Decayeux, J., Djeutchouang, L. M., Dou, X., Duran Rojas, C., Enyo, K., Evans, W., Fay, A. R., Feely, R. A., Ford, D. J., Foster, A., Gasser, T., Gehlen, M., Gkritzalis, T., Grassi, G., Gregor, L., Gruber, N., Gürses, Ö., Harris, I., Hefner, M., Heinke, J., Hurtt, G. C., Iida, Y., Ilyina, T., Jacobson, A. R., Jain, A. K., Jarníková, T., Jersild, A., Jiang, F., Jin, Z., Kato, E., Keeling, R. F., Klein Goldewijk, K., Knauer, J., Korsbakken, J. I., Lan, X., Lauvset, S. K., Lefèvre, N., Liu, Z., Liu, J., Ma, L., Maksyutov, S., Marland, G., Mayot, N., McGuire, P. C., Metzl, N., Monacci, N. M., Morgan, E. J., Nakaoka, S.-I., Neill, C., Niwa, Y., Nützel, T., Olivier, L., Ono, T., Palmer, P. I., Pierrot, D., Qin, Z., Resplandy, L., Roobaert, A., Rosan, T. M., Rödenbeck, C., Schwinger, J., Smallman, T. L., Smith, S. M., Sospedra-Alfonso, R., Steinhoff, T., Sun, Q., Sutton, A. J., Séférian, R., Takao, S., Tatebe, H., Tian, H., Tilbrook, B., Torres, O., Tourigny, E., Tsujino, H., Tubiello, F., van der Werf, G., Wanninkhof, R., Wang, X., Yang, D., Yang, X., Yu, Z., Yuan, W., Yue, X., Zaehle, S., Zeng, N., and Zeng, J.: Global Carbon Budget 2024, Earth Syst. Sci. Data, 17, 965–1039, https://doi.org/10.5194/essd-17-965-2025, 2025.

Gasser, T., Crepin, L., Quilcaille, Y., Houghton, R. A., Ciais, P., and Obersteiner, M.: Historical CO2 emissions from land use and land cover change and their uncertainty, Biogeosciences, 17, 4075–4101, https://doi.org/10.5194/bg-17-4075-2020, 2020.

Gidden, M. J., Gasser, T., Grassi, G., Forsell, N., Janssens, I., Lamb, W. F., Minx, J., Nicholls, Z., Steinhauser, J., and Riahi, K.: Aligning climate scenarios to emissions inventories shifts global benchmarks, Nature, 624, 102–108, https://doi.org/10.1038/s41586-023-06724-y, 2023.

Gillett, N.P., Kirchmeier-Young, M., Ribes, A., Shiogama, H., Hegerl, G.C., Knutti, R., Gastineau, G., John, J.G., Li, L., Nazarenko, L., Rosenbloom, N., Seland, Ø., Wu, T., Yukimoto, S., and Ziehn, T.: Constraining human contributions to observed warming since the pre-industrial period, Nat. Clim. Chang., 11, 207–212, https://doi.org/10.1038/s41558-020-00965-9, 2021.

Gleckler, P. J., Durack, P. J., Stouffer, R. J., Johnson, G. C., and Forest, C. E.: Industrial-era global ocean heat uptake doubles in recent decades, Nat. Clim. Chang., 6, 394–398, https://doi.org/10.1038/nclimate2915, 2016.

Goessling, H. F., Rackow, T., and Jung, T.: Recent global temperature surge intensified by record-low planetary albedo, Science, 387, 68–73, https://doi.org/10.1126/science.adq7280, 2025.

Grassi, G., Stehfest, E., Rogelj, J., Van Vuuren, D., Cescatti, A., House, J., Nabuurs, G.-J., Rossi, S., Alkama, R., Viñas, R. A., Calvin, K., Ceccherini, G., Federici, S., Fujimori, S., Gusti, M., Hasegawa, T., Havlik, P., Humpenöder, F., Korosuo, A., Perugini, L., Tubiello, F. N., and Popp, A.: Critical adjustment of land mitigation pathways for assessing countries' climate progress, Nat. Clim. Chang., 11, 425–434, https://doi.org/10.1038/s41558-021-01033-6, 2021.

Grassi, G., Schwingshackl, C., Gasser, T., Houghton, R. A., Sitch, S., Canadell, J. G., Cescatti, A., Ciais, P., Federici, S., Friedlingstein, P., Kurz, W. A., Sanz Sanchez, M. J., Abad Viñas, R., Alkama, R., Bultan, S., Ceccherini, G., Falk, S., Kato, E., Kennedy, D., Knauer, J., Korosuo, A., Melo, J., McGrath, M. J., Nabel, J. E. M. S., Poulter, B., Romanovskaya, A. A., Rossi, S., Tian, H., Walker, A. P., Yuan, W., Yue, X., and Pongratz, J.: Harmonising the land-use flux estimates of global models and national inventories for 2000–2020, Earth Syst. Sci. Data, 15, 1093–1114, https://doi.org/10.5194/essd-15-1093-2023, 2023.

Guinaldo, T., Cassou, C., Sallée, J.-B., and Liné, A.: Internal variability effect doped by climate change drove the 2023 marine heat extreme in the North Atlantic, Commun Earth Environ, 6, 291, https://doi.org/10.1038/s43247-025-02197-1, 2025.

Gulev, S. K., P. W. Thorne, J. Ahn, F. J. Dentener, C. M. Domingues, S. Gerland, D. Gong, D. S. Kaufman, H. C. Nnamchi, J. Quaas, J.A. Rivera, S. Sathyendranath, S.L. Smith, B. Trewin, K. von Schuckmann, and R. S. Vose: Changing State of the Climate System. In Climate Change 2021: The Physical Science Basis. Contribution of Working Group I to the Sixth Assessment Report of the Intergovernmental Panel on Climate Change[Masson-Delmotte, V., P. Zhai, A. Pirani, S.L. Connors, C. Péan, S. Berger, N. Caud, Y. Chen, L. Goldfarb, M.I. Gomis, M. Huang, K. Leitzell, E. Lonnoy, J.B.R. Matthews, T.K. Maycock, T. Waterfield, O. Yelekçi, R. Yu, and B. Zhou (eds.)]. Cambridge University Press, Cambridge, United Kingdom and New York, NY, USA, pp. 287–422, https://doi.org/10.1017/9781009157896.004, 2021.

Gupta, A. K., Mittal, T., Fauria, K. E., Bennartz, R., and Kok, J. F.: The January 2022 Hunga eruption cooled the southern hemisphere in 2022 and 2023, Commun Earth Environ, 6, 240, https://doi.org/10.1038/s43247-025-02181-9, 2025.

Gütschow, J., Jeffery, M. L., Gieseke, R., Gebel, R., Stevens, D., Krapp, M., and Rocha, M.: The PRIMAP-hist national historical emissions time series, Earth Syst. Sci. Data, 8, 571–603, https://doi.org/10.5194/essd-8-571-2016, 2016.

Gütschow, J., and Busch, D., and Pflüger, M.: The PRIMAP-hist national historical emissions time series v2.6.1 (1750-2023) (2.6.1), Zenodo [data set] https://doi.org/10.5281/zenodo.15016289, 2025.

Hardy, A., Palmer, P. I., and Oakes, G.: Satellite data reveal how Sudd wetland dynamics are linked with globally-significant methane emissions, Environ. Res. Lett., 18, 074044, https://doi.org/10.1088/1748-9326/ace272, 2023.

Hay, C. C., Morrow, E., Kopp, R. E., and Mitrovica, J. X.: Probabilistic reanalysis of twentieth-century sea-level rise, Nature, 517, 481–484, https://doi.org/10.1038/nature14093, 2015.

Hakuba, M. Z., Frederikse, T., and Landerer, F. W.: Earth's energy imbalance from the ocean perspective (2005–2019), Geophys Res Lett, 48, e2021GL093624, https://doi.org/10.1029/2021GL093624, 2021.

Hansen, J. E., Sato, M., Simons, L., Nazarenko, L. S., Sangha, I., Kharecha, P., Zachos, J. C., von Schuckmann, K., Loeb, N. G., Osman, M. B., Jin, Q., Tselioudis, G., Jeong, E., Lacis, A., Ruedy, R., Russell, G., Cao, J., and Li, J.: Global warming in the pipeline, Oxford Open Climate Change, 3, kgad008, https://doi.org/10.1093/oxfclm/kgad008, 2023.

Hansis, E., Davis, S. J., and Pongratz, J.: Relevance of methodological choices for accounting of land use change carbon fluxes, Global Biogeochem. Cy., 29, 1230–1246, https://doi.org/10.1002/2014GB004997, 2015.

Haustein, K., Allen, M. R., Forster, P. M., Otto, F. E. L., Mitchell, D. M., Matthews, H. D., and Frame, D. J.: A real-time Global Warming Index, Sci Rep, 7, 15417, https://doi.org/10.1038/s41598-017-14828-5, 2017.

Harris, I., Osborn, T. J., Jones, P., and Lister, D.: Version 4 of the CRU TS monthly high-resolution gridded multivariate climate dataset, Scientific data, 7, 109, https://doi.org/10.1038/s41597-020-045303, 2020

Hersbach, H., Bell, B., Berrisford, P., Hirahara, S., Horányi, A., Muñoz-Sabater, J., Nicolas, J., Peubey, C., Radu, R., Schepers, D., Simmons, A., Soci, C., Abdalla, S., Abellan, X., Balsamo, G., Bechtold, P., Biavati, G., Bidlot, J., Bonavita, M., De Chiara, G., Dahlgren, P., Dee, D., Diamantakis, M., Dragani, R., Flemming, J., Forbes, R., Fuentes, M., Geer, A., Haimberger, L., Healy, S., Hogan, R. J., Hólm, E., Janisková, M., Keeley, S., Laloyaux, P., Lopez, P., Lupu, C., Radnoti, G., de Rosnay, P., Rozum, I., Vamborg, F., Villaume, S., and Thépaut, J.-N.: The ERA5 global reanalysis, Q. J. R. Meteorol. Soc., 146, 1999–2049, https://doi.org/10.1002/qj.3803, 2020.

Hodnebrog, Ø., Aamaas, B., Fuglestvedt, J. S., Marston, G., Myhre, G., Nielsen, C. J., Sandstad, M., Shine, K. P., and Wallington, T. J.: Updated Global Warming Potentials and Radiative Efficiencies of Halocarbons and Other Weak Atmospheric Absorbers, Rev. Geophys., 58, e2019RG000691, https://doi.org/10.1029/2019RG000691, 2020.

Hodnebrog, Ø., Myhre, G., Jouan, C., Andrews, T., Forster, P. M., Jia, H., Loeb, N. G., Olivié, D. J. L., Paynter, D., Quaas, J., Raghuraman, S. P., and Schulz, M.: Recent reductions in aerosol emissions have increased Earth's energy imbalance, Communications Earth & Environment, 5, 166, https://doi.org/10.1038/s43247-024-01324-8, 2024.

Hoesly, R., Smith, S. J., Ahsan, H., Prime, N., O'Rourke, P., Crippa, M., Klimont, Z., Guizzardi, D., Feng, L., Harkins, C., MCDONALD, B., and Wang, S.: CEDS v_2025_03_18 Aggregate Data (v_2025_03_18), https://doi.org/10.5281/ZENODO.15059443, 2025.

Hoesly, R. M., Smith, S. J., Feng, L., Klimont, Z., Janssens-Maenhout, G., Pitkanen, T., Seibert, J. J., Vu, L., Andres, R. J., Bolt, R. M., Bond, T. C., Dawidowski, L., Kholod, N., Kurokawa, J.-I., Li, M., Liu, L., Lu, Z., Moura, M. C. P.,

O'Rourke, P. R., and Zhang, Q.: Historical (1750–2014) anthropogenic emissions of reactive gases and aerosols from the Community Emissions Data System (CEDS), Geosci. Model. Dev., 11, 369–408, https://doi.org/10.5194/gmd-11-369-2018, 2018.

Hoesly, R., & Smith, S., CEDS v_2024_04_01 Release Emission Data (v_2024_04_01) [Data set], Zenodo. https://doi.org/10.5281/zenodo.10904361, 2024.

Houghton, R. A., and Nassikas, A. A.: Global and regional fluxes of carbon from land use and land cover change 1850–2015, Global Biogeochem. Cy., 31, 456– 472, https://doi.org/10.1002/2016GB005546, 2017.

Houghton, R. A. and Castanho, A.: Annual emissions of carbon from land use, land-use change, and forestry from 1850 to 2020, Earth System Science Data, 15, 2025–2054, https://doi.org/10.5194/essd-15-2025-2023, 2023.

Hu, Y., Yue, X., Tian, C., Zhou, H., Fu, W., Zhao, X., Zhao, Y., and Chen, Y.: Identifying the main drivers of the spatiotemporal variations in wetland methane emissions during 2001–2020, Frontiers in Environmental Science, 11, https://doi.org/10.3389/fenvs.2023.1275742, 2023.

Huang, B., Yin, X., Boyer, T., Liu, C., Menne, M., Rao, Y. D., Smith, T., Vose, R., and Zhang, H.-M.: Extended Reconstructed Sea Surface Temperature, Version 6 (ERSSTv6). Part I: An Artificial Neural Network Approach, Journal of Climate, 38, 1105–1121, https://doi.org/10.1175/JCLI-D-23-0707.1, 2025.

IATA: Air Passenger Monthly Analysis March 2024, https://www.iata.org/en/iata-repository/publications/economic-reports/air-passenger-market-analysis-march-2024/, accessed 20.05.2024, 2024.

IEA: CO2 Emissions in 2023. https://www.iea.org/reports/co2-emissions-in-2023, accessed 20.04.2024, 2024.

IPCC: Sixty-second Session of the IPCC (IPCC-62), Fifteenth Session of the IPCC Working Group I (WGI-15), Thirteenth Session of the IPCC Working Group II (WGII-13), and Fifteenth Session of the IPCC Working Group III (WGIII-15), https://www.ipcc.ch/meeting-doc/ipcc-62/, accessed 20 April 2025, 2025.

IPCC: Climate Change 2013: The Physical Science Basis. Contribution of Working Group I to the Fifth Assessment Report of the Intergovernmental Panel on Climate Change [Stocker, T.F., D. Qin, G.-K. Plattner, M. Tignor, S.K. Allen, J. Boschung, A. Nauels, Y. Xia, V. Bex and P.M. Midgley (eds.)]. Cambridge University Press, Cambridge, United Kingdom and New York, NY, USA, 1535 pp, https://doi:10.1017/CBO9781107415324, 2013.

IPCC: Summary for Policymakers. In: Global Warming of 1.5°C. An IPCC Special Report on the impacts of global warming of 1.5°C above pre-industrial levels and related global greenhouse gas emission pathways, in the context of strengthening the global response to the threat of climate change, sustainable development, and efforts to eradicate poverty [Masson-Delmotte, V., P. Zhai, H.-O. Pörtner, D. Roberts, J. Skea, P.R. Shukla, A. Pirani, W. Moufouma-Okia, C. Péan, R. Pidcock, S. Connors, J.B.R. Matthews, Y. Chen, X. Zhou, M.I. Gomis, E. Lonnoy, T. Maycock, M. Tignor, and T. Waterfield (eds.)]. Cambridge University Press, Cambridge, UK and New York, NY, USA, pp. 3-24, https://doi.org/10.1017/9781009157940.001, 2018.

IPCC: Climate Change 2021: The Physical Science Basis. Contribution of Working Group I to the Sixth Assessment Report of the Intergovernmental Panel on Climate Change, Cambridge University Press, Cambridge, United Kingdom and New York, NY, USA, https://doi.org/10.1017/9781009157896, 2021a.

IPCC: Summary for Policymakers, in: Climate Change 2021: The Physical Science Basis. Contribution of Working Group I to the Sixth Assessment Report of the Intergovernmental Panel on Climate Change, edited by: Masson-Delmotte, V., Zhai, P., Pirani, A., Connors, S. L., Péan, C., Berger, S., Caud, N., Chen, Y., Goldfarb, L., Gomis, M. I., Huang, M., Leitzell, K., Lonnoy, E., Matthews, J. B. R., Maycock, T. K., Waterfield, T., Yelekçi, O., Yu, R., and Zhou, B., Cambridge University Press, Cambridge, United Kingdom and New York, NY, USA, pp.3–32 https://doi.org/10.1017/9781009157896.001, 2021b.

IPCC: Climate Change 2022: Impacts, Adaptation, and Vulnerability. Contribution of Working Group II to the Sixth Assessment Report of the Intergovernmental Panel on Climate Change [H.-O. Pörtner, D.C. Roberts, M. Tignor, E.S. Poloczanska, K. Mintenbeck, A. Alegría, M. Craig, S. Langsdorf, S. Löschke, V. Möller, A. Okem, B. Rama (eds.)]. Cambridge University Press. Cambridge University Press, Cambridge, UK and New York, NY, USA, 3056 pp., https://doi:10.1017/9781009325844, 2022.

IPCC, 2023: Climate Change 2023: Synthesis Report. Contribution of Working Groups I, II and III to the Sixth Assessment Report of the Intergovernmental Panel on Climate Change [Core Writing Team, H. Lee and J. Romero (eds.)]. IPCC, Geneva, Switzerland., Intergovernmental Panel on Climate Change (IPCC), https://doi.org/10.59327/IPCC/AR6-9789291691647, 2023a.

IPCC, 2023: Climate Change 2023: Summary for Policy Makers. Contribution of Working Groups I, II and III to the Sixth Assessment Report of the Intergovernmental Panel on Climate Change [Core Writing Team, H. Lee and J. Romero (eds.)]. IPCC, Geneva, Switzerland., Intergovernmental Panel on Climate Change (IPCC), https://doi.org/10.59327/IPCC/AR6-9789291691647, 2023b.

Iturbide, M., Fernández, J., Gutiérrez, J. M., Pirani, A., Huard, D., Al Khourdajie, A., Baño-Medina, J., Bedia, J., Casanueva, A., Cimadevilla, E., Cofiño, A. S., De Felice, M., Diez-Sierra, J., García-Díez, M., Goldie, J., Herrera, D. A., Herrera, S., Manzanas, R., Milovac, J., Radhakrishnan, A., San-Martín, D., Spinuso, A., Thyng, K. M., Trenham, C., and Yelekçi, Ö.: Implementation of FAIR principles in the IPCC: the WGI AR6 Atlas repository, Sci Data, 9, 629, https://doi.org/10.1038/s41597-022-01739-y, 2022.

Janardanan, R., Maksyutov, S., Wang, F., Nayagam, L., Sahu, S. K., Mangaraj, P., Saunois, M., Lan, X., and Matsunaga, T.: Country-level methane emissions and their sectoral trends during 2009–2020 estimated by high-resolution inversion of GOSAT and surface observations, Environ. Res. Lett., 19, 034007, https://doi.org/10.1088/1748-9326/ad2436, 2024.

Jenkins, S., Povey, A., Gettelman, A., Grainger, R., Stier, P., and Allen, M.: Is Anthropogenic Global Warming Accelerating?, Journal of Climate, 35, 7873–7890, https://doi.org/10.1175/JCLI-D-22-0081.1, 2022.

Jenkins, S., Smith, C., Allen, M., and Grainger, R.: Tonga eruption increases chance of temporary surface temperature anomaly above 1.5 °C, Nature Clim. Chang., 13, 127–129, https://doi.org/10.1038/s41558-022-01568-2, 2023.

Kirchengast, G., Gorfer, M., Mayer, M., Steiner, A. K., and Haimberger, L.: GCOS EHI 1960-2020 Atmospheric Heat Content, https://doi.org/10.26050/WDCC/GCOS_EHI_1960-2020_AHC, 2022.

Kramer, R. J., He, H., Soden, B. J., Oreopoulos, L., Myhre, G., Forster, P. M., and Smith, C. J., Observational evidence of increasing global radiative forcing, Geophys. Res. Lett., 48, e2020GL091585, https://doi.org/10.1029/2020GL091585, 2021.

Lamb, W., Andrew, R., Jones, M., Nicholls, Z., Peters, G., Smith, C., Saunois, M., Grassi, G., Pongratz, J., Smith, S., Tubiello, F., Crippa, M., Gidden, M., Friedlingstein, P., Minx, J., and Forster, P.: Differences in anthropogenic greenhouse gas emissions estimates explained, https://doi.org/10.5194/essd-2025-188, 24 April 2025.

Lamboll, R. D., Jones, C. D., Skeie, R. B., Fiedler, S., Samset, B. H., Gillett, N. P., Rogelj, J., and Forster, P. M.: Modifying emissions scenario projections to account for the effects of COVID-19: protocol for CovidMIP, Geoscientific Model Development, 14, 3683–3695, https://doi.org/10.5194/gmd-14-3683-2021, 2021.

Lamboll, R. D. and Rogelj, J.: Code for estimation of remaining carbon budget in IPCC AR6 WGI, Zenodo [code], https://doi.org/10.5281/zenodo.6373365, 2022.

Lamboll, R. and Rogelj, J.: Carbon Budget Calculator, 2025, Github [code], https://github.com/Rlamboll/AR6CarbonBudgetCalc/tree/v1.0.1, last access: 25 April 2025, 2025.

Lamboll, R. D., Nicholls, Z. R. J., Smith, C. J., Kikstra, J. S., Byers, E., and Rogelj, J.: Assessing the size and uncertainty of remaining carbon budgets, Nature Climate Change, 13, 1360–1367, https://doi.org/10.1038/s41558-023-01848-5, 2023.

Lan, X., Tans, P. and Thoning, K.W.: Trends in globally-averaged CO_2 determined from NOAA Global Monitoring Laboratory measurements, Version Monday, 14-Apr-2025 09:08:57 MDT https://doi.org/10.15138/9N0H-ZH07, 2025.

Lan, X., Thoning, K. W., and Dlugokencky, E.J.: Trends in globally-averaged CH4 N2O, and SF6 determined from NOAA Global Monitoring Laboratory measurements, Version 2023-04, https://doi.org/10.15138/P8XG-AA10, 2023b.

Laube, J., Newland, M., Hogan, C., Brenninkmeijer, A.M., Fraser, P.J., Martinerie, P., Oram, D.E., Reeves, C.E., Röckmann, T., Schwander, J., Witrant, E., Sturges, W.T.: Newly detected ozone-depleting substances in the atmosphere. Nature Geosci., 7, 266–269, https://doi.org/10.1038/ngeo2109, 2014.

Lee, J.-Y., J. Marotzke, G. Bala, L. Cao, S. Corti, J.P. Dunne, F. Engelbrecht, E. Fischer, J.C. Fyfe, C. Jones, A. Maycock, J. Mutemi, O. Ndiaye, S. Panickal, and T. Zhou: Future Global Climate: Scenario-Based Projections and Near-Term Information. In Climate Change 2021: The Physical Science Basis. Contribution of Working Group I to the Sixth Assessment Report of the Intergovernmental Panel on Climate Change[Masson-Delmotte, V., P. Zhai, A. Pirani, S.L. Connors, C. Péan, S. Berger, N. Caud, Y. Chen, L. Goldfarb, M.I. Gomis, M. Huang, K. Leitzell, E.

Lonnoy, J.B.R. Matthews, T.K. Maycock, T. Waterfield, O. Yelekçi, R. Yu, and B. Zhou (eds.)]. Cambridge University Press, Cambridge, United Kingdom and New York, NY, USA, pp. 553–672,https://doi.org/10.1017/9781009157896.006, 2021.

Lee, H., K. Calvin, D. Dasgupta, G. Krinner, A. Mukherji, P. Thorne, C. Trisos, J. Romero, P. Aldunce, K. Barrett, G. Blanco, W.W.L. Cheung, S.L. Connors, F. Denton, A. Diongue-Niang, D. Dodman, M. Garschagen, O. Geden, B. Hayward, C. Jones, F. Jotzo, T. Krug, R. Lasco, J.-Y. Lee, V. Masson-Delmotte, M. Meinshausen, K. Mintenbeck, A. Mokssit, F.E.L. Otto, M. Pathak, A. Pirani, E. Poloczanska, H.-O. Pörtner, A. Revi, D.C. Roberts, J. Roy, A.C. Ruane, J. Skea, P.R. Shukla, R. Slade, A. Slangen, Y. Sokona, A.A. Sörensson, M. Tignor, D. van Vuuren, Y.-M. Wei, H. Winkler, P. Zhai, and Z. Zommers: Synthesis Report of the IPCC Sixth Assessment Report (AR6): Summary for Policymakers. Intergovernmental Panel on Climate Change [accepted], available at https://www.ipcc.ch/report/ar6/syr/, 2023.

Liu, Z., Deng, Z., Davis, S. J., and Ciais, P.: Global carbon emissions in 2023, Nature Reviews Earth & Environment, 5, 253–254, https://doi.org/10.1038/s43017-024-00532-2, 2024.

Loeb, N. G., Johnson, G. C., Thorsen, T. J., Lyman, J. M., Rose, F. G., Kato, S.: Satellite and ocean data reveal marked increase in Earth's heating rate. Geophys. Res. Lett., 48, e2021GL093047, https://doi.org/10.1029/2021GL093047, 2021.

van Marle, M. J. E., Kloster, S., Magi, B. I., Marlon, J. R., Daniau, A.-L., Field, R. D., Arneth, A., Forrest, M., Hantson, S., Kehrwald, N. M., Knorr, W., Lasslop, G., Li, F., Mangeon, S., Yue, C., Kaiser, J. W., and van der Werf, G. R.: Historic global biomass burning emissions for CMIP6 (BB4CMIP) based on merging satellite observations with proxies and fire models (1750–2015), Geosci. Model Dev., 10, 3329–3357, https://doi.org/10.5194/gmd-10-3329-2017, 2017.

McKenna, C. M., Maycock, A. C., Forster, P. M., Smith, C. J., and Tokarska, K. B.: Stringent mitigation substantially reduces risk of unprecedented near-term warming rates, Nature Climate Change, 11, 126–131, https://doi.org/10.1038/s41558-020-00957-9, 2021.

Menne, M. J., Williams, C. N., Gleason, B. E., Rennie, J. J., and Lawrimore, J. H.: The global historical climatology network monthly temperature dataset, version 4, J. Climate, 31, 9835-9854, https://doi.org/10.1175/JCLI-D-18-0094.1, 2018.

Merchant, C. J., Allan, R.P., Embury, O.: Quantifying the acceleration of multidecadal global sea surface warming driven by Earth's energy imbalance, Environ. Res. Lett., 20, 024037, https://doi.org/10.1088/1748-9326/adaa8a, 2025.

Minière, A., von Schuckmann, K., Sallée, J.-B., and Vogt, L.: Robust acceleration of Earth system heating observed over the past six decades, Scientific Reports, 13, 22975, https://doi.org/10.1038/s41598-023-49353-1, 2023.

Minobe, S., Behrens, E., Findell, K. L., Loeb, N. G., Meyssignac, B., and Sutton, R.: Global and regional drivers for exceptional climate extremes in 2023-2024: beyond the new normal, npj Clim Atmos Sci, 8, 138, https://doi.org/10.1038/s41612-025-00996-z, 2025.

Minx, J. C., Lamb, W. F., Andrew, R. M., Canadell, J. G., Crippa, M., Döbbeling, N., Forster, P. M., Guizzardi, D., Olivier, J., Peters, G. P., Pongratz, J., Reisinger, A., Rigby, M., Saunois, M., Smith, S. J., Solazzo, E., and Tian, H.: A comprehensive and synthetic dataset for global, regional, and national greenhouse gas emissions by sector 1970–2018 with an extension to 2019, Earth Syst. Sci. Data, 13, 5213–5252, https://doi.org/10.5194/essd-13-5213-2021, 2021.

NASA: Satellite sea level observations, [data set], https://sealevel.nasa.gov/understanding-sea-level/key-indicators/global-mean-sea-level/, accessed 19 February 2025, 2025.

Nickolay A. Krotkov, Lok N. Lamsal, Sergey V. Marchenko, Edward A. Celarier, Eric J.Bucsela, William H. Swartz, Joanna Joiner and the OMI core team, OMI/Aura NO2 Cloud-Screened Total and Tropospheric Column L3 Global Gridded 0.25 degree x 0.25 degree V3, NASA Goddard Space Flight Center, Goddard Earth Sciences Data and Information Services Center (GES DISC), Accessed: [Data Access 22 April 2024], https://doi.org/10.5067/Aura/OMI/DATA3007, 2019. Nisbet, E. G., Manning, M. R., Dlugokencky, E. J., Michel, S. E., Lan, X., Roeckmann, T., Gon, H. A. D. V. D., Palmer, P., Oh, Y., Fisher, R., Lowry, D., France, J. L., and White, J. W. C.: Atmospheric methane: Comparison between methane's record in 2006-2022 and during glacial terminations, Preprints, https://doi.org/10.22541/essoar.167689502.25042797/v1, 2023.

Nitzbon, J., Krinner, G., Langer, M.: GCOS EHI 1960-2020 Permafrost Heat Content, World Data Center for Climate (WDCC) at DKRZ, https://doi.org/10.26050/WDCC/GCOS_EHI_1960-2020_PHC, 2022.

NOAA: Global sea level timeseries, https://www.star.nesdis.noaa.gov/socd/lsa/SeaLevelRise/LSA_SLR_timeseries.php , [data set], accessed 19 February 2025, 2025.

Palmer, M. D. and McNeall, D. J.: Internal variability of Earth's energy budget simulated by CMIP5 climate models, Environ. Res. Lett., 9, 034016, https://doi.org/10.1088/1748-9326/9/3/034016, 2014.

Palmer, M. D., Domingues, C. M., Slangen, A. B. A., and Boeira Dias, F.: An ensemble approach to quantify global mean sea-level rise over the 20th century from tide gauge reconstructions, Environ. Res. Lett., 16, 044043, https://doi.org/10.1088/1748-9326/abdaec, 2021.

Peng, S., Lin, X., Thompson, R. L., Xi, Y., Liu, G., Hauglustaine, D., Lan, X., Poulter, B., Ramonet, M., Saunois, M., Yin, Y., Zhang, Z., Zheng, B., and Ciais, P.: Wetland emission and atmospheric sink changes explain methane growth in 2020, Nature, 612, 477–482, https://doi.org/10.1038/s41586-022-05447-w, 2022.

Pelz, S., Ganti, G., Lamboll, R., Grant, L., Smith, C., Pachauri, S., Rogelj, J., Riahi, K., Thiery, W., and Gidden, M. J.: Using net-zero carbon debt to track climate overshoot responsibility, Proc. Natl. Acad. Sci. U.S.A., 122, e2409316122, https://doi.org/10.1073/pnas.2409316122, 2025.

Pirani, A., Alegria, A., Khourdajie, A. A., Gunawan, W., Gutiérrez, J. M., Holsman, K., Huard, D., Juckes, M., Kawamiya, M., Klutse, N., Krey, V., Matthews, R., Milward, A., Pascoe, C., Van Der Shrier, G., Spinuso, A., Stockhause, M., and Xiaoshi Xing: The implementation of FAIR data principles in the IPCC AR6 assessment process, https://doi.org/10.5281/ZENODO.6504469, 2022.

Pongratz, J., Schwingshackl, C., Bultan, S., Obermeier, W., Havermann, F., and Guo, S.: Land Use Effects on Climate: Current State, Recent Progress, and Emerging Topics, Curr. Clim. Change Rep., 7, 99–120, https://doi.org/10.1007/s40641-021-00178-y, 2021.

Prinn, R. G., Weiss, R. F., Arduini, J., Arnold, T., DeWitt, H. L., Fraser, P. J., Ganesan, A. L., Gasore, J., Harth, C. M., Hermansen, O., Kim, J., Krummel, P. B., Li, S., Loh, Z. M., Lunder, C. R., Maione, M., Manning, A. J., Miller, B. R., Mitrevski, B., Mühle, J., O'Doherty, S., Park, S., Reimann, S., Rigby, M., Saito, T., Salameh, P. K., Schmidt, R., Simmonds, P. G., Steele, L. P., Vollmer, M. K., Wang, R. H., Yao, B., Yokouchi, Y., Young, D., and Zhou, L.: History of chemically and radiatively important atmospheric gases from the Advanced Global Atmospheric Gases Experiment (AGAGE), Earth Syst. Sci. Data, 10, 985–1018, https://doi.org/10.5194/essd-10-985-2018, 2018.

Purich, A. and Doddridge, E. W.: Record low Antarctic sea ice coverage indicates a new sea ice state, Commun Earth Environ, 4, 314, https://doi.org/10.1038/s43247-023-00961-9, 2023.

Quaas, J., Jia, H., Smith, C., Albright, A. L., Aas, W., Bellouin, N., Boucher, O., Doutriaux-Boucher, M., Forster, P. M., Grosvenor, D., Jenkins, S., Klimont, Z., Loeb, N. G., Ma, X., Naik, V., Paulot, F., Stier, P., Wild, M., Myhre, G., and Schulz, M.: Robust evidence for reversal of the trend in aerosol effective climate forcing, Atmos. Chem. Phys., 22, 12221–12239, https://doi.org/10.5194/acp-22-12221-2022, 2022.

Qin, Z., Zhu, Y., Canadell, J. G., Chen, M., Li, T., Mishra, U., and Yuan, W.: Global spatially explicit carbon emissions from land-use change over the past six decades (1961–2020), One Earth, 7, 835–847, https://doi.org/10.1016/j.oneear.2024.04.002, 2024.

Raghuraman, S.P., Paynter, D. and Ramaswamy, V.: Anthropogenic forcing and response yield observed positive trend in Earth's energy imbalance, Nat. Commun. 12, 4577, https://doi.org/10.1038/s41467-021-24544-4, 2021.

Raghuraman, S. P., Soden, B., Clement, A., Vecchi, G., Menemenlis, S., and Yang, W.: The 2023 global warming spike was driven by the El Niño–Southern Oscillation, Atmos. Chem. Phys., 24, 11275–11283, https://doi.org/10.5194/acp-24-11275-2024, 2024.

Ribes, A., Qasmi, S., and Gillett, N. P.: Making climate projections conditional on historical observations, Sci. Adv., 7, eabc0671, https://doi.org/10.1126/sciadv.abc0671, 2021.

Rogelj, J., D. Shindell, K. Jiang, S. Fifita, P. Forster, V. Ginzburg, C. Handa, H. Kheshgi, S. Kobayashi, E. Kriegler, L. Mundaca, R. Séférian, and M. V. Vilariño: Mitigation Pathways Compatible with 1.5°C in the Context of Sustainable Development. In: Global Warming of 1.5°C. An IPCC Special Report on the impacts of global warming of 1.5°C above pre-industrial levels and related global greenhouse gas emission pathways, in the context of strengthening the global response to the threat of climate change, sustainable development, and efforts to eradicate poverty [Masson-Delmotte, V., P. Zhai, H.-O. Pörtner, D. Roberts, J. Skea, P.R. Shukla, A. Pirani, W. Moufouma-Okia, C. Péan, R. Pidcock, S. Connors, J. B. R. Matthews, Y. Chen, X. Zhou, M. I. Gomis, E. Lonnoy, T. Maycock, M. Tignor, and T. Waterfield (eds.)]. Cambridge University Press, Cambridge, UK and New York, NY, USA, pp. 93-174, https://doi.org/10.1017/9781009157940.004, 2018.

Rogelj, J., Forster, P. M., Kriegler, E., Smith, C. J., and Séférian, R.: Estimating and tracking the remaining carbon budget for stringent climate targets, Nature, 571, 335–342, https://doi.org/10.1038/s41586-019-1368-z, 2019.

Rogelj, J., Lamboll, R.D.: Substantial reductions in non-CO2 greenhouse gas emissions reductions implied by IPCC estimates of the remaining carbon budget. Communications Earth Environ 5, 35. https://doi.org/10.1038/s43247-023-01168-8, 2024.

Rogelj, J., Rao, S., McCollum, D. L., Pachauri, S., Klimont, Z., Krey, V., and Riahi, K: Air-pollution emission ranges consistent with the representative concentration pathways, Nature Clim. Chang., 4 (6), 446–450, https://doi.org/10.1038/nclimate2178, 2014.

Rohde, R., Muller, R., Jacobsen, R., Perlmutter, S., Rosenfeld, A. et al.: Berkeley Earth Temperature Averaging Process, Geoinfor. Geostat.: An Overview 1:2., http://dx.doi.org/10.4172/gigs.1000103, 2013.

Saunois, M., Stavert, A. R., Poulter, B., Bousquet, P., Canadell, J. G., Jackson, R. B., Raymond, P. A., Dlugokencky, E. J., Houweling, S., Patra, P. K., Ciais, P., Arora, V. K., Bastviken, D., Bergamaschi, P., Blake, D. R., Brailsford, G., Bruhwiler, L., Carlson, K. M., Carrol, M., Castaldi, S., Chandra, N., Crevoisier, C., Crill, P. M., Covey, K., Curry, C. L., Etiope, G., Frankenberg, C., Gedney, N., Hegglin, M. I., Höglund-Isaksson, L., Hugelius, G., Ishizawa, M., Ito, A., Janssens-Maenhout, G., Jensen, K. M., Joos, F., Kleinen, T., Krummel, P. B., Langenfelds, R. L., Laruelle, G. G., Liu, L., Machida, T., Maksyutov, S., McDonald, K. C., McNorton, J., Miller, P. A., Melton, J. R., Morino, I., Müller, J., Murguia-Flores, F., Naik, V., Niwa, Y., Noce, S., O'Doherty, S., Parker, R. J., Peng, C., Peng, S., Peters, G. P., Prigent, C., Prinn, R., Ramonet, M., Regnier, P., Riley, W. J., Rosentreter, J. A., Segers, A., Simpson, I. J., Shi, H., Smith, S. J., Steele, L. P., Thornton, B. F., Tian, H., Tohjima, Y., Tubiello, F. N., Tsuruta, A., Viovy, N., Voulgarakis, A., Weber, T. S., Van Weele, M., Van Der Werf, G. R., Weiss, R. F., Worthy, D., Wunch, D., Yin, Y., Yoshida, Y., Zhang, W., Zhang, Z., Zhao, Y., Zheng, B., Zhu, Q., Zhu, Q., and Zhuang, Q.: The Global Methane Budget 2000–2017, Earth Syst. Sci. Data, 12, 1561–1623, https://doi.org/10.5194/essd-12-1561-2020, 2020.

Sato, K., Sato, K., Savita, A., Schweiger, A., Shepherd, A., Seneviratne, S. I., Simons, L., Slater, D. A., Slater, T., Steiner, A. K., Suga, T., Szekely, T., Thiery, W., Timmermans, M.-L., Vanderkelen, I., Wjiffels, S. E., Wu, T., and Zemp, M.: GCOS EHI 1960-2020 Earth Heat Inventory Ocean Heat Content (Version 2), https://doi.org/10.26050/WDCC/GCOS_EHI_1960-2020_OHC_v2, 2023b.

Scarpelli, T. R., Jacob, D. J., Grossman, S., Lu, X., Qu, Z., Sulprizio, M. P., Zhang, Y., Reuland, F., Gordon, D., and Worden, J. R.: Updated Global Fuel Exploitation Inventory (GFEI) for methane emissions from the oil, gas, and coal sectors: evaluation with inversions of atmospheric methane observations, Atmos. Chem. Phys., 22, 3235–3249, https://doi.org/10.5194/acp-22-3235-2022, 2022.

Schamm, K., Ziese, M., Becker A., Finger, P., Meyer-Christoffer, A., Schneider, U., Schroder, M., and Stender, P.: Global gridded precipitation over land: a description of the new GPCC First Guess Daily product, Earth Syst. Sci. Data, 6, 49-60. https://doi.org/10.5194/essd-6-49-2014, 2014.

Schmidt, G.: Climate models can't explain 2023's huge heat anomaly — we could be in uncharted territory, Nature, 627, 467–467, https://doi.org/10.1038/d41586-024-00816-z, 2024.

1809 von Schuckmann, K., Cheng, L., Palmer, M. D., Hansen, J., Tassone, C., Aich, V., Adusumilli, S., Beltrami, H., Boyer,
1810 T., Cuesta-Valero, F. J., Desbruyères, D., Domingues, C., García-García, A., Gentine, P., Gilson, J., Gorfer, M.,
1811 Haimberger, L., Ishii, M., Johnson, G. C., Killick, R., King, B. A., Kirchengast, G., Kolodziejczyk, N., Lyman, J.,
1812 Marzeion, B., Mayer, M., Monier, M., Monselesan, D. P., Purkey, S., Roemmich, D., Schweiger, A., Seneviratne, S.
1813 I., Shepherd, A., Slater, D. A., Steiner, A. K., Straneo, F., Timmermans, M.-L., and Wijffels, S. E.: Heat stored in the
1814 Earth system: where does the energy go?, Earth Syst. Sci. Data, 12, 2013–2041, https://doi.org/10.5194/essd-12-2013-
1815 2020, 2020.

1816 von Schuckmann, K., Minière, A., Gues, F., Cuesta-Valero, F. J., Kirchengast, G., Adusumilli, S., Straneo, F., Ablain,
1817 M., Allan, R. P., Barker, P. M., Beltrami, H., Blazquez, A., Boyer, T., Cheng, L., Church, J., Desbruyeres, D., Dolman,
1818 H., Domingues, C. M., García-García, A., Giglio, D., Gilson, J. E., Gorfer, M., Haimberger, L., Hakuba, M. Z.,
1819 Hendricks, S., Hosoda, S., Johnson, G. C., Killick, R., King, B., Kolodziejczyk, N., Korosov, A., Krinner, G., Kuusela,
1820 M., Landerer, F. W., Langer, M., Lavergne, T., Lawrence, I., Li, Y., Lyman, J., Marti, F., Marzeion, B., Mayer, M.,
1821 MacDougall, A. H., McDougall, T., Monselesan, D. P., Nitzbon, J., Otosaka, I., Peng, J., Purkey, S., Roemmich, D.,
1822 Sato, K., Sato, K., Savita, A., Schweiger, A., Shepherd, A., Seneviratne, S. I., Simons, L., Slater, D. A., Slater, T.,
1823 Steiner, A. K., Suga, T., Szekely, T., Thiery, W., Timmermans, M.-L., Vanderkelen, I., Wjiffels, S. E., Wu, T., and
1824 Zemp, M.: Heat stored in the Earth system 1960–2020: where does the energy go?, Earth System Science Data, 15,
1825 1675–1709, https://doi.org/10.5194/essd-15-1675-2023, 2023a.

1826

1827 Schoeberl, M. R., Wang, Y., Taha, G., Zawada, D. J., Ueyama, R., and Dessler, A.: Evolution of the Climate Forcing
1828 During the Two Years After the Hunga Tonga-Hunga Ha'apai Eruption, JGR Atmospheres, 129, e2024JD041296,
1829 https://doi.org/10.1029/2024JD041296, 2024.
1830 Schwingshackl, C., Obermeier, W. A., Bultan, S., Grassi, G., Canadell, J. G., Friedlingstein, P., Gasser, T., Houghton,
1831 R. A., Kurz, W. A., Sitch, S., and Pongratz, J.: Differences in land-based mitigation estimates reconciled by separating
1832 natural and land-use CO2 fluxes at the country level, One Earth, 5, 1367–1376,
1833 https://doi.org/10.1016/j.oneear.2022.11.009, 2022.
1834 Seneviratne, S.I., X. Zhang, M. Adnan, W. Badi, C. Dereczynski, A. Di Luca, S. Ghosh, I. Iskandar, J. Kossin, S.
1835 Lewis, F. Otto, I. Pinto, M. Satoh, S. M. Vicente-Serrano, M. Wehner, and B. Zhou: Weather and Climate Extreme
1836 Events in a Changing Climate. In Climate Change 2021: The Physical Science Basis. Contribution of Working Group
1837 I to the Sixth Assessment Report of the Intergovernmental Panel on Climate Change [Masson-Delmotte, V., P. Zhai,
1838 A. Pirani, S.L. Connors, C. Péan, S. Berger, N. Caud, Y. Chen, L. Goldfarb, M.I. Gomis, M. Huang, K. Leitzell, E.
1839 Lonnoy, J.B.R. Matthews, T.K. Maycock, T. Waterfield, O. Yelekçi, R. Yu, and B. Zhou (eds.)]. Cambridge
1840 University Press, Cambridge, United Kingdom and New York, NY, USA, pp. 1513–1766,
1841 doi:10.1017/9781009157896.013.1513–1766, https://doi.org/10.1017/9781009157896.013, 2021.

1842 Seo, K.-W., Ryu, D., Jeon, T., Youm, K., Kim, J.-S., Oh, E. H., Chen, J., Famiglietti, J. S., and Wilson, C. R.: Abrupt
1843 sea level rise and Earth's gradual pole shift reveal permanent hydrological regime changes in the 21st century, Science,
1844 387, 1408–1413, https://doi.org/10.1126/science.adq6529, 2025.

Sherwin, E. D., Rutherford, J. S., Zhang, Z., Chen, Y., Wetherley, E. B., Yakovlev, P. V., Berman, E. S. F., Jones, B. B., Cusworth, D. H., Thorpe, A. K., Ayasse, A. K., Duren, R. M., and Brandt, A. R.: US oil and gas system emissions from nearly one million aerial site measurements, Nature, 627, 328–334, https://doi.org/10.1038/s41586-024-07117-5, 2024.

Simmonds, P. G., Rigby, M., McCulloch, A., O'Doherty, S., Young, D., Mühle, J., Krummel, P. B., Steele, P., Fraser, P. J., Manning, A. J., Weiss, R. F., Salameh, P. K., Harth, C. M., Wang, R. H. J., and Prinn, R. G.: Changing trends and emissions of hydrochlorofluorocarbons (HCFCs) and their hydrofluorocarbon (HFCs) replacements, Atmos. Chem. Phys., 17, 4641–4655, https://doi.org/10.5194/acp-17-4641-2017, 2017.

Sippel, S., Zscheischler, J., Heimann, M., Otto, F. E. L., Peters, J., and Mahecha, M. D.: Quantifying changes in climate variability and extremes: Pitfalls and their overcoming, Geophys. .Res. Lett., 42, 9990–9998, https://doi.org/10.1002/2015GL066307, 2015.

Smith, C., Walsh, T., Gillett, N., Hall, B., Hauser, M., Krummel, P., Lamb, W., Lamboll, R., Muhle, J., Palmer, M., Ribes, A., Seneviratne, S., Trewin, B., von Schuckmann, K., and Forster, P.: ClimateIndicator/data: Indicators of Global Climate Change 2024 submission (v2025.06.11), [Data set], https://doi.org/10.5281/zenodo.15639576, 2025a.

Smith, C., Walsh, T., Gillett, N., Hall, B., Hauser, M., Krummel, P., Lamb, W., Lamboll, R., X., Muhle, J., Palmer, M., Ribes, A., Seneviratne, S., Trewin, B., von Schuckmann, K., and Forster, P.: Data repository for Indicators of Global Climate Change, Github [code], https://github.com/ClimateIndicator/data/tree/v2025.06.11 , last access: 11 June 2025, 2025b

Smith, C., Nicholls, Z. R. J., Armour, K., Collins, W., Forster, P., Meinshausen, M., Palmer, M. D., and Watanabe, M.: The Earth's Energy Budget, Climate Feedbacks, and Climate Sensitivity Supplementary Material, in: Climate Change 2021: The Physical Science Basis. Contribution of Working Group I to the Sixth Assessment Report of the Intergovernmental Panel on Climate Change, edited by: Masson-Delmotte, V., Zhai, P., Pirani, A., Connors, S. L., Péan, C., Berger, S., Caud, N., Chen, Y., Goldfarb, L., Gomis, M. I., Huang, M., Leitzell, K., Lonnoy, E., Matthews, J. B. R., Maycock, T. K., Waterfield, T., Yelekçi, O., Yu, R., and Zhou, B., 2021.

Smith, C., Forster, P., Palmer, M., Collins, B., Leach, N., Watanabe, M., Berger, S., Hall, B., Zelinka, M., Lunt, D., Cain, M., Harris, G., and Ringer, M.: IPCC WGI AR6 Chapter 7 (v.1.0). Zenodo. https://doi.org/10.5281/zenodo.5211358, 2021.

Smith, S. J., van Aardenne, J., Klimont, Z., Andres, R. J., Volke, A., and Delgado Arias, S.: Anthropogenic sulfur dioxide emissions: 1850–2005, Atmos. Chem. and Phys., 11, 1101–1116, https://doi.org/10.5194/acp-11-1101-2011, 2011.

Soulie, A., C. Granier, S. Darras, N. Zilbermann, T. Doumbia, M. Guevara, J.-P. Jalkanen, S. Keita, C. Liousse, M. Crippa, D. Guizzardi, R. Hoesly, S. J. Smith Global Anthropogenic Emissions (CAMS-GLOB-ANT) for the Copernicus Atmosphere Monitoring Service Simulations of Air Quality Forecasts and Reanalyses Earth Syst. Sci. Data, 2023.

Storto, A. and Yang, C.: Acceleration of the ocean warming from 1961 to 2022 unveiled by large-ensemble reanalyses, Nature Communications, 15, 545, https://doi.org/10.1038/s41467-024-44749-7, 2024.

Szopa, S., V. Naik, B. Adhikary, P. Artaxo, T. Berntsen, W.D. Collins, S. Fuzzi, L. Gallardo, A. Kiendler-Scharr, Z. Klimont, H. Liao, N. Unger, and P. Zanis: Short-Lived Climate Forcers. In Climate Change 2021: The Physical Science Basis. Contribution of Working Group I to the Sixth Assessment Report of the Intergovernmental Panel on Climate Change [Masson-Delmotte, V., P. Zhai, A. Pirani, S.L. Connors, C. Péan, S. Berger, N. Caud, Y. Chen, L. Goldfarb, M.I. Gomis, M. Huang, K. Leitzell, E. Lonnoy, J.B.R. Matthews, T.K. Maycock, T. Waterfield, O. Yelekçi, R. Yu, and B. Zhou (eds.)]. Cambridge University Press, Cambridge, United Kingdom and New York, NY, USA, pp. 817–922, https://doi:10.1017/9781009157896.008, 2021.

Terhaar, J., Burger, F.A., Vogt, L. et al.: Record sea surface temperature jump in 2023–2024 unlikely but not unexpected, Nature 639, 942–946, https://doi.org/10.1038/s41586-025-08674-z, 2025.

Trewin, B.: Assessing Internal Variability of Global Mean Surface Temperature From Observational Data and Implications for Reaching Key Thresholds, JGR Atmospheres, 127, e2022JD036747, https://doi.org/10.1029/2022JD036747, 2022.

Tibrewal, K., Ciais, P., Saunois, M., Martinez, A., Lin, X., Thanwerdas, J., Deng, Z., Chevallier, F., Giron, C., Albergel, C., Tanaka, K., Patra, P., Tsuruta, A., Zheng, B., Belikov, D., Niwa, Y., Janardanan, R., Maksyutov, S., Segers, A., Tzompa-Sosa, Z. A., Bousquet, P., and Sciare, J.: Assessment of methane emissions from oil, gas and coal sectors across inventories and atmospheric inversions, Communications Earth & Environment, 5, 26, https://doi.org/10.1038/s43247-023-01190-w, 2024.

Vakilifard, N., Williams, R. G., Holden, P. B., Turner, K., Edwards, N. R., and Beerling, D. J.: Impact of negative and positive CO_2 emissions on global warming metrics using an ensemble of Earth system model simulations, Biogeosciences, 19, 4249–4265, https://doi.org/10.5194/bg-19-4249-2022, 2022.

Vanderkelen, I. and Thiery, W.: GCOS EHI 1960-2020 Inland Water Heat Content, https://doi.org/10.26050/WDCC/GCOS_EHI_1960-2020_IWHC, 2022.

Vimont, I. J, B. D. Hall, G. Dutton, S. A. Montzka, J. Mühle, M. Crotwell, K. Petersen, S. Clingan, and D. Nance, [in "State of the Climate in 2022"]. Bull. Amer. Meteor. Soc., 104 , 9, S76–S78, https://doi.org/10.1175/BAMS-D-23-0090.1., 2022.

Vollmer, M. K., Young, D., Trudinger, C. M., Mühle, J., Henne, S., Rigby, M., Park, S., Li, S., Guillevic, M., Mitrevski, B., Harth, C. M., Miller, B. R., Reimann, S., Yao, B., Steele, L. P., Wyss, S. A., Lunder, C. R., Arduini, J., McCulloch, A., Wu, S., Rhee, T. S., Wang, R. H. J., Salameh, P. K., Hermansen, O., Hill, M., Langenfelds, R. L., Ivy, D., O'Doherty, S., Krummel, P. B., Maione, M., Etheridge, D. M., Zhou, L., Fraser, P. J., Prinn, R. G., Weiss, R. F., and Simmonds, P. G.: Atmospheric histories and emissions of chlorofluorocarbons CFC-13 (CClF3), ΣCFC-114 (C2Cl2F4), and CFC-115 (C2ClF5), Atmos. Chem. Phys., 18, 979–1002, https://doi.org/10.5194/acp-18-979-2018, 2018.

Watson-Parris, D., Christensen, M. W., Laurenson, A., Clewley, D., Gryspeerdt, E., and Stier, P.: Shipping regulations lead to large reduction in cloud perturbations, Proc. Natl. Acad. Sci. U.S.A., 119, e2206885119, https://doi.org/10.1073/pnas.2206885119, 2022.

WCRP Global Sea Level Budget Group: Global sea-level budget 1993–present, Earth Syst. Sci. Data, 10, 1551–1590, https://doi.org/10.5194/essd-10-1551-2018, 2018.

Western, L. M., Vollmer, M. K., Krummel, P. B., Adcock, K. E., Fraser, P. J., Harth, C. M., Langenfelds, R. L., Montzka, S. A., Mühle, J., O'Doherty, S., Oram, D. E., Reimann, S., Rigby, M., Vimont, I., Weiss, R. F., Young, D., and Laube, J. C.: Global increase of ozone-depleting chlorofluorocarbons from 2010 to 2020, Nat. Geosci., 16, 309–313, https://doi.org/10.1038/s41561-023-01147-w, 2023.

Western, L. M., Daniel, J. S., Vollmer, M. K., Clingan, S., Crotwell, M., Fraser, P. J., Ganesan, A. L., Hall, B., Harth, C. M., Krummel, P. B., Mühle, J., O'Doherty, S., Salameh, P. K., Stanley, K. M., Reimann, S., Vimont, I., Young, D., Rigby, M., Weiss, R. F., Prinn, R. G., and Montzka, S. A.: A decrease in radiative forcing and equivalent effective chlorine from hydrochlorofluorocarbons, Nat. Clim. Chang., 14, 805–807, https://doi.org/10.1038/s41558-024-02038-7, 2024.

van der Werf, G. R., Randerson, J. T., Giglio, L., van Leeuwen, T. T., Chen, Y., Rogers, B. M., Mu, M., van Marle, M. J. E., Morton, D. C., Collatz, G. J., Yokelson, R. J., and Kasibhatla, P. S.: Global fire emissions estimates during 1997–2016, Earth System Science Data, 9, 697–720, https://doi.org/10.5194/essd-9-697-2017, 2017.

Wild, M., Gilgen, H., Roesch, A., Ohmura, A., Long, C. N., Dutton, E. G., Forgan, B., Kallis, A., Russak, V., and Tsvetkov, A.: From Dimming to Brightening: Decadal Changes in Solar Radiation at Earth's Surface, Science, 308, 847–850, https://doi.org/10.1126/science.1103215, 2005.

World Meteorological Organization (WMO). State of the Global Climate 2024. WMO-No. 1368. 2025. ISBN: 978-92-63-11368-5.

Xu, Q., Wei, S., Li, Z., and Li, Q.: A New Evaluation of Observed Changes in Diurnal Temperature Range, Geophysical Research Letters, 52, e2024GL113406, https://doi.org/10.1029/2024GL113406, 2025.

Zickfeld, K., Azevedo, D., Mathesius, S., and Matthews, H. D.: Asymmetry in the climate–carbon cycle response to positive and negative CO2 emissions, Nat. Clim. Chang., 11, 613–617, https://doi.org/10.1038/s41558-021-01061-2, 2021.

Zhang, Z., Poulter, B., Feldman, A.F., Ying, Q., Ciais, P., Peng, S. and Xin, L.: Recent intensification of wetland methane feedback, Nat. Clim. Chang. 13, 430–433, https://doi.org/10.1038/s41558-023-01629-0, 2023.